OPTIMAL GEOMETRIC DEPOLYMENT OF A GROUND BASED PSEUDOLITE NAVIGATION SYSTEM TO TRACK A LANDING AIRCRAFT

THESIS

Matthew Perri Crawford, Ensign, USN
AFIT/GAE/ENY/06-02

DEPARTMENT OF THE AIR FORCE
AIR UNIVERSITY

AIR FORCE INSTITUTE OF TECHNOLOGY

Wright-Patterson Air Force Base, Ohio

AFIT/GAE/ENG/06-02

OPTIMAL GEOMETRIC DEPOLYMENT OF A GROUND BASED PSEUDOLITE NAVIGATION SYSTEM TO TRACK A LANDING AIRCRAFT

THESIS

Presented to the Faculty

Department of Aeronautics and Astronautics

Graduate School of Engineering and Management

Air Force Institute of Technology

Air University

Air Education and Training Command

In Partial Fulfillment of the Requirements for the

Degree of Master of Science in Aeronautical Engineering

Matthew Perri Crawford, BSAAE

Ensign, USN

JUNE 2006

AFIT/GAE/ENG/06-02

OPTIMAL GEOMETRIC DEPOLYMENT OF A GROUND BASED PSEUDOLITE NAVIGATION SYSTEM TO TRACK A LANDING AIRCRAFT

Matthew Perri Crawford, BSAAE
Ensign, USN

Approved:

/signed/	5 JUN 2006
Professor John F Raquet (Chairman)	date
/signed/	5 JUN 2006
Lt Col Juan Vasquez (Member)	date
/signed/	5 JUN 2006
Major Paul Blue (Member)	date

Abstract

With much of the military and civilian communities becoming dependent on GPS technology to navigate, it has become imperative that the navigation systems be tested in situations in which GPS does not work. This testing is especially necessary for precise tasks such as landing an aircraft. Currently, research is being conducted into using a pseudolite-based reference system to use as a truth model for the GPS jamming test. Pseudolite systems have been proven to provide sub-centimeter level accuracy in the horizontal plane; however in the vertical plane the position error is still in the decimeter to meter level range. This is largely due to the fact that the geometry of a ground based pseudolite system provides poor slant angles in the vertical plane, which contributes to large positioning errors. The goal of this research is to study the effects of system geometry on the vertical plane solution.

The results of this effort show that elevation angles of greater than 20^{o}-30^{o} are necessary to attain reasonably good positioning solutions. Multiple pseudolite deployments, while effective at reducing the geometry errors, are very cost ineffective and the geometries pose significant risks to a landing aircraft. The best geometry involved using an orbiting aircraft, with a pseudolite transmitter and receiver attached, as an elevated pseudolite to create better slant angles and thus better positioning solutions.

To my Mother and Brother

Acknowledgements

First of all I would like to thank all of my family and friends for their love and support, without which I would have lost my sanity long ago. I would also like to thank John Amt for his technical expertise and for serving as a well of knowledge during this endeavor. Lastly I would like to thank my advisor Dr. Raquet for his guidance and patience.

Ensign Matthew Crawford, USN

Table of Contents

List of Figures

List of Tables

List of Symbols

List of Abbreviations

OPTIMAL GEOMETRIC DEPOLYMENT OF A GROUND BASED PSEUDOLITE NAVIGATION SYSTEM TO TRACK A LANDING AIRCRAFT

I. Introduction

1.1 Motivation

The introduction of the Global Positioning System (GPS) heralded in a new era of navigation. With the ability to determine ones position to within a few meters of error, GPS gives a more precise alternative to a complex system of maps, compasses, and Inertial Navigation Systems (INS) and allows the US military to better track and manage its forces around the globe. In the beginning, only the US military and government were privy to the signals that gave accuracy to within a few meters, because of a Selective Availability (SA) that intentionally added position error on the order of hundreds of meters. Then on 1 May 2000, President Bill Clinton ordered that SA be turned off [17]. At that point the rest of the world realized the true capability of GPS, which could accurately determine position to within a few meters. Since that time, the demand for more precise measurements has increased dramatically.

Several methods have been developed that dramatically increase the accuracy of GPS to decimeter and centimeter level accuracy. One of these methods is known as Differential GPS (DGPS). DGPS takes advantage of the fact that position errors between two nearby receivers are nearly identical. Thus if one receiver is placed in a known location the GPS error corrections can be calculated and transmitted (either through a

cable or a wireless connection) to the second receiver. With DGPS the position error reduces to either decimeter level or centimeter level, depending on the method used [17]. Another method for improving the accuracy of GPS is to combine its readings with those of an INS, which would also yield a robust position solution. Both the military and the civilian communities are working to incorporate GPS into automated precision approaches for landing aircraft.

The problem with GPS, and its subsequent error reducing methods, is that many military, government, and civilian systems are now dependent on receiving GPS signals from the orbiting satellites. This dependency has shown a growing infrastructure vulnerability which a savvy enemy could take advantage of by jamming those signals. Therefore, to stay one step ahead of the enemy, the United States Air Force (USAF) has embarked on a scientific effort to test the robustness of GPS in jamming or interference environments.

Developing this robust system poses a unique problem to the USAF. How does one test a system that is currently the standard for which most other systems are based? A truth measurement system must be established that is at least an order of magnitude smaller than the system being tested. With GPS this would mean that the truth system would have to, at the very least, achieve centimeter level accuracy. Past systems for testing GPS in jamming environments used one of the GPS frequencies as a truth measurement while the other was jammed. Currently the 746th Test Squadron's (TS) Central Inertial Guidance Test Facility (CIGTF) based at Holloman Air Force Base (AFB), NM is the Air Force's testing center for new flight navigation systems. The 746th uses an Embedded GPS/INS (EGI), a second INS, and a second GPS receiver, along with

a transponder/integrator in a system called the CIGTF Reference System (CRS) to conduct tests on GPS under single frequency jamming conditions [1]. In a real life interference situation, the enemy would jam both GPS frequencies. Therefore the truth measurement system must be completely independent of the GPS signal and therefore unaffected by the jamming of the GPS signals. Currently the 746th TS does not have such a system.

Ironically, one of the ideas for designing this new truth reference system has its roots in the early design of GPS. Pseudo-satellites (also known as pseudolites) were used in the early days of GPS development to test the basic concepts of GPS before the satellites were built [14]. It is this same technology, only enhanced, that may offer a solution to finding a truth model that is completely independent from GPS. Pseudolites can be deployed on the ground and transmit GPS-like signals but on different frequencies than GPS. A correctly deployed array of pseudolites would therefore provide the Air Force with a system with enough robustness to test GPS in a jamming environment. However, the question then becomes, would a pseudolite deployment yield the desired accuracy to test GPS? This is the question that must be carefully considered if pseudolites are to be implemented in a testing environment.

There have already been studies into the simulation of the pseudolite environment [8], and the development and testing of a pseudolite network for use in tracking ground vehicles over changing terrain [1]. This research has shown that in the horizontal plane it is possible to get decimeter level accuracy with a pseudolite network given certain conditions such as terrain are known. However, the vertical position error remains imprecise due to poor geometry. Several solutions have been proposed to solve this

vertical deficiency. One solution is to use more rigorous mathematics to squeeze every bit of measurement accuracy out of the signal. This solution has already begun to reach its limit. Another option is to augment the pseudolite network with an image-aided inertial system. The third option is to try and achieve the very best geometry for a given area by studying the effects of pseudolite position and its effects on the solution. The geometry optimization option is of particular interest because an optimized geometry could possibly yield a large increase in precision for a very low cost.

1.2 Problem Definition

When implementing a pseudolite network, it is relatively easy to achieve good geometry (centimeter level accuracy) in the horizontal plane. In the vertical direction, however, the level of precision decreases greatly. This decrease in precision is a result of low observability in the vertical plane due to poor elevation angles between transmitter and receiver. For example consider the case of a pseudolite placed on a tower of equal height to the tallest aircraft control tower in the world, which currently resides at the Kuala Lumpor International Airport and is 130 meters tall [11]. According to FAA regulations on airspace obstructions [12], a tower of this size must be no closer than 6 kilometers away from a 3,000 meter long runway. Given these parameters, the best elevation angle between a pseudolite on the tower and a receiver on the runway would be 1.24^{o}. Even if the tower were closer to the runway, say 1 kilometer away instead of 6 kilometers, the maximum elevation angle from the receiver to the pseudolite would be 7.40^{o}. Given these inherent problems in pseudolite reference systems, caused by poor elevation angles, it is the purpose of this research to systematically investigate possible

options of increasing the vertical observability of the reference system by varying the pseudolite network's deployment geometry.

1.3 Proposed Solution

There is no single geometric positioning approach that will yield sub-centimeter level measurements. Every different application of pseudolite technology will yield a different optimal geometry. The general goal, however, is to encompass the test area in all three dimensions. For this study, the test area will be a 3,000-meter by 120-meter runway. A small, unmanned, landing aircraft will be modeled as a point source. This aircraft will travel along a 3^{o} glide slope, starting at 500 feet, and perform a rollout maneuver upon touch down. The glide slope and the pseudolite network will be modeled in Matlab®, and a nonlinear, iterative, weighted, batch least squares estimation method developed by John Amt at the Air Force Institute of Technology (AFIT) [1], will be used to simulate the measurements generated by the pseudolite network.

Several different geometry simulations will be generated during the course of this research. The first simulation will be a study into the influence that the elevation angle of a single transmitter has on the quality of a pseudolite network's geometry. The next family of simulations involves varying the number of pseudolites, aligning them in different configurations along the runway, and studying their effect on the network's accuracy. The last test group involves using a mobile pseudolite/receiver combination on an orbiting aircraft to increase the vertical observability of the pseudolite system.

1.4 Scope

This research will further the development of a pseudolite-based reference system for which to test GPS in an interference environment. A systematic approach will be developed for studying the effects of system geometry on position solutions. During the course of simulating the different geometric deployments, new ways to visualize the effect of geometry on measurement precision will be created. All of the pseudolite networks will be simulated in a Matlab® 7.0 environment.

The pseudolites being modeled in this research are based on those manufactured by Locata, Inc. These pseudolites use a method of time synchronization to eliminate the pseudolite clock error that typically occurs between stationary pseudolites.

1.5 Assumptions

The following assumptions were made during the course of this research:

1. Carrier phase ambiguities can be neglected for all tests except for the real-life based orbiting aircraft test, because the goal of this research is to study the effects of only the pseudolite network geometry, not the ability to resolve ambiguities.
2. Real time solutions are not necessary, because the ultimate goal of this research is to aid in the development of a truth reference system for a GPS interference test. All data can, therefore, be post-processed.
3. No signal interference analysis is required because the pseudolites will be operating at a different frequency than GPS.

4. The time offset that is, in most situations, inherent in pseudolite-based reference systems can be neglected because of the unique TimeLoc system developed the Locata, Inc [2, 3, 4, 5, 6, &7].
5. Tropospheric errors can be ignored in all simulations in order to focus solely on the errors from geometric positioning.

1.6 Related Research

1.6.1 Pseudolite Research

Pseudolites have been used, in the past, for testing and designing GPS. Over the last 15 years their usefulness as a possible alternative or addition to GPS has been investigated.

1.6.1.1 Pseudolite Transceiver Applications

Reference [18] is an excellent source for the background development of pseudolite transmitters, which form the basic technology behind the development of the Locata positioning system. Included in the discussion are the differences between prior pseudolite systems and pseudolite transceivers. The major distinction made is that prior pseudolite systems required the use of a reference receiver to synchronize the pseudolites in the network. With the Locata system, each of the LocataLites (pseudolites) are time synchronized so no reference receiver is required. Another benefit to the antenna/transmitter design of these pseudolites is the potential ability to self-difference inside the network to reduce clock errors (as Locata does). Possible applications for this technology, including but not limited to Mars exploration, open-pit mining, and formation flying spacecraft are also discussed. More information can be found in [18].

1.6.1.2 Simulation of a Pseudolite Reference System

The development and simulation of a pseudolite-based reference system is given in [8]. Carrier phase measurements were used to track the truth trajectory of a simulated C-12 cargo aircraft. Instead of batch least squares estimation, this research used double differenced measurements and a Kalman filter with optimal smoothing to resolve carrier-phase ambiguities and solve for position. Tropospheric errors are first reduced using a modified troposphere model [10], with the residual error being reduced through the differencing techniques. The tropospheric error remaining after the modeling still results in higher than desired position solutions. Two methods were tested to further reduce the tropospheric error term. The first method involved weighting the state covariance matrix, while the second method added states to the Kalman filter to specifically model the residual error. This research shows that single frequency operation is sufficient to yield centimeter level precision, which means that widelane techniques are not required. Another significant finding of this research is that change in relative geometry is necessary to resolve the carrier-phase ambiguities. Lastly, this paper also shows that another significant source of error (other than the troposphere) is pseudolite network alignment.

1.6.1.3 Height Determination in a Pseudolite Reference System

Amt [1] attempts to solve the vertical geometry problem by using a batch least squares technique with single differencing to resolve the floating point ambiguities (integer ambiguities plus various errors terms such as the receiver clock error and tropospheric error). The research found that decimeter-level precision is attained in the vertical domain by constraining the height to a grid. Two real world tests were run where

a Locata network tracks a ground vehicle. The first test has the ground vehicle traveling along a straight road, while the second test had the vehicle traveling on a track that appears to 'wiggle' from side to side. The height constraining method works well in surveyed geographic environments for land and sea based applications. However, the grid-constrained solution would not work for an aircraft simulation, because the vertical position of an aircraft is not limited by a known surface. The Matlab® simulation developed during Amt's research is the base simulator on which the test cases in this thesis were run.

1.6.1.4 Inverted Pseudolite System

In 1995, a proof-of-concept demonstration was performed showing that pseudolite-based reference systems can be used to accurately track the position of a moving object. This test, conducted by the 746th Test Squadron at Holloman AFB, involves using two pseudolite transmitters and an array of GPS receivers. One pseudolite transmitter was located at a precisely known (surveyed) location, while the other pseudolite was placed in a mobile platform. The ultimate goal was for the mobile platform to be an aircraft. GPS receivers were then deployed in a non-coplanar array and used as references to calculate the position of the pseudolite onboard the mobile platform, as shown in Figure 1. This test concluded that a pseudolite-based reference system could be used to track a mobile pseudolite with decimeter level accuracy. This approach shows promise for future applications, including the use of an orbiting aircraft (whose position has been found using a pseudolite network) to track a landing aircraft. Further details on the inverted pseudolite system can be found in [16].

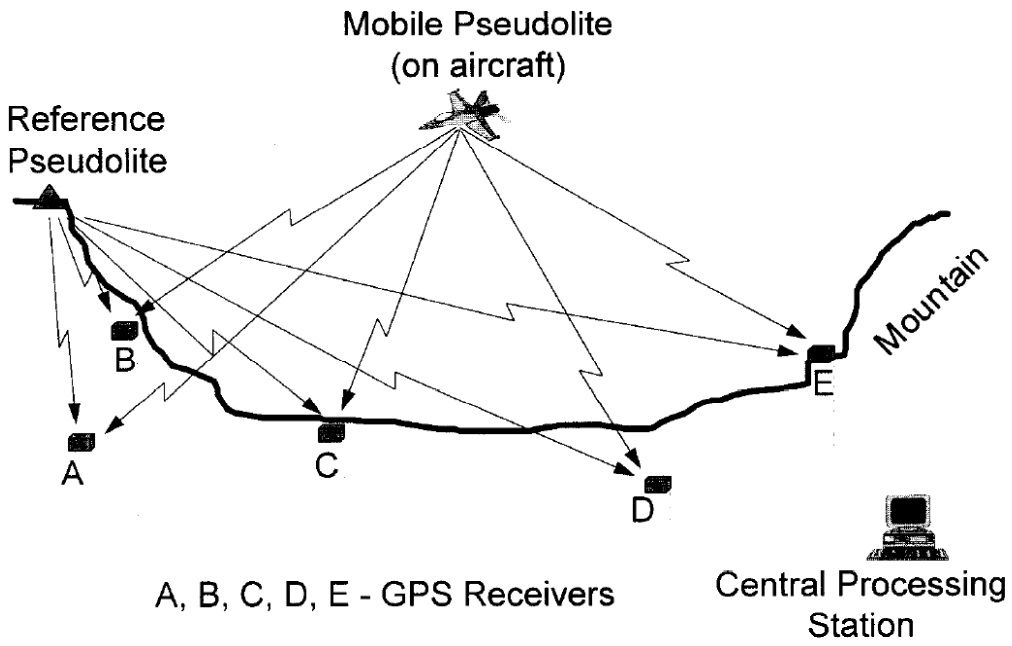

Figure 1: The Inverted Pseudolite Network [16]

1.6.1.5 Pseudolite Augmentation for GPS Airborne Applications

An investigation, led by the Satellite Navigation and Positioning (SNAP) group at the University of New South Wales, into the use of pseudolite transmitters to augment GPS for aircraft applications was conducted in 2002 [13]. This study yielded some interesting results, the first being that the offset between the GPS antenna (located on the top of the aircraft) and the pseudolite antenna (located on the bottom of the aircraft), see Figure 2, must be corrected for in order to get precise measurements. Secondly, this study showed that for a pseudolite system that is used to augment GPS, adding more than three pseudolite transmitters to the system would not significantly improve measurement results. Lastly, it was found that the use of pseudolites to augment GPS significantly improves the reference system geometry and the signal availability to the airborne

receivers. This information would be very helpful in the implementation of a test for a pseudolite reference system for use in a landing environment.

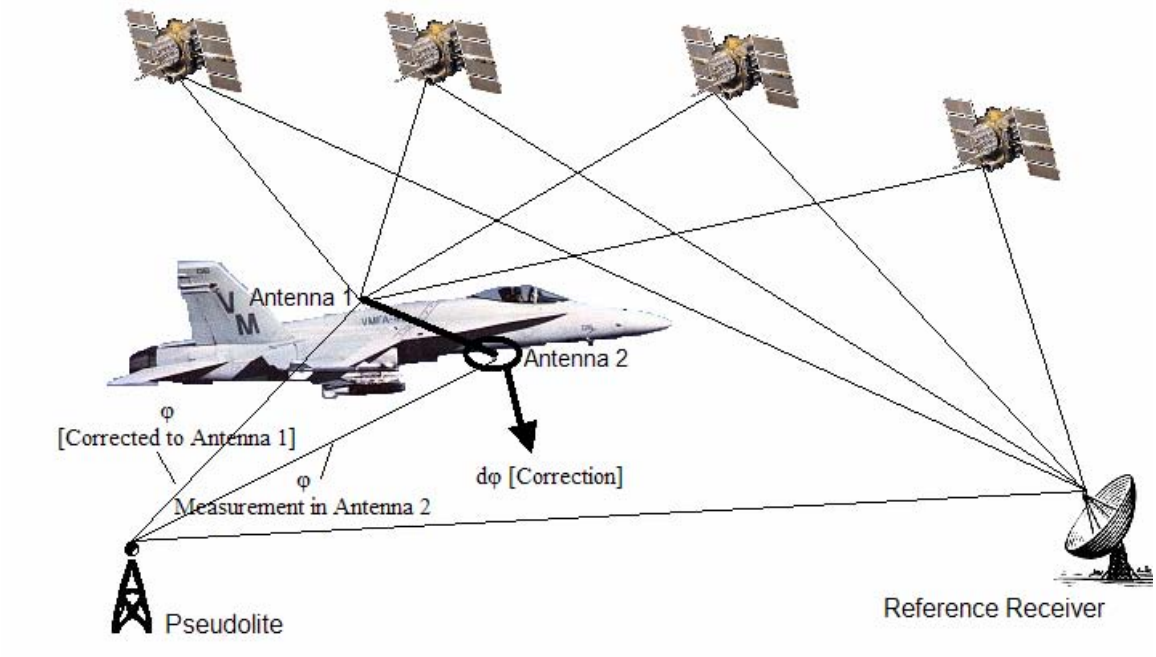

Figure 2: Pseudolite Augmentation for an Airborne Application

1.6.1.6 GPS/ Pseudolite Based Relative Navigation

The Navigation Systems Testing Laboratory (NSTL) at NASA's Johnson Space Center in Houston, Texas conducted research that focuses on the use of a Kalman filter algorithm to process the double differenced measurements from pseudolites. This research tests a pseudolite environment for use with precision guidance approach and docking of the Space Shuttle to the International Space Station. Results from this study show that less than 1 meter of error is possible if one could reduce or eliminate the numerous cycle slips, which occur in the data collection process. More information can be found in [14].

1.6.1.7 Pseudolite Applications: Progress and Problems

Wang [19] gives a summary of much of the research into pseudolites that has been conducted over the past 20+ years. Key topics include the definitions of different types of pseudolites, their possible applications, pseudolite only positioning system strengths and weaknesses, pseudolites used in conjunction with GPS/INS, and the problems associated with pseudolites. The problems associated with pseudolite systems include multipath, tropospheric error and time synchronization of pseudolites with imprecise clocks. For more information refer to [19].

1.6.2 Precision Guided Landing

There are several systems which have been tested with the goal of precisely tracking the approach of a landing aircraft. These tests demonstrate previous examples in which a tracking system, independent from GPS, has been required.

1.6.2.1 Carrier Phase DGPS/INS Flight Test

In 1995 NASA Ames Research Center worked to assess the feasibility of using DGPS in conjunction with INS to safely execute the precision landing of an aircraft (in accordance with the Category III flight criteria set by the FAA for precision landing systems) [15]. The thinking behind the combined system (DGPS/INS) is that alone each system has weaknesses, which prohibit their sole use in Category III flight. DGPS, while very accurate, does not provide the desired reliability and INS (which is a proven and reliable system) is not precise enough for a landing environment. To test this system, a King Air 200 was used as test bed with both an INS and a DGPS receiver. Both systems are combined inside the onboard computer system to provide the pilot with real time positioning data. The criteria for this test is that the aircraft must stay inside the approach

tunnel (a 3^{o} glide slope) 95% of the time, until 50 feet above the ground, where the pilot will then take over the controls and complete the landing. A laser-tracking device, which must be precisely tuned before each test run, was used to generate a truth trajectory, which is only accurate to 0.2 meters. This research is relevant because it details the standard glide slope approach trajectory used for landing aircraft, and it shows the limits to using a laser tracker for tracking the truth trajectory of a landing aircraft.

1.6.2.2 GPS/Pseudolite Flight Test

This flight test, conducted in 1993, uses a GPS/pseudolite combination to perform a precision landing [9]. In this test, a single pseudolite was used to send a GPS-like signal from the ground. This ground signal improved the reliability and geometry of the GPS system, and yielded more precise position measurements. A laser tracker was used to provide the truth trajectory for comparison to the GPS/pseudolite. The laser tracker used in this research once again shows the limits of laser technology for use in navigation as it was only accurate to 1 meter in all directions, when the aircraft was about 1.5 miles away from the runway. This study correlates with the results from [13], in which the use of pseudolites in a local area can greatly enhance the geometry of GPS to provide more precise measurements. More information can be found in [9].

1.6.3 Locata Pilot Studies

There have been several studies done in the design and implementation of Locata, Inc.'s LocataNet technology.

1.6.3.1 Industrial Machine Guidance Using LocataNet

In this pilot study [3], conducted at the BlueScope Steel warehouse in Port Kembla, Australia, the LocataNet system was used to track an indoor moving crane,

which is used to move steel slabs to specific locations. This proved to be a challenging environment for Locata because the heavily metallic environment, created by the machines and steel, made the possibility of mulitpath error very large. Despite the obvious multipath difficulties, a LocataNet is able to yield sub-centimeter level precision and centimeter level absolute accuracy. This feat is accomplished by careful positioning of the Locatalites to minimize the effects of multipath. The fact that careful positioning successfully reduced the multipath errors gives hope that the same principle of careful positioning can be used to optimize the geometry of a LocataNet for a landing aircraft environment.

1.6.3.2 Structural Deformation Monitoring Using Locata

In the past GPS has been used to monitor structural deformation, however due to poor satellite geometry and observability it can be extremely difficult to get precise measurements with GPS. In 2004, the Locata, Inc team tested their reference system for use as a GPS alternative for structural deformation monitoring at the Parsley Bay footbridge in Sydney Harbor, Australia [4]. This location was chosen because the bridge had been previously used in a study on using GPS to monitor structural deformation. When compared, the LocataNet provided sub-centimeter level accuracy comparable to the GPS case. Poor geometry led to larger positioning errors in the vertical plane, and shows the importance of geometry in obtaining precise measurements.

1.7 Thesis Overview

Chapter 2 covers the relevant background theory needed to accomplish this research. The topics covered in Chapter 2 include a basic overview of GPS and how it is used in precision approaches and landings, a comparison between pseudolite and GPS based reference systems, least squared estimation techniques, and the impact of geometry on GPS and pseudolite systems. Chapter 3 will detail the methods used in developing the Geometric Normalized Accuracy of Position (GNAP) plot, and the reason for its development. Also included in Chapter 3 will be a section describing the batch least squares simulator which will be used in this thesis, and another section which discusses the results of a Monte Carlo analysis on a sample simulation. Chapter 4 will be an in depth description of each family of simulations and the results from each test run. Lastly, Chapter 5 will draw conclusions from the results of this research and offer recommendations for future research in pseudolite deployment optimization.

II. Background

2.1 Overview

This section begins with a discussion on GPS signals and how they are used to compute position solutions. This is followed by an introduction into pseudolite technology and comparisons between pseudolites and GPS. Next, the specific pseudolites that are used in this research known as Locatalites, are described. The last section of this chapter details the batch least squares iteration technique used to calculate the position solutions.

2.2 GPS Signals

2.2.1 GPS Basics

GPS signals are transmitted from a constellation of satellites orbiting the planet at a distance roughly three times the radius of the Earth. These satellites transmit two types of encoded Pseudo-Random Noise (PRN) signals down to receivers around the globe. This is done on two frequencies. The first frequency is L1 (1575.42 MHz) which contains both the Precise Code (P-code) and the Coarse-Acquisition Code (C/A-code). Transmitted with the L1 frequency is the L2 frequency (1227.60 MHz) that carries only the P-code. When GPS satellites transmit these signals down to the receivers they also transmit navigation data that includes the satellites ephemeris data, which can be used to determine position at the time of signal reception (by the ground receiver). Receivers compare the PRN-code that they create internally to the PRN-code transmitted by the satellites. This comparison is what allows the receiver to judge the difference in time

between the satellite transmission and the reception of the signal. The time difference, coupled with the known speed of light, allows the receiver to determine its range in relation to the satellite that transmitted the code. However, this data does not give the true range of the receiver to the satellite, because it also includes clock errors. The true range is found by adjusting the original "pseudorange" measurement for clock and environmental errors. Another measurement that receivers can use to calculate the true position is called the carrier-phase measurement. Carrier-phase measurements are much more precise (on the order of centimeters) than pseudorange measurements, and are found by tracking the phase component of the carrier signal. With this type of measurement one must know the integer number of signal cycles that occurred before the time of signal reception to solve the equation. Once the integer ambiguities are determined, the carrier-phase measurement can be found by simply dividing the phase by the wavelength of the signal. A more thorough discussion on GPS fundamentals can be found in [17].

2.2.2 Pseudorange Measurements

The following equation represents the pseudorange measurement, which can also be called "code" measurements [17]:

$$\rho = r + c(\delta t_u - \delta t_{sv}) + T + I + m_\rho + v_\rho \tag{2.1}$$

Where:

ρ = pseudorange measurement (meters)

r = true range from the transmitter to the receiver (meters)

c = the speed of light (meters/second)

δt_u = receiver clock error (seconds)

δt_{sv} = transmitter clock error (seconds)

T = troposphereic error (meters)

I = ionospheric error (meters)

m_ρ = pseudorange multipath error (meters)

v_ρ = pseudorange receiver noise error (meters)

The pseudorange measurement is the uncorrected range between the transmitter and receiver. Tropospheric and Ionospheric errors deal with the fact that the electromagnetic signal transmitted by the satellites change speed and direction upon entering a denser medium. Multipath errors take into account that some portions of the signal may bounce off local objects and arrive at the receiver at different times. Noise error involves the random noise that the receiver may have in its internal workings. By far the largest errors come from imprecision in the transmitter and receiver clocks. This is due to the high magnitude of the speed of light, which takes a nanosecond clock difference and translates it to about a foot of error. The satellite clock error is very small because each satellite is equipped with an atomic clock which is very precise, and the satellite clock errors are modeled and transmitted to the user. However, most receivers have cheaper and comparatively imprecise clocks. Therefore, the receiver clock error must be removed or accounted for via differencing or estimation.

2.2.3 Carrier-Phase Measurements

Pseudorange measurements are easier to conceptualize than carrier-phase measurements; however they are less precise and usually result in measurements that have errors in the meter range. Carrier-phase measurements are much more precise and can be described as [17]:

$$\phi = \frac{1}{\lambda}\left(r + c(\delta t_u - \delta t_{sv}) + T - I + m_\phi + v_\phi\right) + N \qquad (2.2)$$

Where:

ϕ = carrier phase measurement (cycles)

λ = signal wavelength (cycles/meter)

r = true range from the transmitter to the receiver (meters)

c = the speed of light (meters/second)

δt_u = receiver clock error (seconds)

δt_{sv} = transmitter clock error (seconds)

T = tropospheric error (meters)

I = ionospheric error (meters)

m_ϕ = pseudorange multipath error (meters)

v_ϕ = pseudorange receiver noise error (meters)

N = integer ambiguity (cycles)

The carrier phase equation is very similar to the pseudorange equation in terms of its errors. Note that, like the pseudorange equation, the carrier phase equation has multipath, noise, tropospheric, ionospheric, and clock error terms. The addition of the signal wavelength is to convert the units of the of the right hand side of the equation from meters to cycles so as to match the units of the carrier phase measurement. The integer ambiguity is another new term whose function is to correct the equation for the number of cycles that have passed in the signal by the time of reception.

2.2.4 Single Differencing

A technique known as single differencing is often used to reduce or eliminate some of the errors in either the pseudorange or carrier-phase measurements, allowing the receiver to solve for the true range between it and the transmitter. Single differencing uses linear combinations of similar measurements (such as between two transmitters, two receivers, or two times) to eliminate common error terms. Equation (2.3) is the formula for single differencing between two pseudolite transmitter pseudorange measurements.

$$\nabla\rho_A^{12} = \rho_A^1 - \rho_A^2 \tag{2.3}$$

In Equation (2.3) the $\nabla\rho_A^{12}$ term represents the single difference operation between the pseudorange measurement from transmitter 1 to receiver A (ρ_A^1), and the pseudorange measurement from transmitter 2 to receiver A (ρ_A^2). Expanding Equation (2.3) using Equation (2.1) yields the following equation:

$$\nabla\rho_A^{12} = r_A^1 + c(\delta t_{uA}^1 + \delta t_{pl}^1) + T_A^1 + I_A^1 + m_{\rho A}^1 + v_{\rho A}^1 - (r_A^2 + c(\delta t_{uA}^2 + \delta t_{pl}^2) + T_A^2 + I_A^2 + m_{\rho A}^2 + v_{\rho A}^2) \tag{2.4}$$

When like terms in Equation (2.4) are combined, the receiver clock error (which is the same for both pseudorange equations) is eliminated, yielding:

$$\nabla\rho_A^{12} = (r_A^1 - r_A^2) + c(\delta t_{pl}^1 - \delta t_{pl}^2) + (T_A^1 - T_A^2) + (I_A^1 - I_A^2) + (m_{\rho A}^1 - m_{\rho A}^2) + (v_{\rho A}^1 - v_{\rho A}^2) \tag{2.5}$$

Since each measurement is taken in reference to the same receiver, the differences can be rewritten with the ∇ symbol as in Equation (2.6):

$$\nabla\rho_A^{12} = \nabla r_A^{12} + c\nabla\delta t_A^{12} + \nabla T_A^{12} + \nabla I_A^{12} + \nabla m_{\rho A}^{12} + \nabla v_{\rho A}^{12} \tag{2.6}$$

The same process used above can be used to remove the receiver clock error in the carrier phase measurement equation, which is shown below in Equation (2.7):

$$\nabla \phi_A^{12} = \frac{1}{\lambda}(\nabla r_A^{12} + c\nabla \delta t_A^{12} + \nabla T_A^{12} + \nabla I_A^{12} + \nabla m_{\phi A}^{12} + \nabla v_{\phi A}^{12}) + \nabla N_A^{12} \quad (2.7)$$

Using single differencing, "In the GPS case... will reduce the tropospheric error, but will increase the multipath and measurement noise by a factor of $\sqrt{2}$." [1]. A technique known as double differencing can also be used to further reduce Equations (2.6) and (2.7) by eliminating the transmitter clock error. Double differencing will also further reduce the atmospheric error terms and increase the multipath and noise errors. However the transceivers used in this study, invented by Locata, Inc., effectively eliminate the transmitter clock error, so double differencing techniques are not needed for most cases.

2.3 Pseudolites

2.3.1 Pseudolites versus GPS

Pseudo-satellites, termed pseudolites, are usually ground-based transmitters which transmit PRN signals that are very similar to GPS signals. Early in the GPS development process, pseudolites were used to test the signals and frequencies that would later be implemented on the satellites [14]. Other applications of pseudolite technology include using pseudolites in addition to GPS signals to get more precise navigation solutions [13,14], and using pseudolites independently from GPS to track in environments where GPS does not perform well (such as indoors or in a jamming environment) [2, 3, 4]. While the signals that are generated by pseudolites are very similar to GPS, they do not necessarily have to be either the L1 or L2 signal (unless they are specifically designed to interact with the GPS system). Some pseudolite systems are designed to operate with completely different chipping rates than GPS satellites, including the Locata reference system used in this research [2].

2.3.2 Pseudolite Equations

The equations for pseudolite reference systems are very similar to those for the GPS reference system. Listed below are the equations associated with the pseudolite pseudorange and carrier-phase measurements:

$$\rho = r + c(\delta t_u + \delta t_{pl}) + T + m_\rho + v_\rho \tag{2.8}$$

$$\phi = \frac{1}{\lambda}\left(r + c(\delta t_u - \delta t_{pl}) + T + m_\phi + v_\phi\right) + N \tag{2.9}$$

Notice that the ionospheric error has been removed because the pseudolite signals do not pass through the ionosphere.

2.3.3 Pseudolite Errors

Though pseudolites share similar signals with GPS, there are many differences between GPS and pseudolites, specifically when dealing with the errors associated with the pseudorange and carrier phase measurements.

2.3.3.1 Clock Errors

The first major error in pseudolite-based systems is that the transmitter clock error (in most pseudolites) can no longer be neglected as it is in the GPS satellites, because most pseudolites have simpler, cheaper, less precise internal clocks than the GPS satellites. Not knowing the precise transmit time will lead to very large position errors. When pseudolites are used to augment GPS, they can be synchronized to the clocks on board the GPS satellites, which would once again reduce the transmitter clock error to acceptable levels. However, for stand-alone pseudolite-based systems in an environment where GPS is unavailable (such as the one being used in this study), synchronization with the atomic clocks onboard the satellite is not an option. Double differencing techniques

can be used to eliminate the transmitter clock error [1]. Locata, Inc. has developed a novel way to deal with the transmitter clock error, which will be discussed in Section 2.4.

2.3.3.2 Atmospheric Errors

Ionospheric error can be completely neglected in most pseudolite equations because the path of the signal from transmitter to receiver never travels through the ionosphere. Tropospheric error can be a very large source of position error, and mostly occurs in the portion of the atmosphere between 0 km and 10 km. The pseudolite reference system used for this study will operate solely in this area of the atmosphere. As light passes through the troposphere, it is slowed down, and when one is dealing with a system in which centimeter level precision is desired, even the slightest delay could lead to large errors. The amount of delay is ultimately dependent on the density of the air (both "wet" and "dry") in the troposphere. The "dry" portion of the density causes about 90% of the delay while the "wet" air causes only 10% [1]. For GPS, the tropospheric dry air density can be predicted to about 1% at the zenith (90^o elevation angle). Unfortunately it is much harder to predict the wet air density, which is only predictable to 10-20% at zenith [1]. The tropospheric error is usually found at the zenith position and then mapped to other elevation angles using a mapping function. However, this method of determining tropospheric error is not sufficient for pseudolite applications, so alternative models must be used. Further reduction of tropospheric error can be achieved by differencing the measurement equations. For the simulations in this study, tropospheric error has been ignored in order to solely study the effects of geometric deployments on position solution.

2.3.3.3 Multipath

Multipath error is similar for both GPS and pseudolite systems. The problem stems from the "truth signal", which is supposed to travel directly from the transmitter to the receiver, being reflected off surrounding objects. These reflections cause an error because the same signal can hit the receiver from multiple reception paths [1]. This error increases when dealing with pseudolite systems (especially in indoor applications); because the path of the signal is more tangential to the ground and thus is more readily reflected off the surrounding ground clutter (such as trees, rocks, and buildings). For an example of a pseudolite system in a high multipath environment refer to [3]. Another factor that increases multipath error is the effect of differencing the measurements to reduce the clock and tropospheric error. When dealing with GPS, the satellites are in constant motion around the planet, so the multipath error tends to change over time. In most pseudolite systems the transmitters are at a fixed location, so the receiver can get a biased multipath. The biased multipath is called "standing multipath". Standing multipath is difficult to eliminate and to do so requires the use of special antennas and gain shaping techniques [8].

2.3.3.4 The Near-Far Problem

Another difference between GPS and pseudolites is the "near-far" problem, which defines the extreme ranges of a pseudolite reference system. If pseudolites in a network are positioned too closely to one another then the signals will begin to interfere with each other. Pseudolites placed too far from either each other or the receiver will not be able to maintain a lock on that object. An illustration of the near-far radii of a pseudolite network is shown in Figure 3. Obviously the near-far radii will change depending on the

type of pseudolite hardware that is used. The most common ways to reduce the near-far problem are to pulse the signal using Time Division Multiple Access (TDMA), reduce the interference using Frequency Division Multiple Access (FDMA), or to concatenate the C/A-codes in Code Division Multiple Access (CDMA). More information on the reduction of the near-far problem can be found in [8].

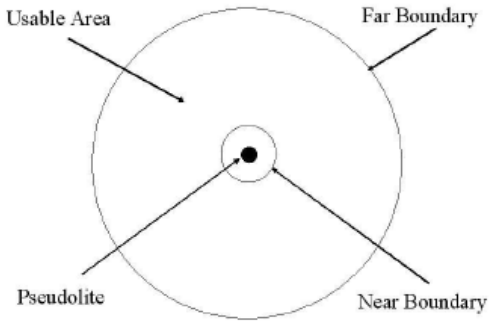

Figure 3: The Near Far Problem [8]

2.3.3.5 Transmit Positioning Error

Due to the fact that pseudolites are not in orbit around the planet they, "do not have orbital or ephemeris error, but rather a position error that is dependent on the type of surveying accuracy used to estimate the phase center of the pseudolite antenna," [8]. Lastly, because of the large distance between the GPS satellite and a GPS receiver, the GPS measurement model can be well approximated by a linear expression. With a pseudolite system, however, the receiver is much closer to the transmitters and thus the measurement model is more non-linear.

2.3.4 Geometry Effects

Proper transmitter geometry is crucial for precise measurement solutions. With GPS, the transmitters are located very far from the receivers on the ground, and the slant angles are usually favorable (between 10^{o}-90^{o}) in all directions. When a satellite is rising

or setting, its position relative to the receiver will appear to be near the horizon. At this point the slant angle is less than favorable; however, since there are other satellites, with better elevation angles visible to the receiver at any given time, the position error is generally not affected by a single satellite rising or setting. In fact the only time that GPS would yield poor positioning due to low elevation angles would be when all the measurements are at low elevation angles. To accommodate for possible bad GPS geometry, in a specific geographic area, pseudolites transmitting GPS type signals may be used [14]. This is especially useful when trying to track a receiver attached to a flying aircraft, because as the receiver is traveling above the transmitters, the slant angle is relatively good even if the GPS satellite geometry is poor [13].

As an augmentation to GPS, pseudolites have been shown to actually improve transmitter geometry [13, 14]. However, as a stand-alone system, pseudolites have large errors associated with the geometric deployment, especially in the vertical plane. This is due to the fact that in a ground-based pseudolite system most, if not all, the measurements are taken at low elevation angles. Proper deployment of the pseudolites in an area is crucial to getting precision positioning solutions.

2.4 Locatalites

Locata, Inc. has developed pseudolites that make centimeter level positioning solutions possible when using a pseudolite-based reference system [2, 3, 4, 5, 6, & 7]. Each pseudolite is in fact a transceiver, which allows the Locatalites to receive correcting signals from one another while transmitting. Several successful test case studies have been done over the past 5 years, which prove that LocataNet has the robustness and precision needed to implement a pseudolite only positioning system in environments in

which GPS does not perform. The goal of Locata, Inc. is to design a positioning system, independent of GPS, which could provide centimeter level positioning in areas where GPS is not available. At the same time, this system is also designed to be able to work with GPS to get better solutions when GPS is available. Figure 4 below shows a pictorial view of the Locata positioning concept [6].

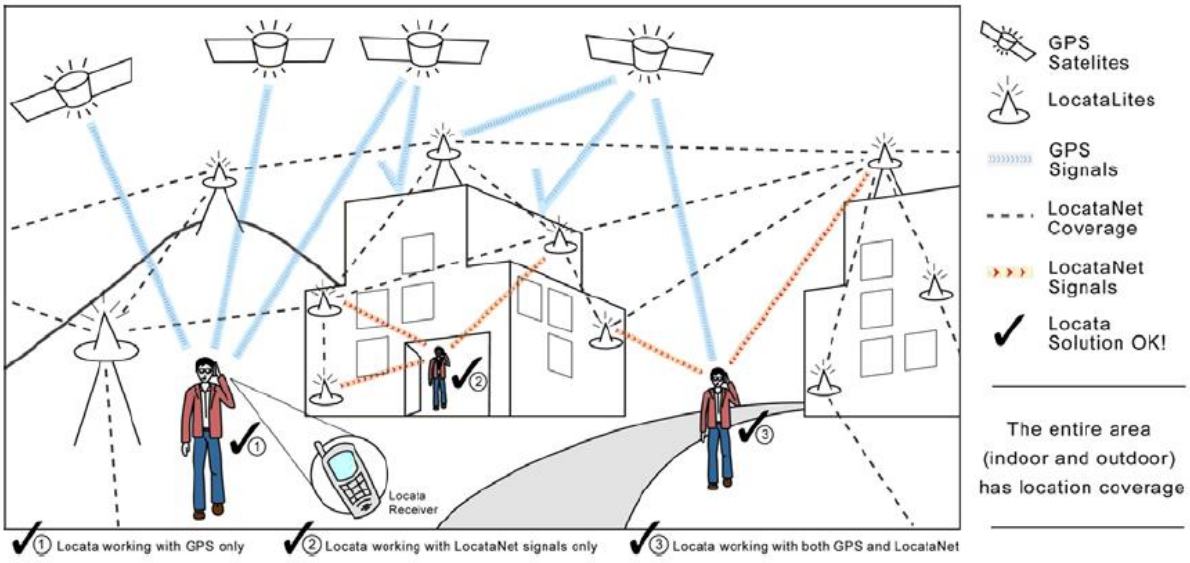

Figure 4: Locata Positioning Concept [6]

2.4.1 TimeLoc

What makes the Locata system so innovative is the Time-Loc technology, which synchronizes the clocks of all the Locatalites in the LocataNet to within 30 picoseconds [3]. This allows the transmitter clock error to be eliminated without having to use any differencing techniques. The TimeLoc process that synchronizes one Locatalite to another is explained in detail in the following steps [7]:

1. Locatalite A transmits a C/A code and carrier signal on a particular PRN code.
2. The receiver section of Locatalite B acquires, tracks and measures the signal (C/A code and carrier-phase measurements) generated by Locatalite A.

3. Locatalite B generates its own C/A code and carrier signal on a different PRN code to A.
4. Locatalite B calculates the difference between the code and carrier of the received signal and it's own locally generated signal. Ignoring propagation errors, the differences between the two signals are due to the difference in the clocks between the two devices, and the geometric separation between them.
5. Locatalite B adjusts its local oscillator using Direct Digital Synthesis (DDS) technology to bring the code and carrier differences between itself and Locatalite A to zero. The code and carrier differences between Locatalite A and B are continually monitored so that they remain zero. In other words, the local oscillator of B follows precisely that of A.
6. The final stage is to correct for the geometrical offset between Locatalite A and B, using the known coordinates of the Locatalites, and after this TimeLoc is achieved.

This TimeLoc process effectively reduces Equations (2.8) and (2.9) down to the following:

$$\rho = r + c\delta t_u + T + m_\rho + v_\rho \tag{2.10}$$

$$\phi = \frac{1}{\lambda}\left(r + c\delta t_u + T + m_\phi + v_\phi\right) + N \tag{2.11}$$

Notice that the transmitter clock error has been eliminated due to the TimeLoc synchronization of the LocataNet. This process can be applied to all the Locatalites in a network and only requires that each Locatalite know its exact position. Once TimeLoc is achieved the LocataNet operates independently of GPS.

2.4.2 Locata Signal Structure

Locata's signal, like the TimeLoc ability, is also unique to this system. The signal operates in the 2.4 GHz Industry Scientific and Medical (ISM) band and has a transmit power of up to 1 watt [2]. This transmit power allows a Locata to receive a signal from a Locatalite up to 10 kilometers away. The exact frequencies and PRN code information are proprietary information of Locata, but what is known is that they are completely

separate from the GPS frequencies and PRN codes (though they are similarly structured). The new signal makes the following possible [2]:

1. Interoperability with GPS and no licensing requirement.
2. Capability for On-The-Fly ambiguity resolution using dual-frequency measurement data.
3. Better multipath mitigation on code measurements due to higher 10MHz chipping rate, and theoretically less carrier phase multipath than GPS due to the higher frequency used.
4. Transmit power of up to 1 watt giving line-of-sight range of 10 kilometers.

Another benefit of the stronger Locata signal (which is several orders of magnitude stronger than GPS [2]) is that it is strong enough to penetrate the walls of most buildings. This ability allows a LocataNet to operate inside office buildings where line of sight communication may not be possible because of walls that separate rooms. This signal strength allows for a very large LocataNet to be built with the range to cover the span of a runway, which is imperative to creating a pseudolite network test environment for tracking a landing aircraft without GPS. More in depth descriptions of the hardware, software, and case studies that test the technology can be found in [2, 3, 4, 5, 6, & 7].

2.5 Batch Least Squares Estimation

The method of estimation used to find the measurements for this research will be non-linear batched Least Squares Estimation (LSE). The first part of this section will outline the basics of the LSE technique. Following that sub-section will be a discussion of non-linear LSE, followed by a definition of the batched LSE process. Lastly, Dilution of Precision (DOP) plots will be discussed along with how the plots are found using LSE techniques and their usefulness in measuring the geometry of a system.

2.5.1 Least Squares Estimation Basics

Least squares estimation is a powerful and common way to estimate the states (or characteristics) of a system given a set of measurements from some sort of observer. LSE is the estimation technique used in the simulator, developed by Amt [1] that is to be used in this research. The thing to keep in mind is that the desired result of the LSE is to find the position states of the receiver using the measurements from the pseudolite transmitter signal at each epoch in time. To begin the process of estimating the states, assume that there is a linear relationship between the measurements and the characteristics of the system as shown in Equation (2.12) [1]:

$$z = Hx + v \tag{2.12}$$

where:

z = the *m*-dimensional measurement vector

H = the *m x n* measurement matrix

v = is the *m*-dimensional error vector

x = the *n*-dimensional unknown state vector

In order to solve Equation (2.12), there must be more measurements (*m*) than there are states (*n*). If that is the case then Equation (2.12) is over-determined can yield many solutions. Only one solution will exist if $m = n$, and the solution will be under-determined, and unsolvable, if there are more states than measurements ($n > m$). In the case of GPS and pseudolite-reference systems, it is very rare that $n > m$, because by design the systems have more measurements than states. Another condition for being able to solve Equation (2.12) is that **H** must be completely observable, meaning **H** must be of rank *n* [1].

The premise behind the LSE method is that it minimizes the difference between the measurements and an estimate (or educated guess) of the measurements of the unknown states **x** and the known characteristic matrix **H**. The LSE scalar error term (**J**), which is to be minimized, is defined as the following [1]:

$$J = (z - Hx)^T (z - Hx) \tag{2.13}$$

To minimize the difference between the estimated and known measurements, the derivative of **J** is taken with respect to **x** and then set equal to zero. The unknown state matrix **x** is then solved for in the resulting equation, yielding the following [1]:

$$\hat{x} = (H^T H)^{-1} H^T z \tag{2.14}$$

If **H** does not have a rank of *n* then $(\mathbf{H^T H})^{-1}$ will be singular and non-invertible, which would mean that Equation (2.14) could not be solved.

To be as precise as possible, it is important to have as much information about the system as possible. This includes adjusting the error vector from Equation (2.12) to include measurement errors, which in this case is modeled as zero-mean, Gaussian noise with a covariance matrix **R**, where [1]:

$$R = E\{vv^T\} \tag{2.15}$$

This measurement covariance matrix, **R**, is used to account for the errors that are to be expected in the measurements, along with any correlation between measurement errors. With this new term in the LSE process, Equation (2.14) now becomes [1]:

$$\hat{x} = (H^T R^{-1} H)^{-1} H^T R^{-1} z \tag{2.16}$$

Notice that the unknown state vector is now a function of the error covariance matrix, which accounts for the measurement errors. This yields a more precise estimate for the

unknown states. This method, which accounts for the errors in measurements, is called Weighted Least Squares Estimation

2.5.2 Non-linear Least Squares Estimation

Many real life situations cannot be simply represented by the linear approach used in Section 2.5.1. Therefore, it is necessary to solve for the non-linear representation of the states which is shown below [1]:

$$z = h(x) + v \tag{2.17}$$

In Equation (2.17), h(**x**) cannot be assumed to be linear, so linear LSE cannot be used. It is now necessary to use iterative linearization techniques to solve for the estimated state vector. Iterative Least Squares Estimation (ILS) involves taking an initial estimate of the state vector $\hat{x}_o$ and then uses those initial guesses to find the corrected state measurement $\hat{x}_c$, which becomes the new initial state vector for the next iteration. The following formula is used to create the corrected state estimate [1]:

$$\hat{x}_c = \hat{x} + \Delta\hat{x} \tag{2.18}$$

In Equation (2.18) $\Delta\hat{x}$ is the estimated error in the state vector estimate. The difference between the actual measurements, represented by vector **z**, and the current state estimate $\hat{x}$ is known as the measurement residual, and can be shown in the following relationship [1]:

$$\Delta z = z - h(\hat{x}) \tag{2.19}$$

Equation (2.19) can be expanded to relate the measurement residual to the state correction Δx. This expansion is shown in Equation (2.20) [1]:

$$\Delta z = H\Delta x + v \tag{2.20}$$

The characteristic matrix, **H**, is also known as the sensitivity matrix, and in this case **H** is the matrix of partial derivatives evaluated from the current state estimate. An equation form of **H** is shown in Equation (2.21) [1].

$$H = \left.\frac{\partial h(x)}{\partial x}\right|_{x=\hat{x}} \tag{2.21}$$

As in the linear case, **H** is an *m* x *n* matrix which relates the states to the measurements. Using **H**, **R**, and $\Delta\mathbf{z}$ it is now possible to solve for the estimated state error vector can now be calculated to be [1]:

$$\Delta\hat{x} = (H^T R^{-1} H)^{-1} H^T R^{-1} \Delta z \tag{2.22}$$

Notice that Equation (2.22) looks very similar to Equation (2.16). In Equation (2.22) the sensitivity matrix, **H,** must be re-evaluated for all iterations at the current state estimate. The iterative process repeats until the solution converges, where convergence is indicated when the state estimate $\Delta\hat{x}$ becomes sufficiently small.

2.5.3 Batch Least Squares Estimation

In the ILS technique described above, the states and measurements are evaluated at each separate epoch. However, there are many terms in the measurements that are common for every epoch. An example of such a term is the integer ambiguity. The batch process considers all the states and measurements over all measurement times together [2]. This means that the states and measurements are not constrained to a single time epoch. By using the batch process, the ambiguity terms, and other common terms between epochs, can be estimated in the correct manner.

2.5.4 Dilution of Precision

Dilution of Precision, otherwise known as DOP, is a relationship between the measurement errors and position errors. Position errors are very dependent on the measurement geometry and thus DOP, or some variant of DOP, will be crucial for evaluating the geometry of a given pseudolite deployment.

Mathematically, the covariance matrix of measurements, **R**, has already been described in Section 2.5.3 and is thus defined as:

$$R = \begin{bmatrix} \sigma_{\rho 1}^2 & \sigma_{\rho 1 \rho 2} & \cdots & \sigma_{\rho 1 \rho n} \\ \sigma_{\rho 1 \rho 2} & \sigma_{\rho 2}^2 & \cdots & \sigma_{\rho 2 \rho n} \\ \vdots & \vdots & \ddots & \sigma_{\rho 3 \rho n} \\ \sigma_{\rho 1 \rho n} & \sigma_{\rho 2 \rho n} & \sigma_{\rho 2 \rho n} & \sigma_{\rho n}^2 \end{bmatrix} \tag{2.23}$$

The covariance matrix for the positions ($\mathbf{C_x}$) is defined as follows:

$$C_x = \begin{bmatrix} \sigma_{xu}^2 & \sigma_{xuyu} & \sigma_{xuzu} & \sigma_{xu\delta tu} \\ \sigma_{xuyu} & \sigma_{yu}^2 & \sigma_{yuzu} & \sigma_{yu\delta tu} \\ \sigma_{xuzu} & \sigma_{yuzu} & \sigma_{zu}^2 & \sigma_{zu\delta tu} \\ \sigma_{xu\delta tu} & \sigma_{yu\delta tu} & \sigma_{zu\delta tu} & \sigma_{\delta tu}^2 \end{bmatrix} \tag{2.24}$$

From LSE theory [17], the following relation between Equations (2.23) and Equation (2.24) exists:

$$C_x = (H^T R^{-1} H)^{-1} \tag{2.25}$$

Equation (2.25) can therefore be inserted into Equation (2.22), which would yield the following equation:

$$\Delta \hat{x} = C_x H^T R^{-1} \Delta z \tag{2.26}$$

Notice that the $\mathbf{C_x}$ matrix is a multiplier of the $\Delta\mathbf{z}$ term, which is in fact the measurement error. Therefore, assuming that the measurement error remains constant, if $\mathbf{C_x}$ is "large" then the position error will be large and if $\mathbf{C_x}$ is "small" then the position error is small.

In GPS, the covariance matrix of position and clock error is used to develop the DOP that can be used, as described above, as a quantitative method for evaluating deployment geometry. There are some key assumptions made during this process. The first assumption is that all the measurements in the **R** matrix have the same variance. In other words the diagonal terms of the **R** matrix are all equal to each other. Secondly, DOP assumes that the measurement errors are uncorrelated, which means that the off-diagonal terms of the **R** matrix are zero. Using these assumptions, Equation (2.23) reduces down to:

$$R = I\sigma_\rho^2 \tag{2.27}$$

Where **I** is the identity matrix and the σ term is a scalar, white noise term. Substituting Equation (2.27) into Equation (2.25) yields the following relationship:

$$C_x = (H^T H)^{-1}\sigma_\rho^2 \tag{2.28}$$

The matrix $\mathbf{(H^T H)^{-1}}$ is referred to as the DOP matrix, which directly relates the measurement errors σ_ρ to the position errors C_x.

It is important to note the assumptions that are made in the derivation of DOP. In GPS positioning these assumptions are acceptable; however, they may not be applicable to pseudolite-based reference systems due to the many differences between GPS and pseudolite systems. This will be discussed in depth in the next chapter.

2.6 Summary

An introduction into both GPS and pseudolite technology has been discussed. The Locata reference system has also been described in detail. Lastly, the iterative batch LSE process used in research has been described in detail, along with an explanation of DOP. The next chapter will discuss the Matlab® simulation used in this research along with a DOP alternative and a Monte Carlo analysis which was run on the simulation.

III. Methodology

3.1 Overview

This chapter covers the development of the tools needed to conduct a study into the effects that geometry has on position error. Immediately following the chapter overview will be a section on the Locata batch LSE simulator (developed by John Amt) which has been modified, for use in this research, to simulate various LocataNet configurations tracking a landing aircraft. The second section will cover the development of the simulation parameters used as inputs to the Locata simulator, including the East/North test simulation (ENtest) which produces a LocataNet deployment which is used as a global geometry for all other simulations. Following the simulator parameters discussion will be a section showing the results of a Monte Carlo analysis on the ENtest simulation which will statistically validate the data generated by this simulator. Lastly, there will be an in-depth discussion on the development of the Geometric Normalized Accuracy of Position (GNAP), and why it is used in this research instead of DOP.

3.2 The Locata Simulator

The Locata simulator that is used for this research can be described using the block diagram shown in Figure 5. Before the simulation parameters can be entered into the simulator, they must first be generated in Matlab®. Among other things, these simulation parameters consist of the glide slope truth trajectory of the mobile receiver, the positions of each Locatalite in the LocataNet, and the measurement noise. There are

a variety of assumptions that are made about the simulation parameters used in this research, which will isolate the effects of geometry on the final position:

1. The receiver's trajectory remains constant for all tests
2. There is no clock error due to the TimeLoc technology, and the differencing of the carrier phase measurements.
3. The measurement noise, $\sigma = 0.01$ meters for all tests
4. There are no cycle slips used in these simulations.
5. The ambiguities are assumed to be known for all tests except for the "real world" orbiting aircraft study.

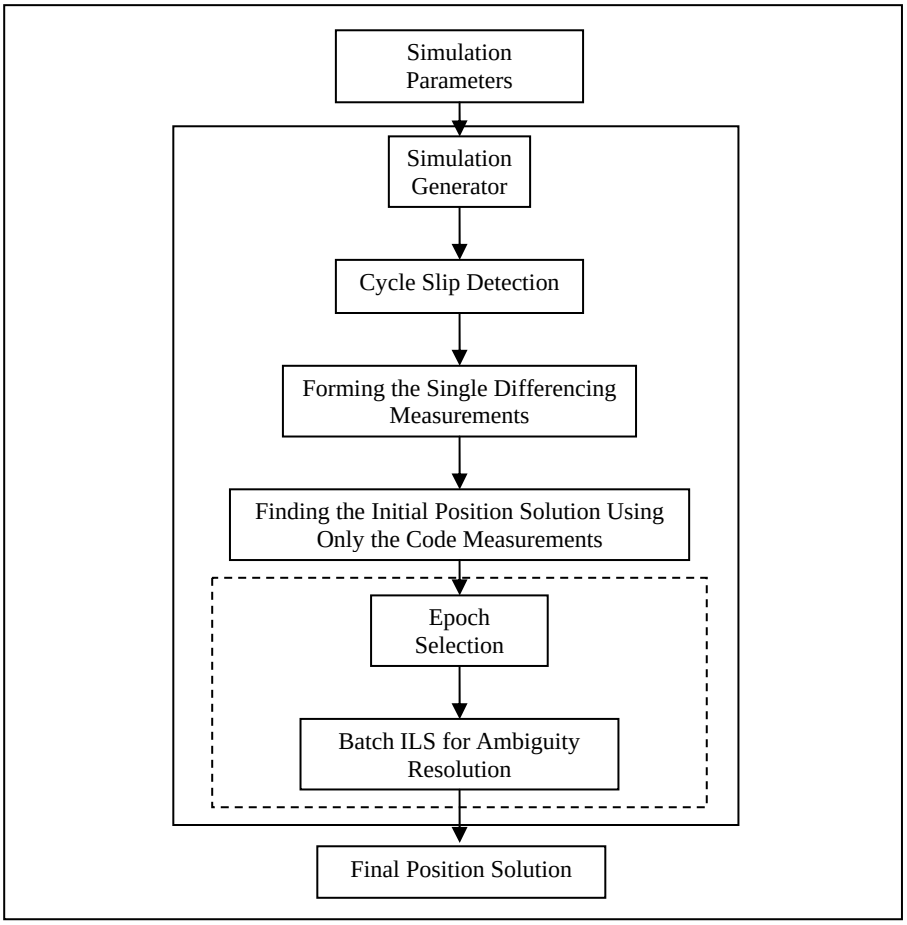

Figure 5: Locata Simulation Flow Chart

With the simulation parameters prepared, they are now ready to be passed into the simulator. The first step is the simulation generator, which generates the simulated measurements. These simulated measurements are then passed through a program that is used to detect any cycle slips in the system. For this research, it is assumed that there are no cycle slips, so the simulated measurements pass through the cycle slip detection program and into an algorithm that forms the single difference measurements. These single difference measurements are then passed on to an algorithm that finds the initial position solution using only the code (or pseudorange) measurements. Recall that the code measurements are much less precise than the carrier-phase measurements. However the code measurements are easier to solve for, and in this simulator it is necessary to solve for the initial position using the code measurements in order to find the more precise solution using carrier-phase measurements. Once the initial position solution is found, it is now possible to initialize the iterative batch LSE technique to solve for the carrier phase ambiguities. Notice that in Figure 5, the Epoch Selection and Batch ILS portions of the simulator are blocked off with a dotted line. This blocked, dotted line section is skipped for all tests done in this research except for the "real life" orbiting aircraft test, due to the fact that, except for the "real life" orbiting aircraft test, the ambiguities have been assumed to be known. With the carrier-phase measurements now calculated from the Batch ILS, it is now possible to find the final position solution for the system. This solution is computed epoch by epoch, so other than the use of the initial code measurement generated position to start the process; none of the position solutions are dependent on the solution before it. For more information on the simulation process see [2].

3.3 Pre-Simulation Development

As mentioned in section 3.2, there are several parameters that need to be created as inputs to the Batch LSE simulator. Two of those inputs are the positions of each Locatalite in the LocataNet, and the glide slope trajectory of the landing receiver.

3.3.1 Glide Slope Development

The glide slope used for this experiment is designed for a small landing aircraft. Based on prior research [10], the receiver aircraft's approach angle is the standard approach glide angle used in most air traffic control schemes, which is 3^{o} from ground level. Aircraft landing speed is 25 knots during the descent to simulate a small UAV's approach velocity. Using that airspeed the aircraft takes 257 seconds (about 4 minutes 16 seconds) and just under 3,000 meters to descend from 152 meters (500 feet). After touchdown there is a short rollout period, which is included in the glide slope trajectory so that the "on the ground" geometry can be studied. It should be noted that most aircraft would need more than the allotted space to complete rollout. For simplicity purposes the "runway" begins when the aircraft begins its descent from 500 feet and ends shortly after the rollout. It should be noted that although this research calls this area the runway, an aircraft would start its descent well before the actual tarmac landing strip traditionally known as a runway. Figure 6 shows the modeled approach, touchdown and rollout of the receiver that from here on will be known as the glide slope.

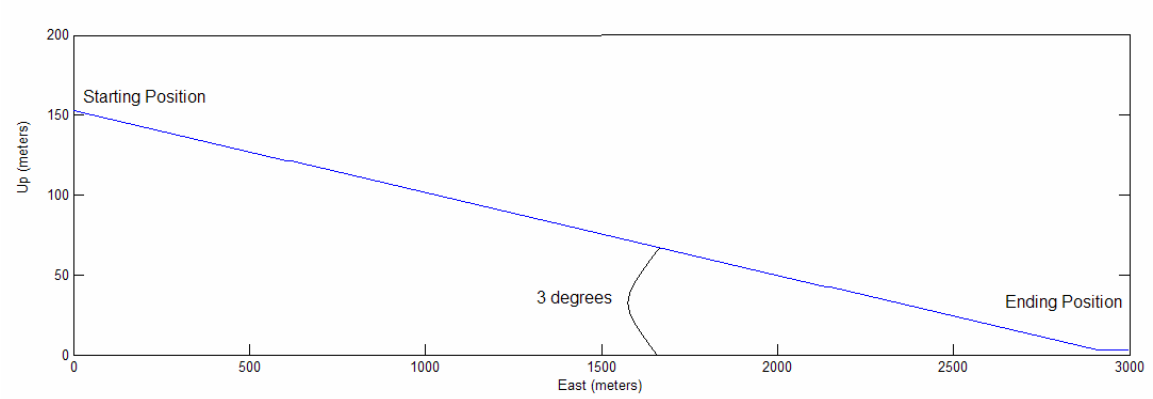

Figure 6: Glide Slope Trajectory of the Receiver

It should be noted that the receiver antenna would be located underneath the undercarriage of the aircraft, not the wheels, and thus the glide slope appears to not actually touch down but hover about 3 meters above the ground.

3.3.2 East/North Verification Test

Recall that the focus of this thesis is to investigate methods of geometric improvement in the vertical range for tracking an aircraft that is close to the ground. In order to assure that the results of the simulations are not skewed by bad horizontal geometry, it is first necessary to find a reasonably good geometry in the horizontal plane. Several different horizontal geometries were simulated to see which would yield the best horizontal geometry. Of these geometries the one that produced the best geometric values in the East and North directions was the rectangular deployment displayed in Figure 7.

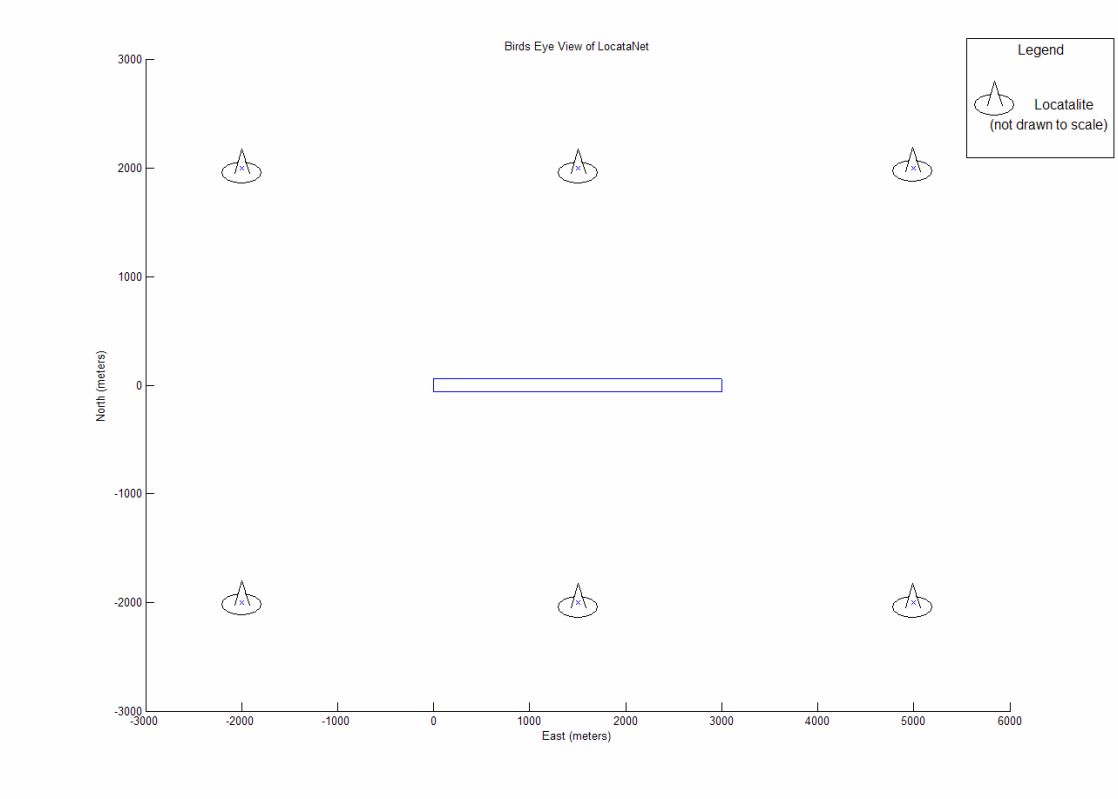

Figure 7: Rectangular Deployment of the LocataNet

The rectangular configuration of the in Figure 7 shows that the Locatalites are deployed about two kilometers away from the runway in the North and East directions. This is to ensure that the runway is completely encompassed by the LocataNet. It should also be noted that none of the Locatalites in this deployment are elevated above the ground level, which lead to extremely poor vertical geometry. This geometry is so poor that a Locatalite needs to be placed in the center of the LocataNet at an altitude of 200 kilometers in order to ensure that the simulation would converge on a solution. This high altitude Locatalite does not affect the horizontal plane; it simply allows the simulation to be run in the LSE simulator. Once the quality of the horizontal plane geometry is assured, the high altitude Locatalite will be removed from this global LocataNet (leaving just the six ground based Locatalites).

3.4 The Monte Carlo Analysis

Before the simulator can be used as a tool for studying geometric effects it must be confirmed that the calculated standard deviations from the Covariance matrix, $\mathbf{C_x}$, match the standard deviation of the position errors. To do this, a statistical tool known as a Monte Carlo analysis is preformed. A Monte Carlo analysis runs a simulation multiple times and plots the mean and standard deviation of the data from each run. The mean of the position errors should average to zero over a number of simulations, and the standard deviation of the position errors should match the calculated standard deviations from the diagonals of the $\mathbf{C_x}$ matrix. In this case, a Monte Carlo analysis of 100 runs is conducted on the ENtest simulation's position errors in the East, North and Up directions. The results of this Monte Carlo analysis can be seen in Figure 8.

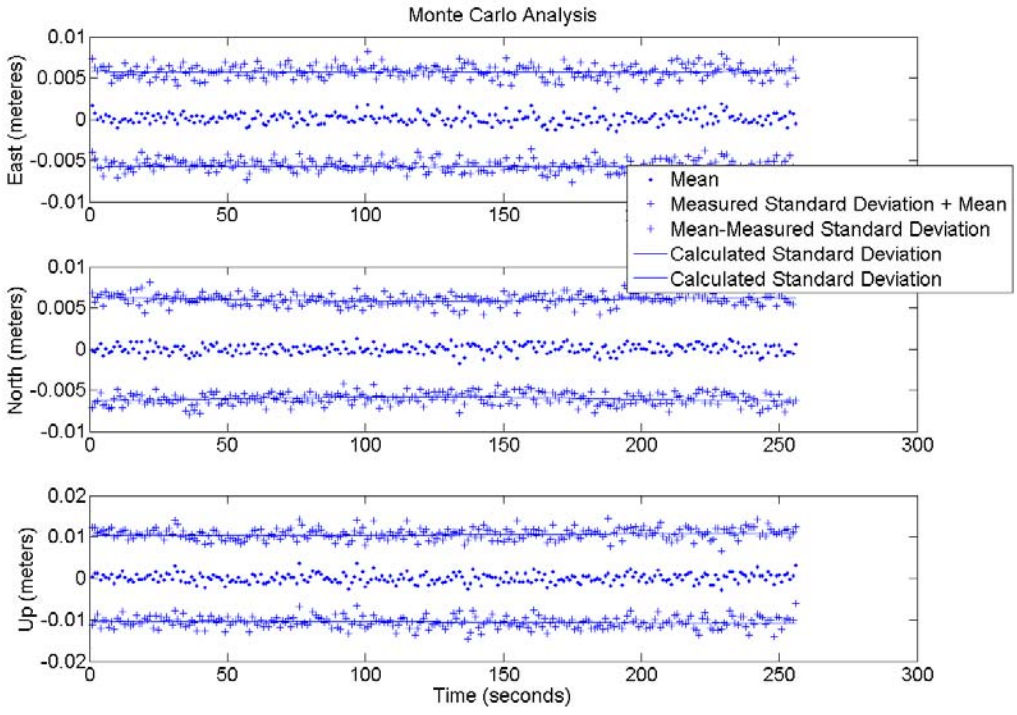

Figure 8: Results from a 100 run Monte Carlo Analysis Conducted on the ENtest Simulation

As can be seen from Figure 8 there is a nearly zero mean position error and more importantly, the standard deviations from the mean of the position errors closely follow the calculated standard deviations. This therefore proves that the simulator is producing results that match what is expected from theoretical calculations.

3.5 GNAP Development

3.5.1 Where DOP Fails

The Geometric Normalized Accuracy of Precision is very similar to the more traditionally used DOP in that both are used as a relative gauge of the reference system's deployment to the receiver. However, DOP has a flaw in the fact that it relies on the assumption that the off-diagonal terms of the **R** matrix are zero. This assumption is not true for the simulations used in this research. Therefore it is necessary to create a new relation, based on the same principles of DOP, in which the **R** matrix off-diagonal terms are non-zero.

To illustrate why DOP should not be used, consider the DOP plots for the ENtest simulation shown in Figure 9. According to DOP theory, described in Section 2.5.4, multiplying the DOP by the single difference measurement error ($\sigma = 0.01*\sqrt{2}$) should give the standard deviation of the position error. Table 1 compares the standard deviation of the DOP position error, calculated using the DOP value of the first epoch for each state, to the mean position error standard deviation calculated from the Monte Carlo analysis conducted in Section 3.4.

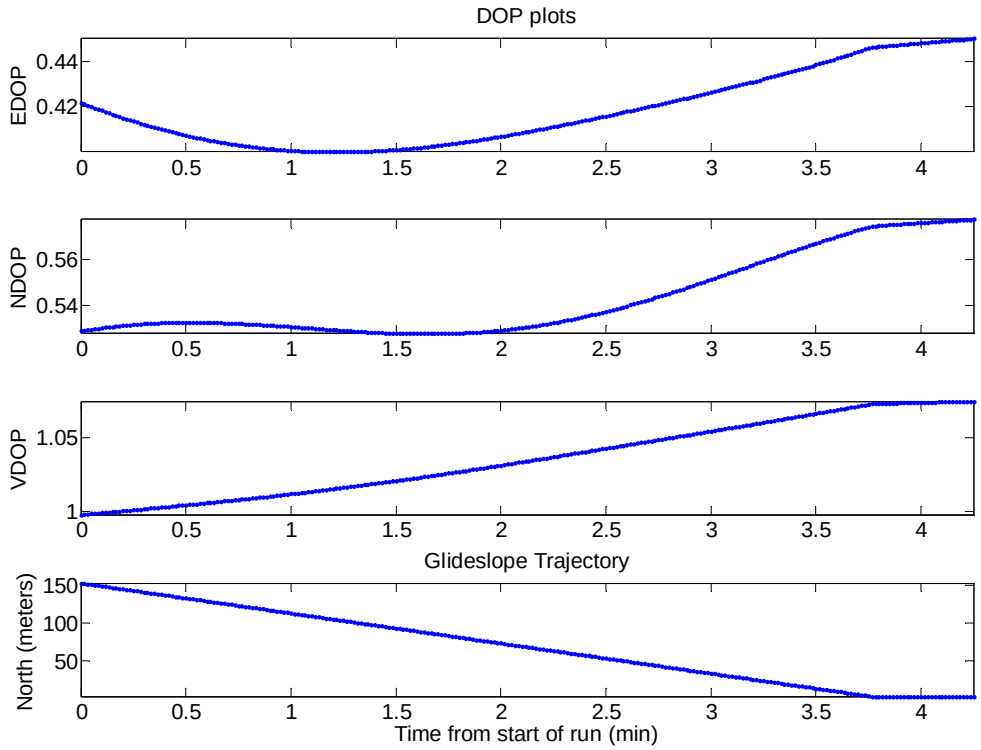

Figure 9: ENtest DOP Plots

Table 1: Comparison between DOP and Monte Carlo Standard Deviations for the ENtest Simulation

State	$DOP_{Epoch\ 1}$	STD of Position $Error_{DOP\_1}$ (m)	STD of Position $Error_{MC}$ (m)
East	0.422	0.0060	0.0057
North	0.529	0.0075	0.0061
Up	0.998	0.0141	0.0107

As can clearly be seen in Table 1 the standard deviations of the position errors calculated using the DOP values do not match the standard deviations of the position errors found using the Monte Carlo analysis. It can reasonably be concluded that the difference between the standard deviations is a result of DOP assuming that the off-diagonal terms of the **R** matrix are zero. GNAP accounts for these off diagonal terms.

3.5.2 GNAP Definition

Recall from Equation (2.25) that the state covariance matrix, $\mathbf{C_x}$, is formed by $(\mathbf{H^T R^{-1} H})^{-1}$, and that DOP assumes that the off diagonal terms of the **R** matrix are zero. In the single difference case the off diagonals are non-zero and are actually one half of the diagonal terms. This is due to the fact that carrier phase cross covariances are assumed to be half of the carrier phase variance due to the fact that half of the measurements are in common due to differencing [1]. The **R** matrix for this case is thus formed by the following equation:

$$R = \begin{bmatrix} \sigma_\phi^2 & \frac{1}{2}\sigma_\phi^2 & \cdots & \cdots \\ \frac{1}{2}\sigma_\phi^2 & \ddots & \ddots & \ddots \\ \vdots & \ddots & \ddots & \ddots \\ \vdots & \ddots & \ddots & \ddots \end{bmatrix}$$

$$\sigma_\phi = \frac{0.01 * \sqrt{2}}{\lambda} \tag{3.1}$$

Note that for all tests the white noise (σ) will be 1 centimeter, which is then divided by the wavelength to put σ in units of cycles. The $\sqrt{2}$ term is a result of the single differencing of the measurements. To find the GNAP, take the square roots of the main diagonal terms of the Cx matrix, also known as the state variances, and normalize them by the measurement noise in this case 0.01 meters. This normalization removes the impact of the Gaussian noise on the $\mathbf{C_x}$ matrix and thus allows that matrix to be used as a relative measure of the system geometry even with the off diagonal, non-zero terms in the **R** matrix.

3.5.3 Analytical GNAP Demonstration

To show that GNAP can be used as a viable alternative to DOP in these simulations, take the case a receiver is placed at the origin of a 3-D space defined by the East, North, and Up vectors. This receiver remains in that position throughout time. Surrounding this receiver are six Locatalites that are arranged in the LocataNet shown whose coordinates are shown in Table 2:

Table 2: LocataNet for GNAP Proof

PRN #	East	North	Up
1	0	-10	0
2	0	10	0
3	10	0	0
4	-10	0	0
5	0	0	10
6	0	0	-10

For this demonstration, the base (or reference) Locatalite will be PRN #1. Neglecting tropospheric, multipath, and noise errors, the equation for the carrier phase measurements between a Locatalite (superscript *i*) and the receiver (subscript *r*) becomes:

$$\phi_r^i = \frac{1}{\lambda}(r_r^i + c\delta t_r) \tag{3.2}$$

Now when Equation 3.2 is single differenced with respect to the base Locatalite, the following single difference relationship is found:

$$\nabla \phi_r^{1i} = \frac{1}{\lambda}(r_r^1 - r_r^i) \tag{3.3}$$

Notice that the receiver clock error has now been eliminated from Equation (3.2) and the carrier-phase measurement is now solely a function of the Euclidean ranges between each Locatalite and the receiver.

$$r_r^i = \sqrt{(E_i - E_r)^2 + (N_i - N_r)^2 + (U_i - U_r)^2} \tag{3.4}$$

Where:

E_i = East Coordinate of LocataLite PRN # "i"

E_r = East Coordinate of the Reference LocataLite

N_i = North Coordinate of LocataLite PRN # "i"

N_r = North Coordinate of the Reference LocataLite

U_i = Up Coordinate of LocataLite PRN # "i"

U_r = Up Coordinate of the Reference LocataLite

A carrier-phase measurement is made for each single difference between the reference Locatalite and another Locatalite. So for this example there will be five single differenced carrier-phase measurements stored in the following vector:

$$\vec{h}(x) = \begin{bmatrix} \nabla \phi_r^{12} \\ \nabla \phi_r^{13} \\ \nabla \phi_r^{14} \\ \nabla \phi_r^{15} \\ \nabla \phi_r^{16} \end{bmatrix} \tag{3.5}$$

Where (x) represents the ENU coordinates of the receiver:

$$x = [E_r, N_r, U_r] \tag{3.6}$$

Recall from Equation (2.21) that the **H** matrix is composed of the partial derivatives of the **h(x)** vector in Equation (3.5) with respect to Equation (3.6). A sample derivative of the $\mathbf{h_{11}(x)}$ term with respect to E_r would yield the following:

$$\frac{\partial h_{11}}{\partial E_r} = \frac{1}{\lambda}\left[\frac{-(E_1 - E_r)}{r_r^1} + \frac{(E_2 - E_r)}{r_r^2}\right] = \frac{-e_E^1 + e_E^2}{\lambda} \tag{3.7}$$

This sample derivative would form the $\mathbf{H_{11}}$ term in the 5 x 3 H matrix. Where the rows correspond to the single differenced rows in Equation (3.5) and the columns correspond to the East, North, and Up coordinate variables. Note that in Equation (3.7) the term *e* represents a unit vector. Going through this process for each differenced pair results in the following **H** matrix:

$$H = \begin{bmatrix} \frac{-e_E^1 + e_E^1}{\lambda} & \frac{-e_N^1 + e_N^1}{\lambda} & \frac{-e_U^1 + e_U^1}{\lambda} \\ \vdots & \vdots & \vdots \\ \frac{-e_E^1 + e_E^6}{\lambda} & \frac{-e_N^1 + e_N^6}{\lambda} & \frac{-e_U^1 + e_U^6}{\lambda} \end{bmatrix} \tag{3.8}$$

Using the **H** and **R** matrices from Equations (3.1) and (3.8) in this example yields the following $\mathbf{C_x}$ matrix:

$$C_x = \begin{bmatrix} 0.000025 & 0 & 0 \\ 0 & 0.000025 & 0 \\ 0 & 0 & 0.000025 \end{bmatrix} \tag{3.9}$$

The GNAP values for each state can easily be found by taking the square roots of the diagonals of the $\mathbf{C_x}$ matrix in Equation (3.9) and then dividing them by the measurement noise standard deviation (0.01). The GNAP values for this demonstration are shown in Table 3.

Table 3: GNAP Proof Values for a Point Receiver at (0, 0, 0)

State	GNAP Value
East	0.50
North	0.50
Up	0.50

When this same demonstration is run on the Locata simulator it yields the same results as seen in Table 3. This demonstration thus proves that the GNAP results found using the Locata simulator are congruent with results found analytically.

3.5.4 GNAP vs. Monte Carlo Test

To show that GNAP gives an accurate mapping between the measurement errors and the positioning errors it is subjected to the same test as the DOP was in Section 3.5.1. Table 4 shows the standard deviations of the position errors calculated using ENtest GNAP and the single difference measurement error compared to the position errors found in the Monte Carlo analysis of ENtest.

Table 4: Comparison between GNAP and Monte Carlo Standard Deviations for the ENtest Simulation

State	$GNAP_{Epoch\ 1}$	STD of Position $Error_{GNAP\_1}$ (m)	STD of Position $Error_{MC}$ (m)
East	0.4081	0.0058	0.0057
North	0.4430	0.0063	0.0061
Up	0.7343	0.0104	0.0107

Notice that in Table 4 the standard deviation of the position errors found using the GNAP closely matches the standard deviation found in the Monte Carlo analysis. This proves that the GNAP, by taking the measurement correlations into account, does a much better job than DOP at correlating the measurement errors to the position errors.

3.6 Summary

Chapter 3 began by describing the basic processes involved in the Locata simulator used in this research. Following that was a section describing the ENtest geometry. The geometry from ENtest was then used in a Monte Carlo analysis which showed that the calculated standard deviations matched the position error standard deviations. Following the Monte Carlo analysis was an in-depth description of GNAP and why it is used in this study instead of DOP to measure the geometry of a system. The next chapter will discuss the results found by using the Locata simulator on various geometric LocataNet deployments.

IV. Results and Discussion

4.1 Chapter Overview

This chapter begins with a section that discusses the results of performing a GNAP analysis on the ENtest geometry and how that geometry is then used as the global geometry to ensure good horizontal geometry during the following simulations. The next section will detail the LocataNet deployment and results for the study of elevation angle effects on the vertical geometry. After the angle study will be a section covering various LocataNet deployments and results in which the number of Locatalites is varied in three configurations along the runway. Lastly, a section will describe the effects of attaching a Locatalite and receiver to an orbiting aircraft in hope that the orbiting transmitter will aid in the vertical geometry of the system.

4.2 East North Verification Results

Recall from Section 3.3.2 that the ENtest simulation is based on a LocataNet deployment which produced favorable geometric solutions in the horizontal plane. The GNAP of the rectangular deployment of the LocataNet can be seen in Figure 10.

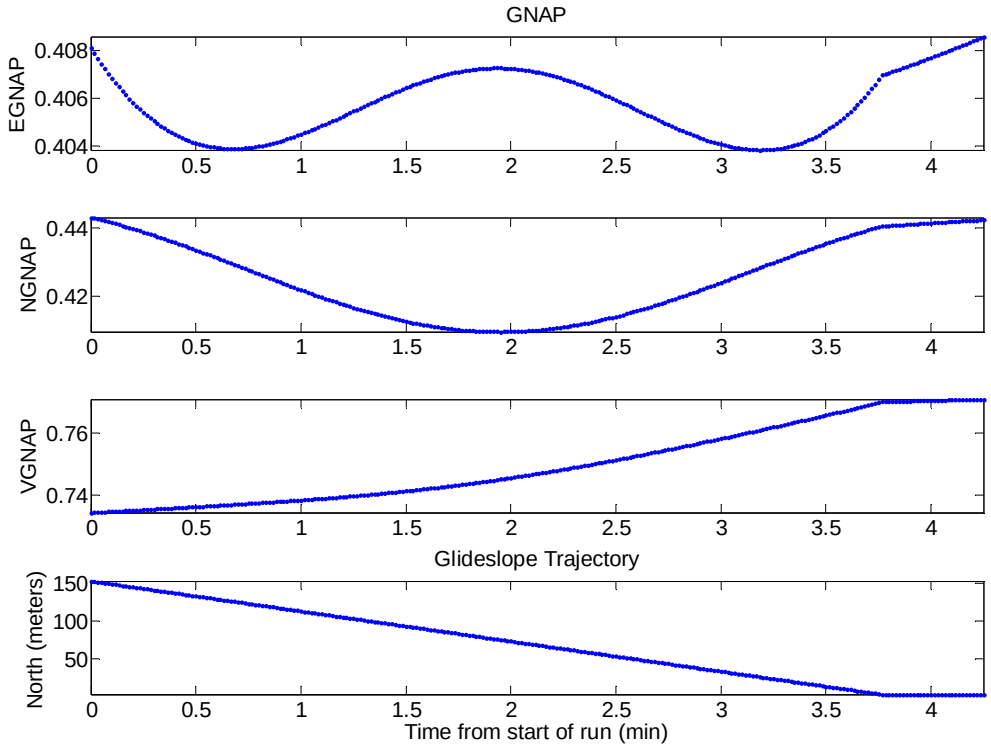

Figure 10: GNAP of Rectangular Deployment (ENtest)

Notice that the EGNAP is practically constant, hovering between 0.404 and 0.408, while the NGNAP fluctuates between 0.41 and 0.44. Also note that the VGNAP appears to be favorable in this simulation, with 'favorable' meaning the VGNAP of 0.74 multiplied by a standard deviation measurement error of 0.01 m would yield a standard deviation position error of 0.0074 m which is sub-centimeter level. The VGNAP seems to be favorable in this simulation because of the high altitude LocataLite located in the center of the LocataNet, which is being used to aid the simulator in converging to a solution. Once this high altitude Locatalite is removed, this geometry yields high VGNAP values. Recall that for the study in which six Locatalites surround a single receiver the GNAP values averaged to be around 0.5. Therefore it is reasonable to conclude that the rectangular deployment yields favorable geometry in the horizontal plane. This

deployment will be used as a standard global LocataNet to ensure good horizontal coverage for all tests.

4.3 Angle Variation Test Case

The goal of this test case is to study the effect that elevation angle has on the vertical positioning error. To conduct this test, the global rectangular Locatalite deployment will be used to ensure good horizontal plane geometry. A seventh Locatalite was located 10 kilometers (10,000 meters) north of the center of the runway, as can be seen in Figure 11. The Locatalite was placed far from the runway, on the very edge of a Locatatlite's transmit range, in order to ensure that every point of the runway will receive equal coverage from this transmitter. This extra Locatalite's height was varied so as to create elevation angles ranging from 10^{o} to 80^{o}. A visualization of the elevation angle between two Locatalites can be seen in Figure 12.

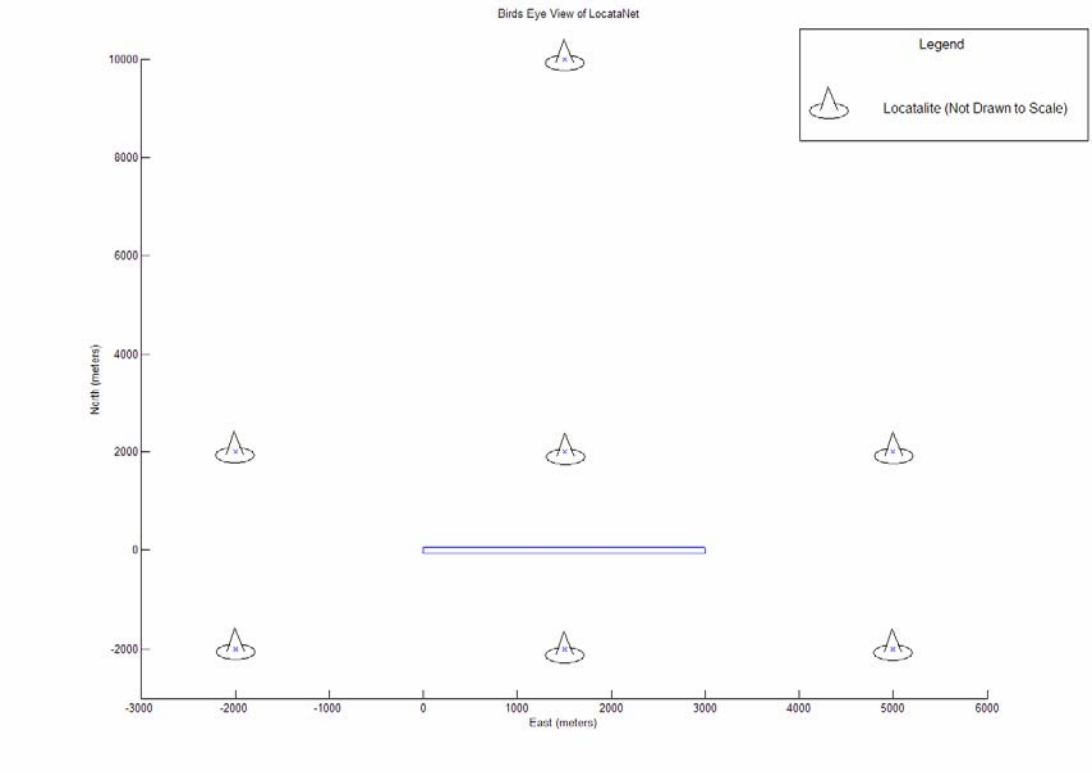

Figure 11: Bird's Eye View of the Angle Study LocataNet

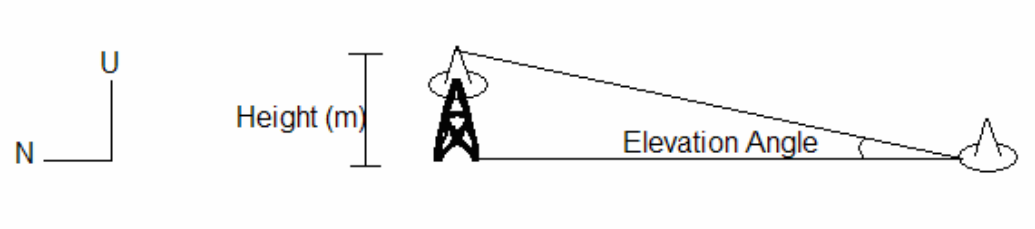

Figure 12: Visualization of Elevation Angle

The GNAP plots for each run of this test case were saved after the simulation was completed. These plots can be seen in the Appendix, and show that the EGNAP and NGNAP remain constant through all the runs for this test case. Figure 13 shows the VGNAP vs. Time of each run of this test case. Note that the VGNAP increases as the aircraft gets lower to the ground and remains constant once the aircraft touches down and rolls out. Also notice that the variation in the VGNAP over time becomes nearly constant after 20^{o}.

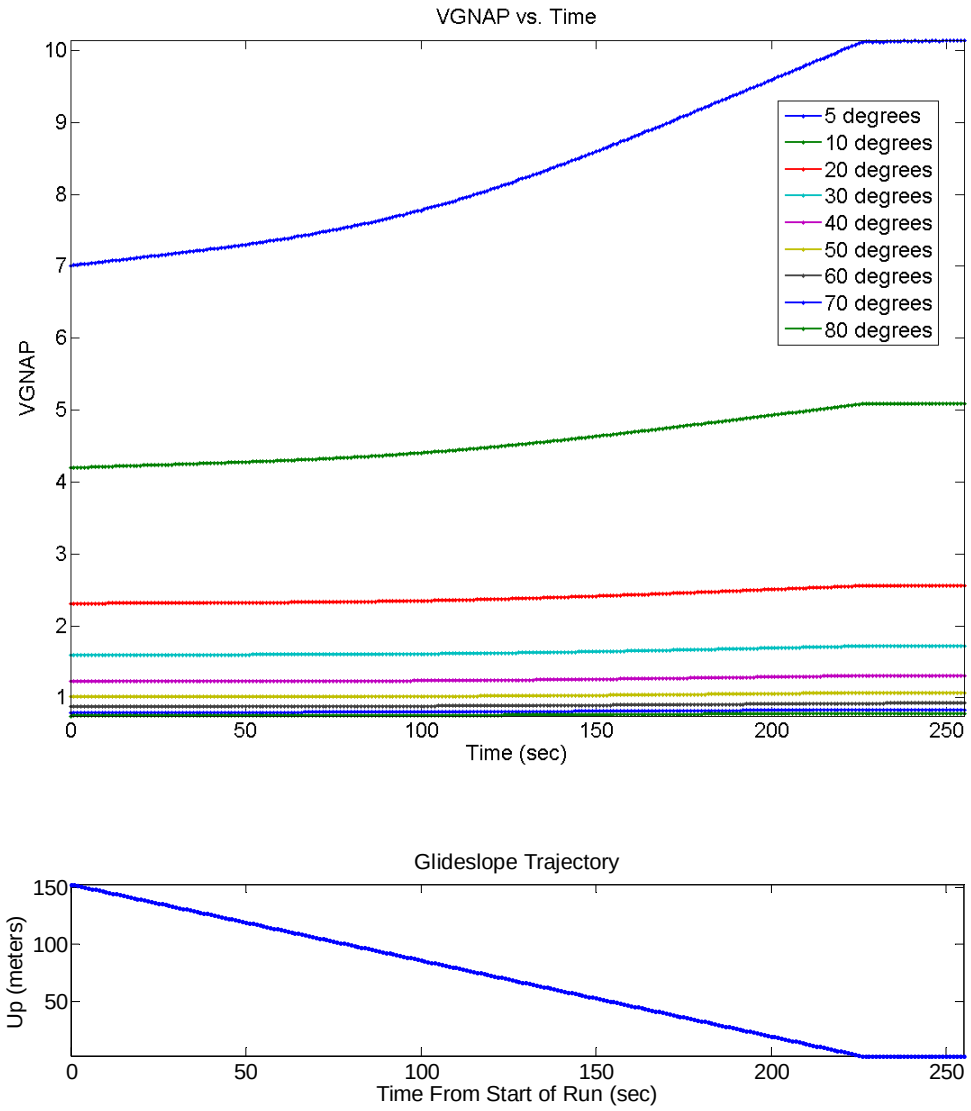

Figure 13: Angle Test Case VGNAP vs. Time with Glide Slope Trajectory

The average of each of the VGNAP plots, from 3.5 minutes until the end of the rollout, is plotted against its corresponding elevation angle in Figure 14. The reason for taking the average VGNAP from only 3.5 minutes on is that after this time (where the aircraft is about 100 feet above the ground) the VGNAP begins to increase significantly due to the fact that the aircraft based receiver is almost coplanar with the LocataNet.

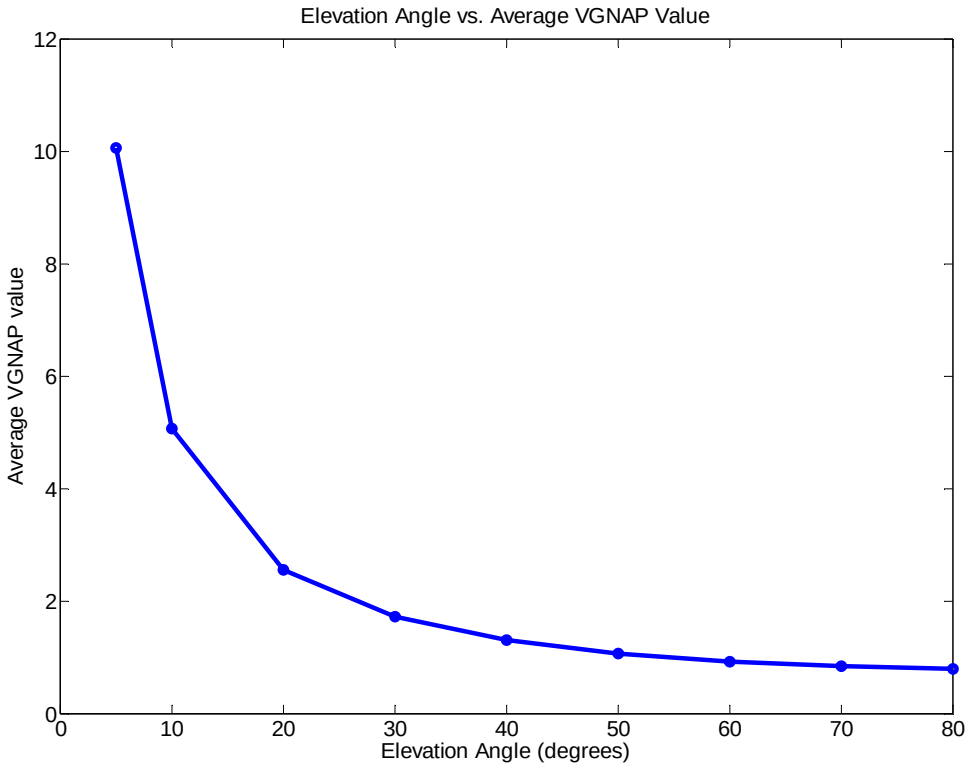

Figure 14: Elevation Angle vs. Average GNAP

Notice that as elevation angle increases, the average VGNAP value decreases in a decaying exponential fashion. It can clearly be seen that after an elevation angle of 20^{o} the decrease in VGNAP begins to level out. This is important because it shows that diminishing returns begin to occur after 20^{o} of elevation.

4.4 Multiple Locatalite Test Cases

Simulations in this section deal with varying the number of Locatalites aligned in various patterns along the runway. The thinking behind this family of tests is that if the Locatalites are deployed very near the runway then the geometry between an individual Locatalite and the receiver on the airplane will be favorable as the aircraft passes over or near that particular Locatalite. With a sufficient number of Locatalites deployed in this

fashion along the length of the runway then the aircraft will always be flying near at least a few of the Locatalites, and the increased elevation angles from the near Locatalites will help to decrease the position error. In each of these cases, the runway is encompassed in the horizontal plane by the global rectangular LocataNet deployment. There will be three test cases run in this family of simulations.

4.4.1 The Lots Test Case

The first of these test cases will be called the "Lots" study. During this test a number of Locatalite pairs will be arranged along either side of the runway. For these simulations, all the Locatalites are located on the ground. The number of Locatalite pairs will range from 3 to 500. A bird's eye view of the LocataNet with 10 Locatalite pairs can be seen in Figure 15.

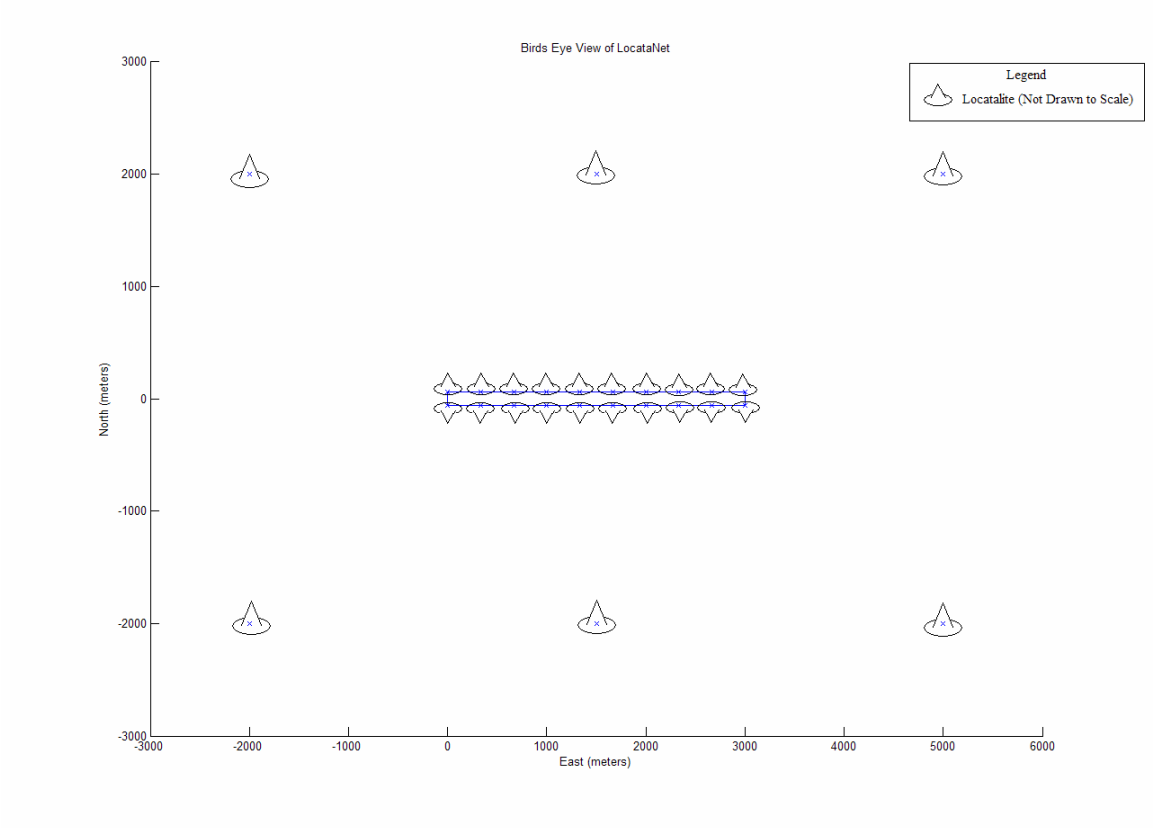

Figure 15: Bird's Eye view of Lots Study LocataNet with 10 Locatalite Pairs Along the Runway

The thought in this study is that the sheer number of Locatalites will be able to provide enough coverage of each part of the runway to allow the vertical position to be precisely solved. The individual GNAP plots for each simulation can be found in the Appendix.

Figure 16 shows the VGNAP versus time for the Lots study. Note that the VGNAP for all the simulations rise sharply as the aircraft passes through t = 3.5 minutes. It is also important to note that 20 Locatalites are needed to get the spike value of the VGNAP, as it passes through the 3.5-minute threshold, down to value of 10. Compare that to the Elevation Angle study where only one extra pseudolite, 10 kilometers away and raised to an elevation angle of 10^{o} achieved the same result. A plot of the Average VGNAP (taken

after the 210 second (3.5 min) threshold) versus the number of Locatalite pairs along the runway can be found in Figure 17.

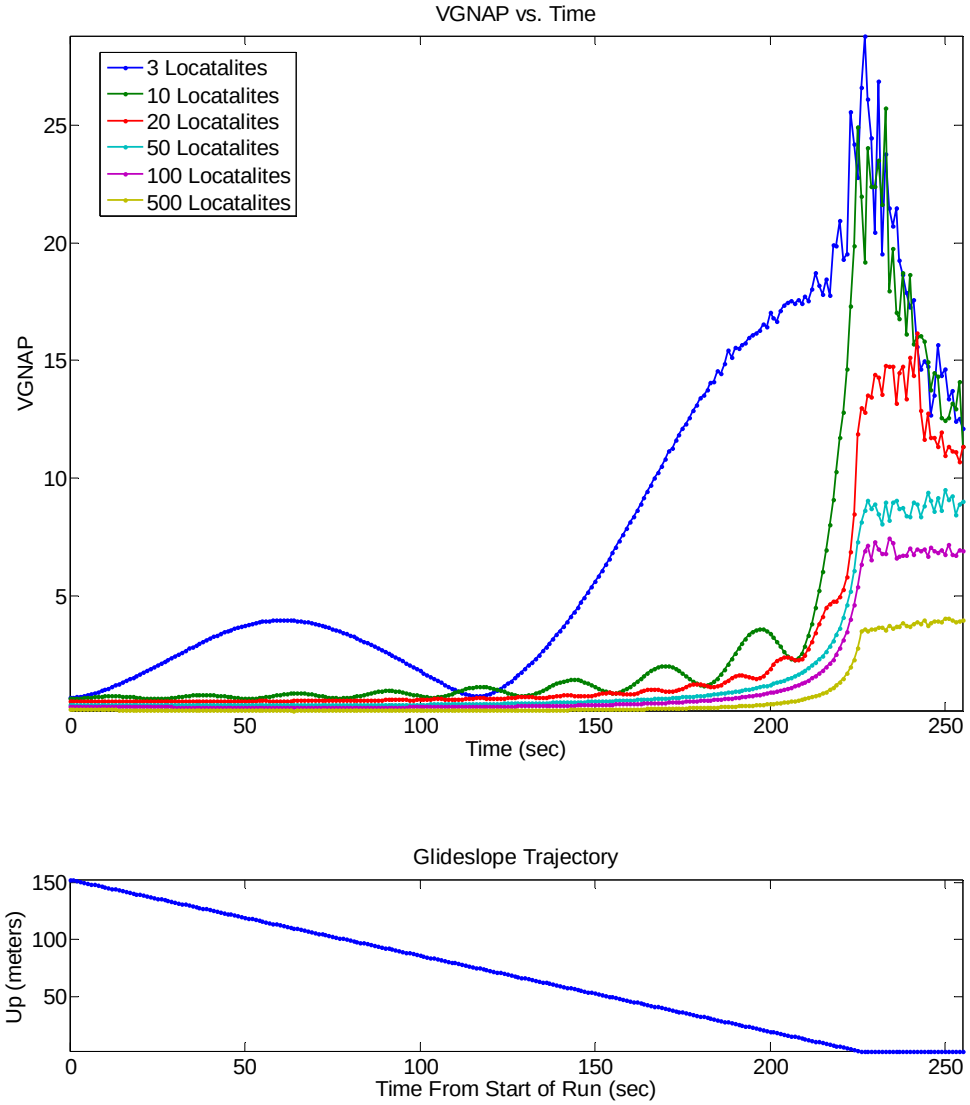

Figure 16: Lots Study VGNAP vs. Time with Glide Slope Trajectory

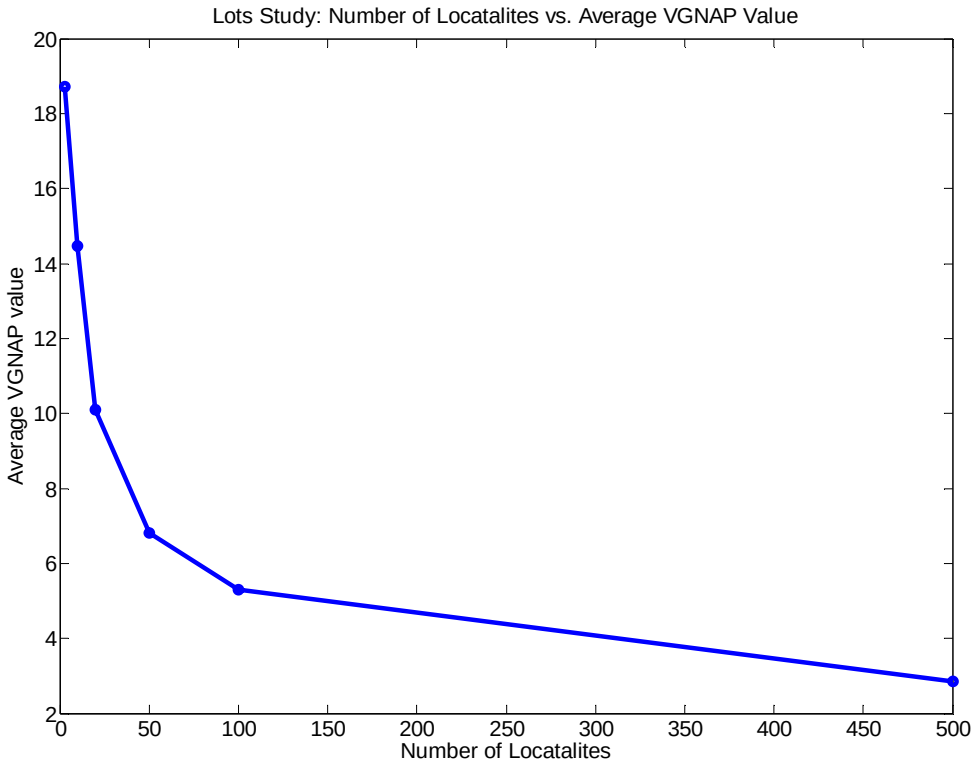

Figure 17: Lots Study Average VGNAP (taken after t = 210 sec) vs. the Number of Locatalite Pairs in the LocataNet

Figure 17 shows that the point of diminishing return for the number of Locatalites needed does not occur until about 100 Locatalite pairs are aligned along the runway. This case shows that placing numerous the Locatalites alongside the runway on the ground level is probably not an efficient way to reduce the VGNAP.

4.4.2 The Stairs Case Study

Before ruling out placing multiple Locatalite pairs along the side of the runway as a way to reduce the vertical position error, a test needs to be done to determine if raising these Locatalite pairs out of the ground plane will improve the results from the Lots study. However, the Locatalite pairs cannot all be simply raised to the same height, because the aircraft would then still pass through a now elevated plane in which the

vertical elevation angle from each of the Locatalites to the receiver would be poor. The next intuitional step would be to say that as the aircraft descends the Locatalite pairs should ascend, so that when the aircraft is at the two extreme ends of the glide slope the vertical geometry would be favorable. This is only partly true, because if all of the Locatalites were to be incrementally raised in this fashion, then there would still appear to be 3D "space" in the middle of the glide slope where the geometry would be unfavorable. This would be caused by the aircraft passing through the slanted plane created by the Locatalites. One approach is to incrementally raise every other Locatalite pair. The skipped over Locatalite pairs would remain on the ground. In theory this should eliminate the "plane" in which the aircraft passes through and should yield good geometry throughout the glide slope. A 3D visualization of this LocataNet can be seen in Figure 18. Again the entire runway and Stair LocataNet is encompassed by the global LocataNet to ensure good geometry in the horizontal plane. For the purposes of these simulationss the Locatalite pairs are incremented from zero to 100 meters above ground.

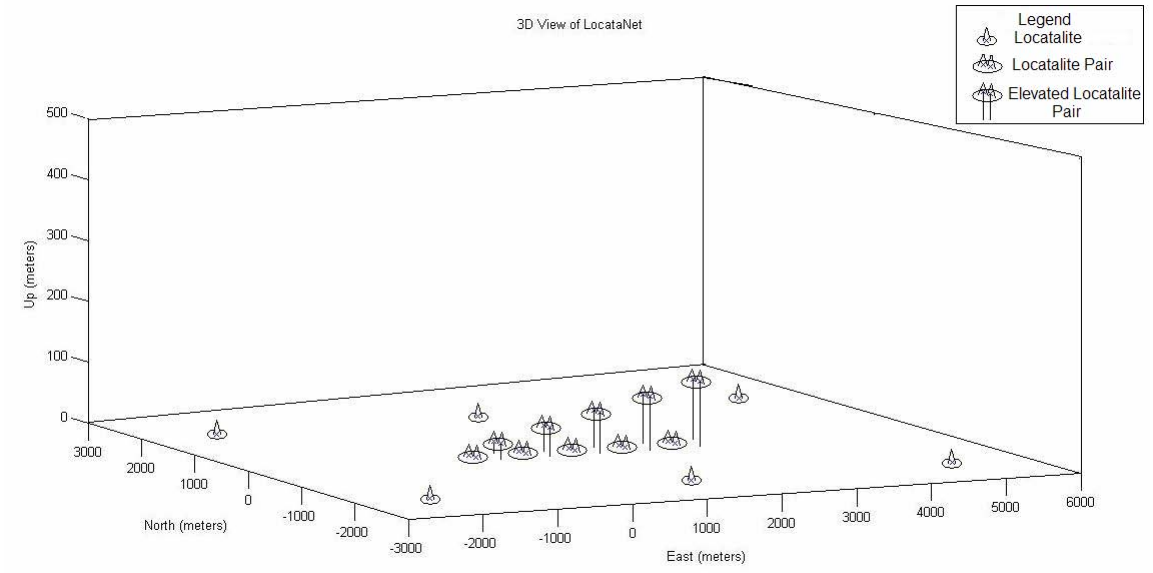

Figure 18: 3D View of the Stair Case Study LocataNet

The VGNAP versus time plot for this configuration is shown in Figure 19 and it can be seen that the VGNAP is fewer than 10 with just three Locatalite pairs arranged in this configuration (recall that in the Lots study it required over 20 Locatalite pairs to get the VGNAP spike less than 10). Also note that the spike that occurs in the Lots and Elevation Angle studies at t = 3.5 minutes does not occur in these simulations. Instead the spikes occur near the middle of the glide-slope as the aircraft passes through the 3D poor geometry space. This spaces effect, however, seems to be lessened by the staggering of the Locatalites. Figure 20 shows the average VGNAP (taken over the entire time, because there is no definitive spike point) versus the number of Locatalite pairs. Notice that the point of diminishing returns at only 20 Locatalite pairs, while the Lots study needed over 100. Also note that the point of diminishing returns occurs well below a VGNAP of 1. Even after 500 Locatalite pairs the Lots study is still over a VGNAP = 3.

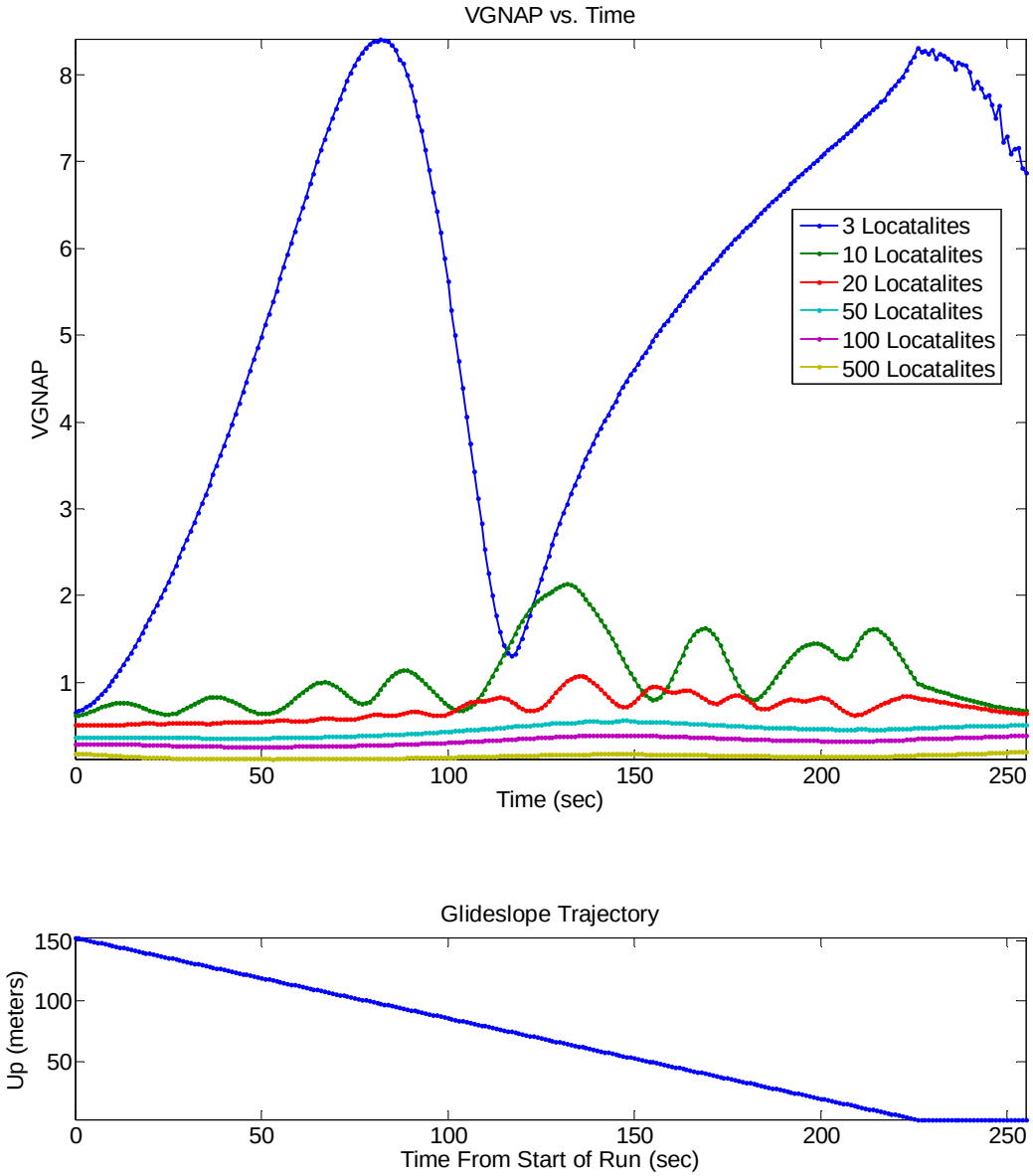

Figure 19: Stair Study VGNAP vs. Time with Glide Slope Trajectory

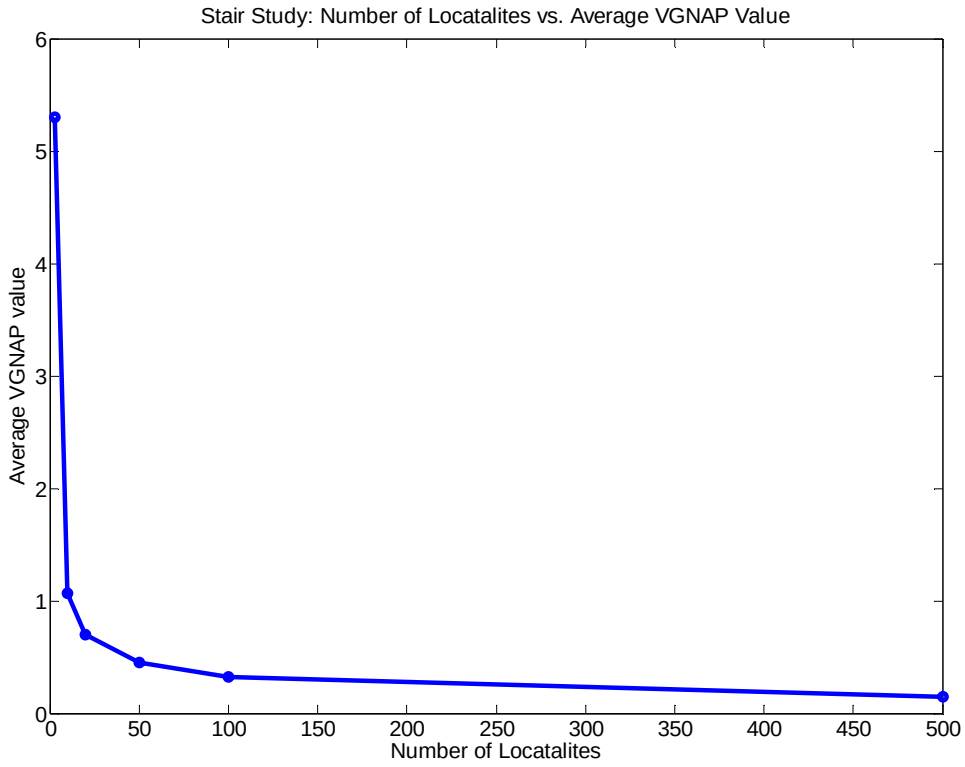

Figure 20: Stair Study Average VGNAP versus the Number of Locatalite Pairs in the LocataNet

The problem with the Stair simulation is that it is a very impractical scheme to implement in the real world. Firstly, building 100-meter towers near a landing strip would violate several safety rules and federal regulations [12]. Also, even with the best of pilots, trying to land in a situation where there are obstacles on either side of the landing strip is a perilous exercise.

4.4.3 The Center Case Study

This case study does not involve Locatalite pairs. Instead, the Center study takes a varying number of Locatalites and evenly spaces them down the center of the runway, as can be seen in Figure 21.

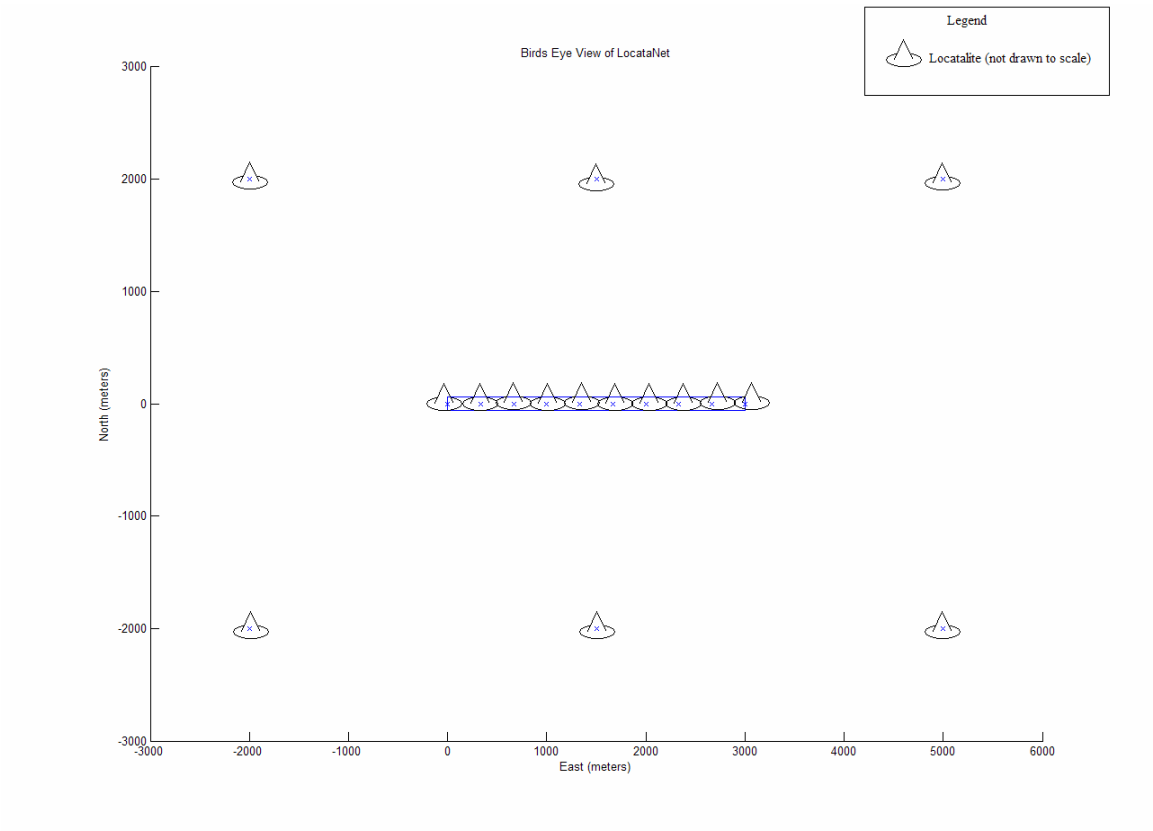

Figure 21: Bird's Eye View of the Center Study LocataNet

The premise behind this test is that as the aircraft is landing it will fly directly over these Locatalites. Due to the fact that the receiver is in fact on the under carriage, and not the tires, even when the aircraft is on the ground there should be 3 meters of elevation to generate angles between the aircraft and the Locatalites directly beneath it (or in its general area). The height of the under carriage will obviously change depending on the aircraft being used, for this research it is assumed that the under carriage is 3 meters off the ground. The plot of the VGNAP versus time of the Center case study can be seen in Figure 22. Notice that once again there is a spike in the data around t = 210 sec (3.5 min), where the VGNAP rises considerably due to poor geometry right as the plane is about to land.

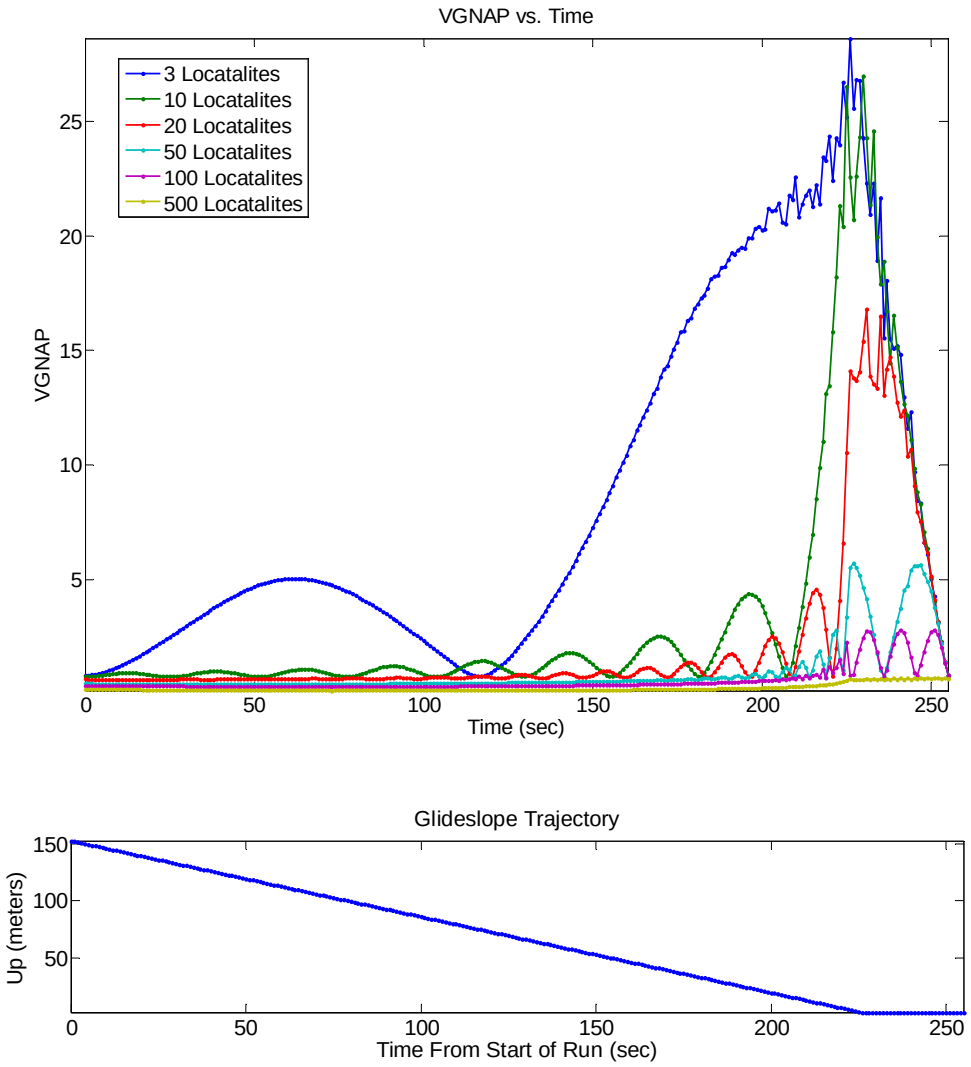

Figure 22: Center Case Study VGNAP vs. Time with Glide Slope Trajectory

Average VGNAP versus the number of Locatalites aligned along the center of the runway is shown in Figure 23. This plot shows that the point of diminishing return for the number of Locatalites needed occurs at around 50 Locatalites. While this is much less than the Lots case study, which required about 100 Locatalites before reaching point of diminishing returns, it is much greater than the same point for the Stair study.

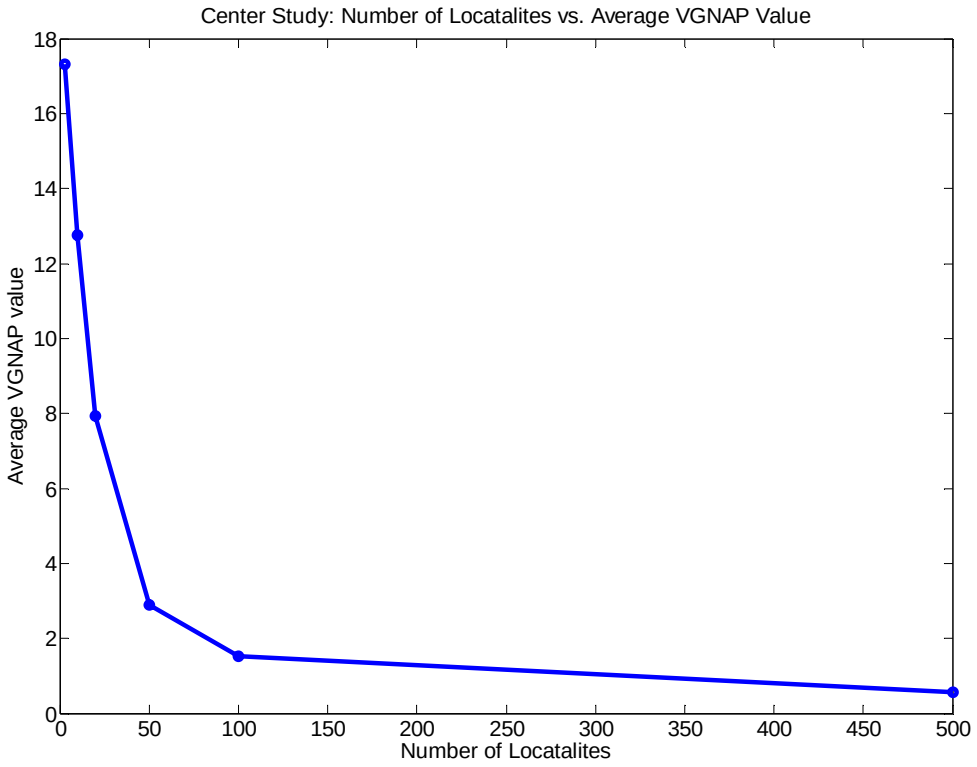

Figure 23: Center Study Average VGNAP (taken after t = 3.5 min) vs. the Number of Locatalites

Although the results from the Center study do not produce VGNAP values that are as low as the Stair study, the premise of embedding Locatalites into the runway seems more feasible for tracking a landing aircraft than the idea of placing hundred foot tall towers along the sides of the runway. See Figure 24 below for a final comparison between the VGNAP vs. the Number of Locatalites needed. Bear in mind that for the Stair and Lots studies in Figure 24, the number of Locatalites actually refers to the number of Locatalite pairs lined up along either side of the runway. Figure 24 clearly shows that the best VGNAP for the least amount of Locatalites occurs with the Stair configuration.

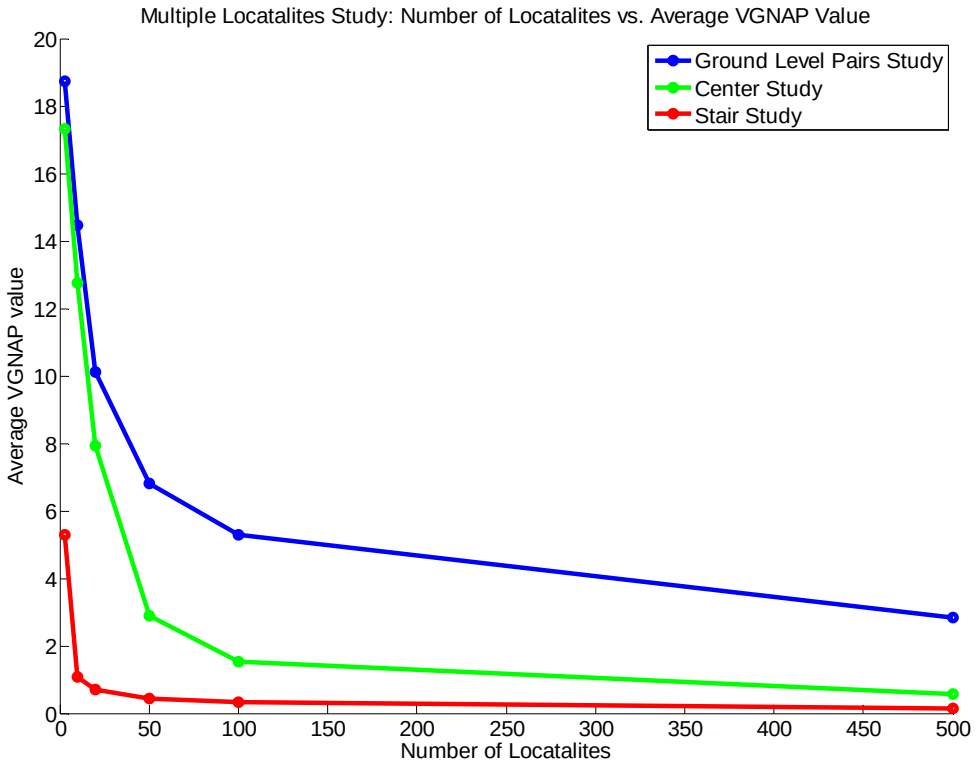

Figure 24: Multiple Locatalite Study VGNAP vs. Number of Locatalites

4.5 Orbiting Aircraft Study

This test case involves an approach in which a Locatalite is placed in an aircraft, which will be orbiting the runway as the mobile receiver lands. The promising aspect of this case for improving the vertical positioning error is that it creates the coverage and elevation angle equivalent to having a very tall tower close to the runway without the dangerous tower. Development of this case study will be broken down into sections covering different ways to improve upon the system. It is important to note that in order to solve for both the orbiting aircraft position and the landing aircraft position it will be necessary to turn on the ambiguity resolution in the batch ILS simulator. Also some

alterations to the carrier phase measurements section of the code will need to be made. These changes will be discussed in Section 4.5.2.

4.5.1 The Perfect Orbiting Aircraft Track

In this case, the orbiting aircraft's position was assumed to be known and was a perfect match to the truth trajectory flown by the orbiter. Another assumption made in this simulation is that the orbiting Locatalite is perfectly synchronized with all the other Locatalites. The orbiting aircraft was flying in a perfect circle at an altitude of 15,000 meters and at 54.1 meters/second. This speed allowed the orbiter's circular track to lie within the LocataNet for the entire test. The ground based LocataNet was the same global LocataNet that has been used for all other previous studies. By treating the orbiter as simply a moving Locatalite whose position is exactly known, solving for this problem requires no code alterations or ambiguities. Figure 25 shows the GNAP plot for this case study.

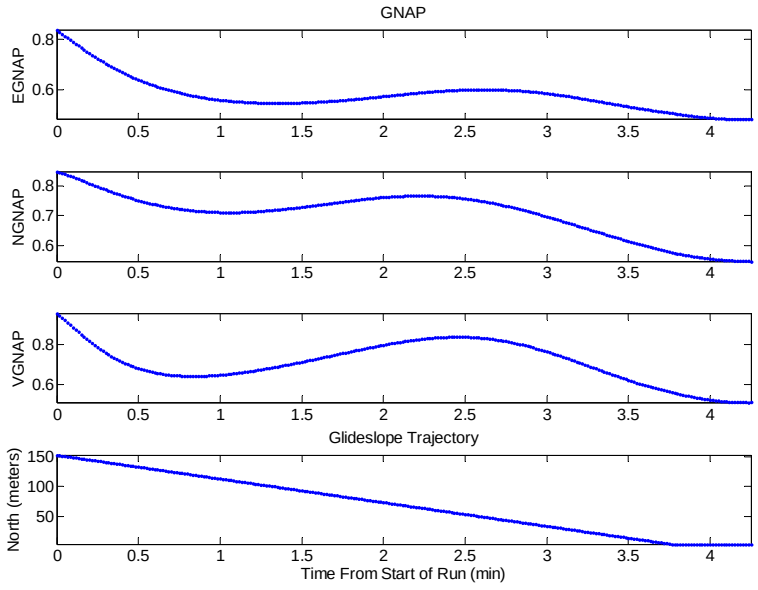

Figure 25: VGNAP vs. Time for the Orbiter with a Perfect Track

Looking at Figure 25 it is clear to see that, for this case, the VGNAP values are very good, ranging from 0.95 to 0.5. However in the real world one cannot assume that the orbiting aircraft's track is perfectly known.

4.5.2 Measurement Code Development Differences

For a more realistic approach to using an orbiting aircraft to solve for the position of the landing aircraft, one cannot assume that the orbiting aircraft's trajectory is known and that it is being perfectly tracked. Therefore the orbiter's position must be solved for, using the same LocataNet used to track the landing aircraft, before its position can be used to solve for the position of the landing receiver. Two things need to happen before the position solution of the orbiter can be found. The first is that the carrier-phase ambiguities can no longer be assumed to be known (as they had been for all previous tests). Secondly, a base receiver must be added to the LocataNet. This base receiver is needed because the dynamics of the orbiter in relation to the landing aircraft adds another clock error term to the system, δt_{orbit}. One way to account for this clock error is to perform double differencing between the reference receiver and the landing receiver measurements. Equation (4.1) and Equation (4.2) show the new **h(x)** matrix with the double differenced term added as the sixth row.

$$h(x) = \begin{bmatrix} \nabla\phi_R^{12} \\ \nabla\phi_R^{13} \\ \nabla\phi_R^{14} \\ \nabla\phi_R^{15} \\ \nabla\phi_R^{16} \\ \Delta\nabla\phi_R^{17} \end{bmatrix} \tag{4.1}$$

$$\Delta\nabla\phi_R^{17} = \nabla\phi_R^{17} - \nabla\phi_B^{17} \tag{4.2}$$

Where $\nabla\phi_B^{17}$ is the single difference measurement between the reference Locatalite for the LocataNet, and the orbiting Locatalite with the base receiver as the reference. With the base receiver added to the system, the double difference term added to the batch ILS process, and the ambiguities turned on, it is now possible to solve for both the orbiter's position and the landing aircraft's position.

4.5.3 High Orbit inside of the LocataNet

The first test case run with the new orbiting model was to fly the orbiting aircraft at a very high altitude. According to the Elevation Angle study, flying the orbiting aircraft at a high altitude directly over the runway should be a favorable geometry for the landing aircraft. Figure 26 shows the configuration of the LocataNet, orbiting aircraft, and landing aircraft.

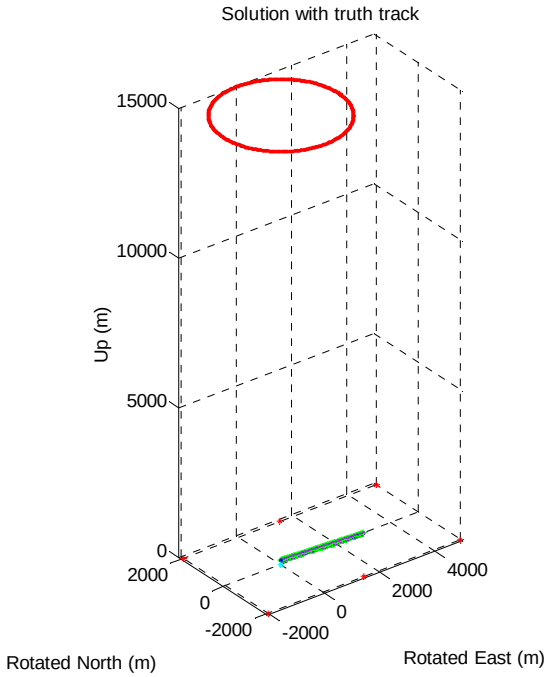

Figure 26: 3D View of the LocataNet with Orbiting Aircraft at 15,000 meters and Landing Aircraft

Figure 27 through Figure 30 show the results of having a high altitude orbiting aircraft whose orbit is inside of the global LocataNet. The orbiting aircraft's GNAP is shown in Figure 27, and it can be seen that the VGNAP values are very poor. These poor GNAP values correlate to a biased vertical positioning error plot in Figure 28. The poor GNAP values and the bias in the positioning error for the orbiting aircraft can be explained by the fact that the geometric change in position of the orbiting aircraft in relation to the global LocataNet is too small to solve for the ambiguites of the orbiter, which leads to large errors.

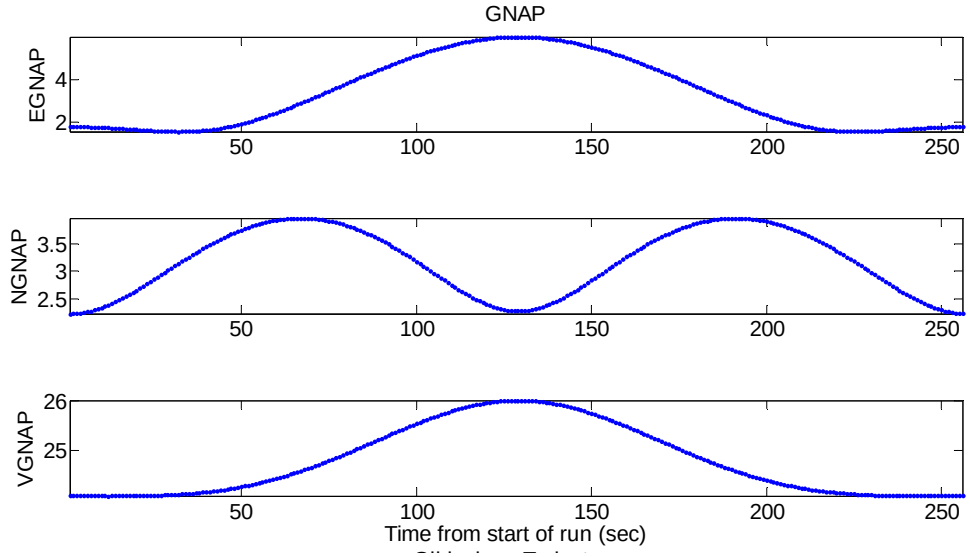

Figure 27: Orbiter GNAP Plots for h = 15,000 meters

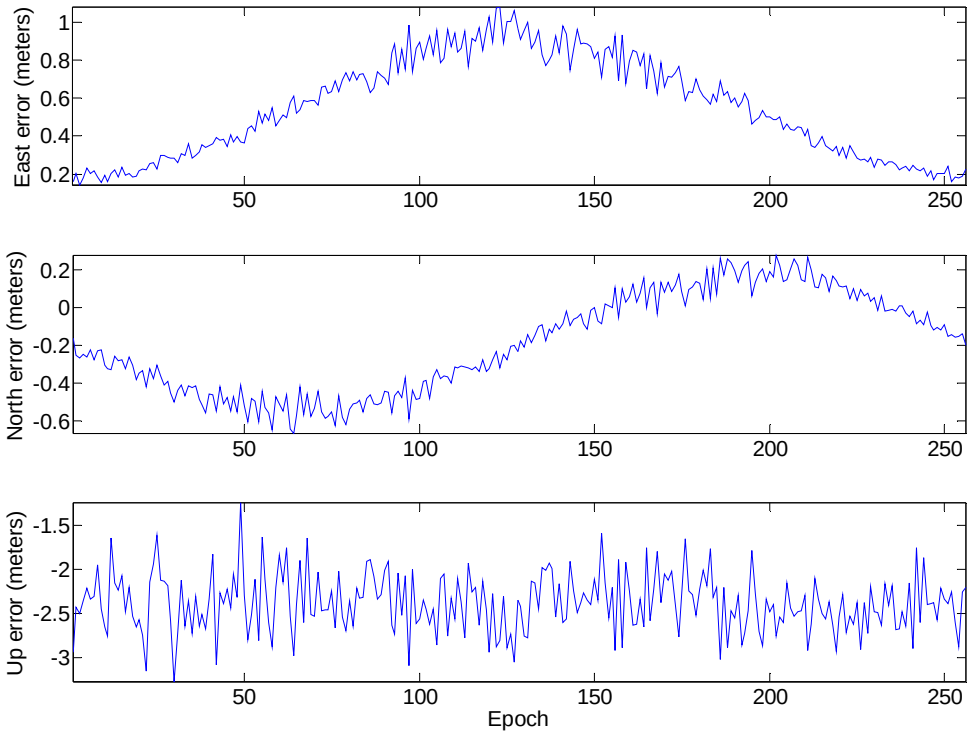

Figure 28: Orbiter Position Error for h = 15,000 meters

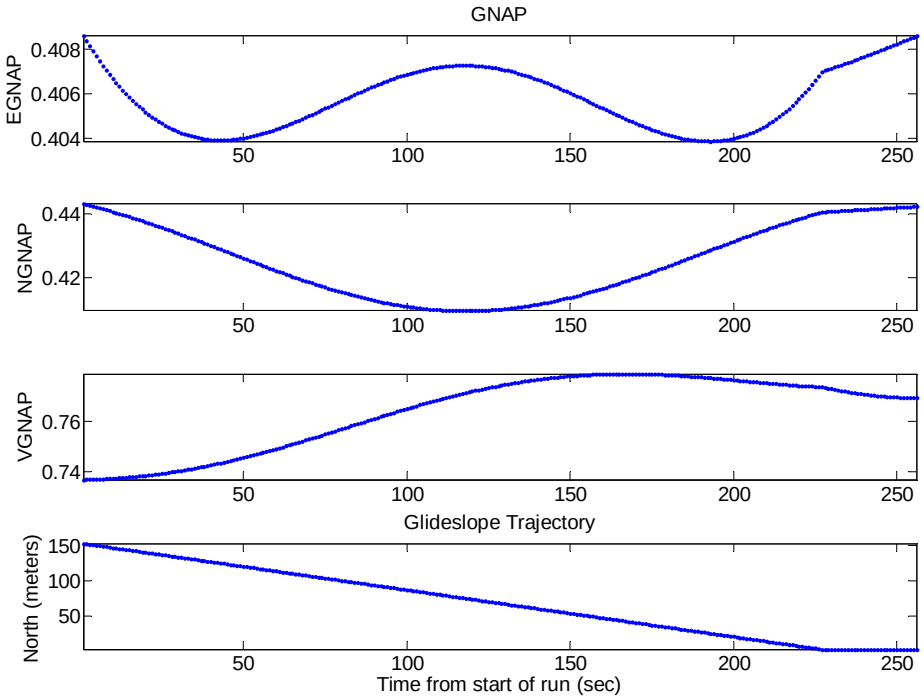

Figure 29: Landing A/C GNAP for h = 15,000 meters

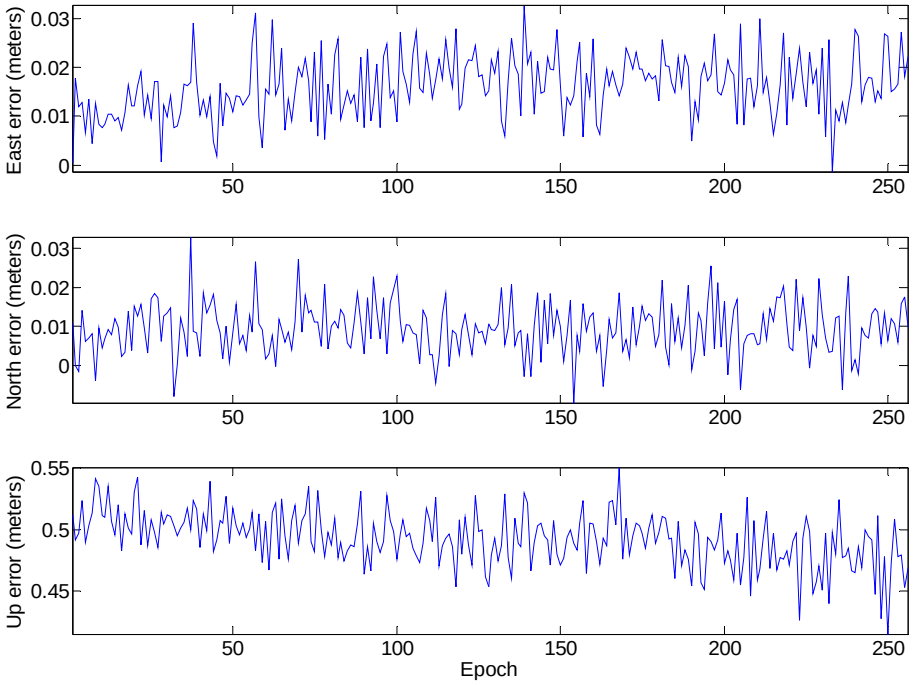

Figure 30: Example of Landing A/C Position Error for h = 15,000 meters

It should be noted that the GNAP for the landing aircraft, shown in Figure 29 appears to be very good and comparable to the "perfectly tracked" orbiting aircraft, however recall that the position solution of the landing aircraft is based on accurately knowing the position of the orbiting aircraft, and with the orbiting GNAP and position errors being as high as they are, the landing data cannot be trusted. Also notice that while the GNAP solution appears good, the bias in the vertical positioning error from the orbiting aircraft has carried over into the landing vertical positioning error, which is also biased as shown in Figure 30. This bias, which was not present in the "perfectly tracked" orbiting test, showcases the effect that adding the ambiguities has on the system performance.

4.5.3 Lower Altitude/Larger Radius Orbiting Aircraft

To try and fix the problems in Section 4.5.2 involving poor ambiguity resolution of the orbiting aircraft, the orbiter's altitude was lowered to 4,000 meters. Also, to aid in the ambiguity resolution further, the speed of the orbiter is increased to 100 meters/second. This speed increase effectively increases the radius of the circular orbit, which yields a larger geometry change in reference to the global LocataNet. To account for the increase in radius, one of the Locatalites in the global LocataNet must be moved out to its max range so that the horizontal plane of the orbiting aircraft is still enclosed by the global LocataNet. A 3D plot of this configuration can be seen in Figure 31.

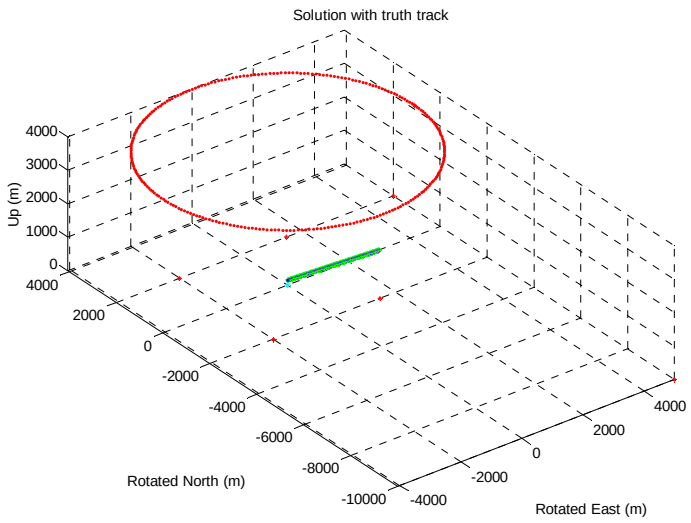

Figure 31: 3D View of the Orbiting Aircraft at 4,000 feet with a Larger Orbit

The following plots, shown in Figure 32 through Figure 35, show the resulting GNAP and position error values for both the orbiter and the landing aircraft for this configuration. Notice in Figure 32 that the GNAP values for the orbiter are much better than the GNAP values from when the orbiter was at 15,000 meters, however the GNAP numbers are still in the high range. The good news is that now the position error for the orbiter has a zero mean in all three directions which is a major improvement from the 15,000 meters case (see Figure 28). Note that now that the orbiting aircraft is lower (and thus closer) to the landing aircraft, the angle of elevation has reduced and, even though the GNAP has been decreased and the position error is no longer biased for the orbiter, the GNAP has gotten worse for the landing aircraft, which can be seen by comparing Figure 34 to Figure 29. The bias in the vertical position error of the landing aircraft has decreased as a result of the greater geometry change of the orbiter relative to the LocataNet. The remaining vertical position error bias in the landing aircraft is due to not enough change in geometry between the orbiting aircraft and the landing aircraft.

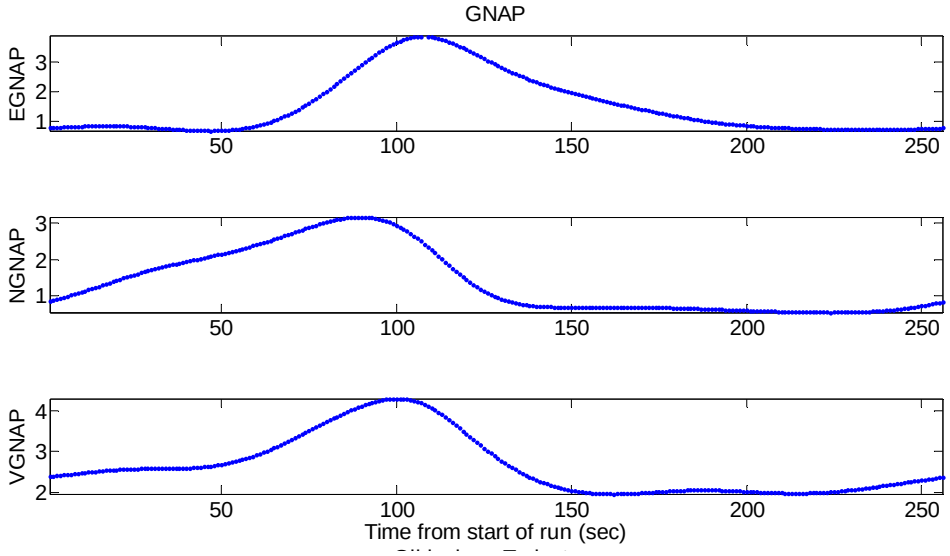

Figure 32: Orbiter GNAP vs. Time for h = 4,000 meters

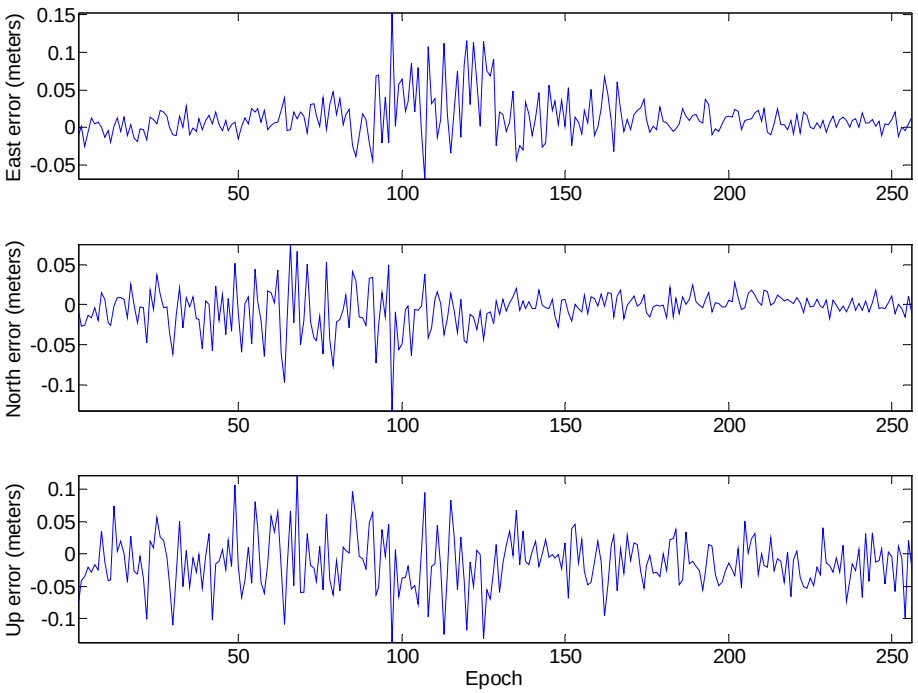

Figure 33: Orbiter Position Error vs. Time for h = 4,000 meters

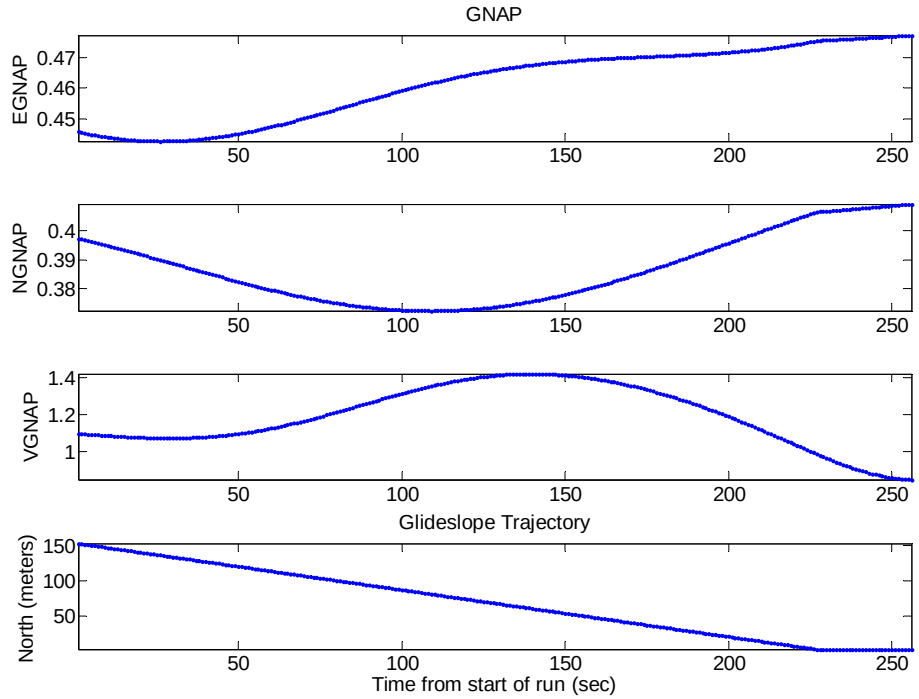

Figure 34: Landing A/C GNAP vs. Time for h = 4,000 meters

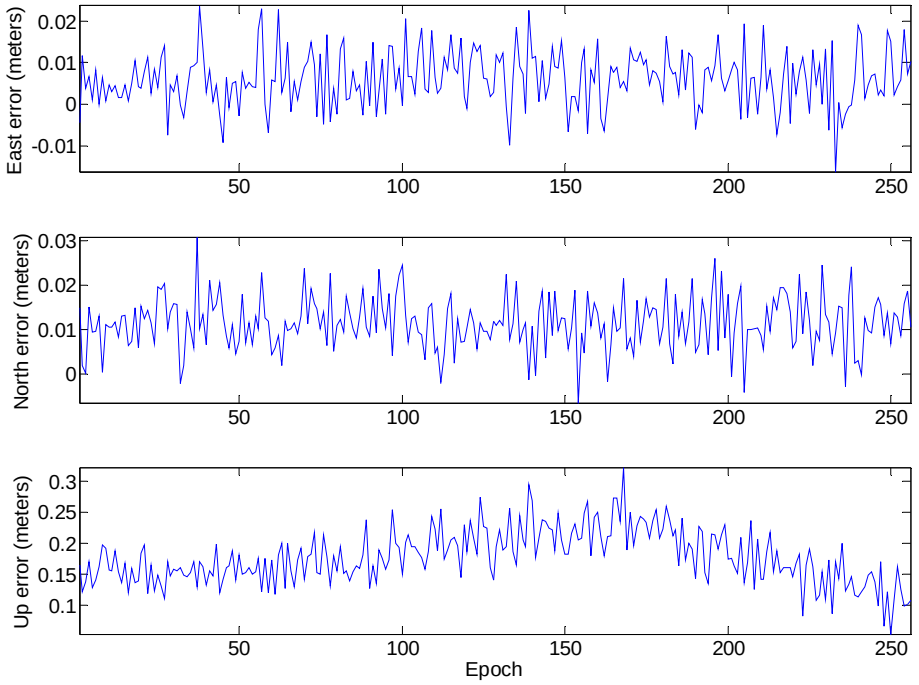

Figure 35: Example of Landing A/C Position Error for h = 4,000 meters

4.5.4 Sinusoidal Orbiter

The last simulation in this family of tests attempted to further resolve the ambiguities between the orbiting aircraft and the landing aircraft in order to reduce the bias in the vertical position error of the landing aircraft. To do this the orbiting aircraft now orbits at the same radius as in Section 4.5.3, however now it is changing altitude in a sinusoidal fashion in an attempt to vary the geometry enough to solve the ambiguities between it and the landing aircraft. This new orbiting geometry can be seen in Figure 36.

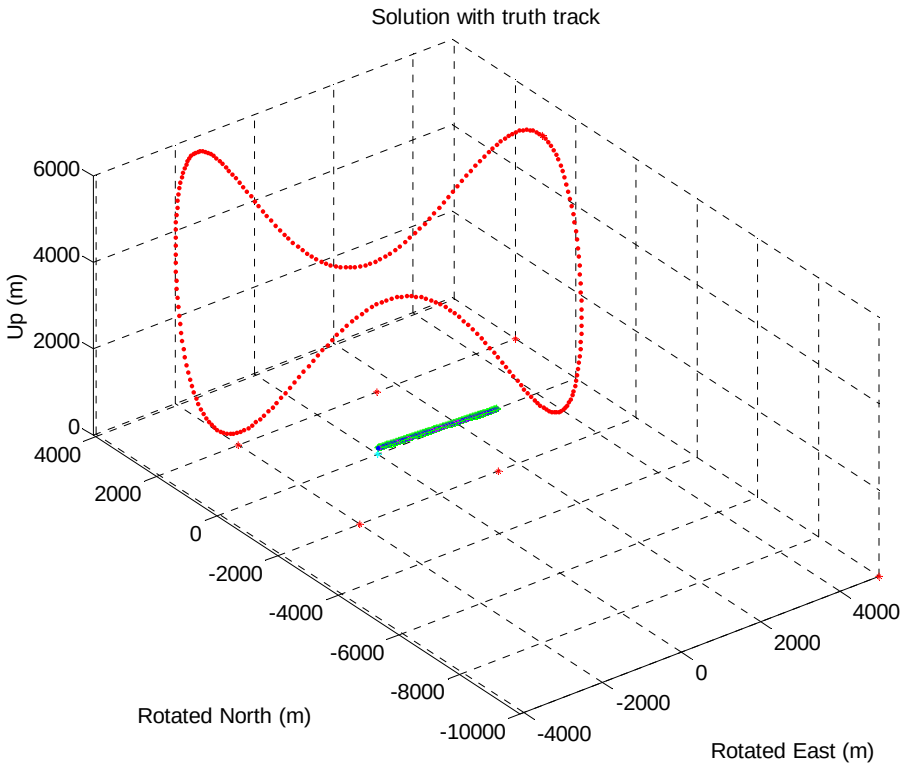

Figure 36: 3D Visualization of the Sinusoidal Orbit

The results from this simulation can be seen in Figure 37 through Figure 40.

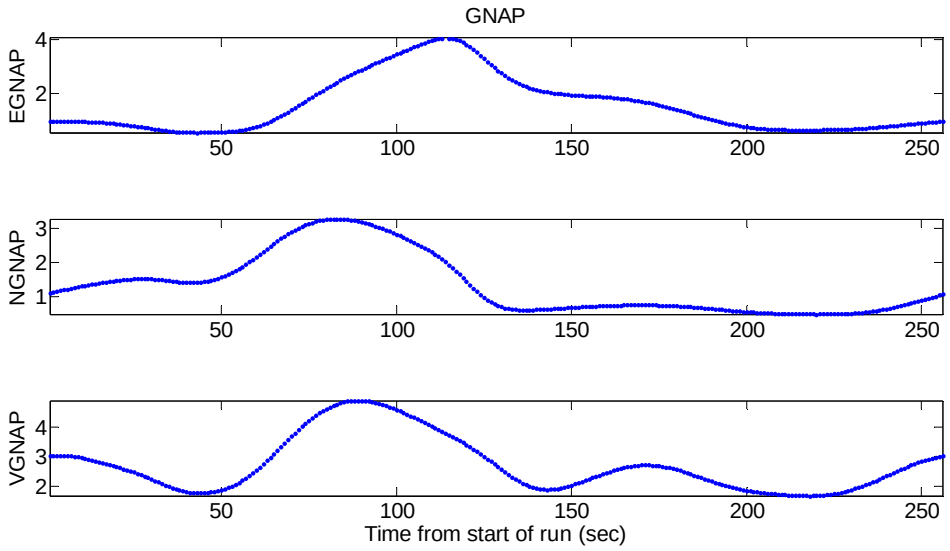

Figure 37: Orbiting Aircraft GNAP vs. Time for h = 4,000 meters Varying with Altitude Varying in a Sinusoidal Fashion

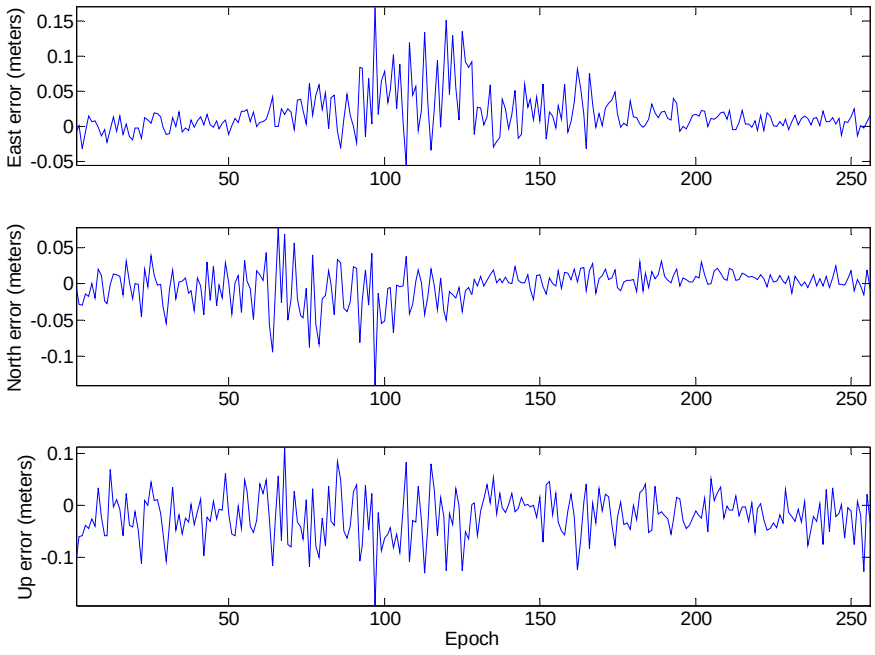

Figure 38: Orbiting Aircraft ENU Position Error for h = 4000 meters and Altitude Varying in a Sinusoidal Fashion

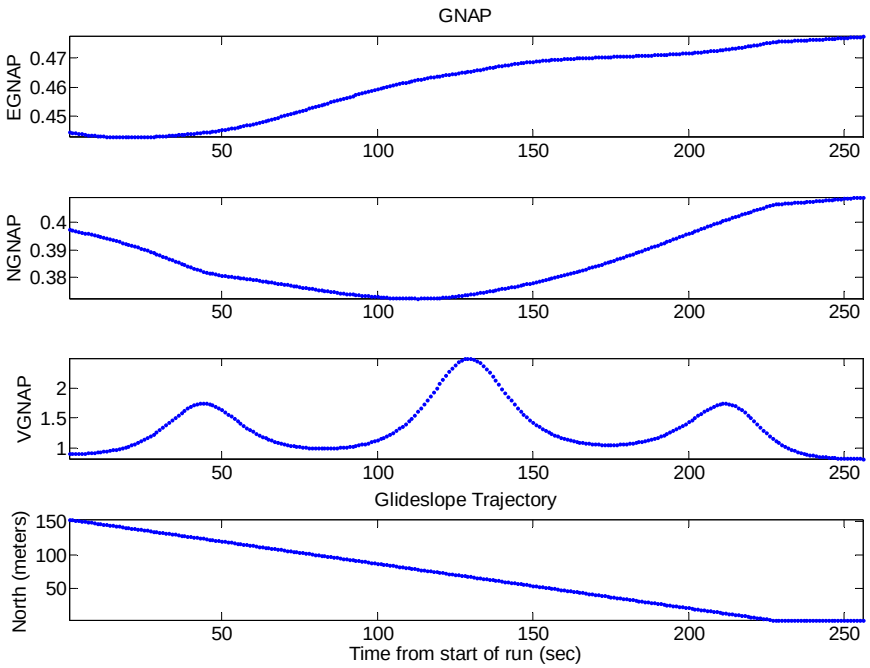

Figure 39: Landing Aircraft GNAP vs. Time for h = 4,000 meters Varying with Altitude Varying in a Sinusoidal Fashion

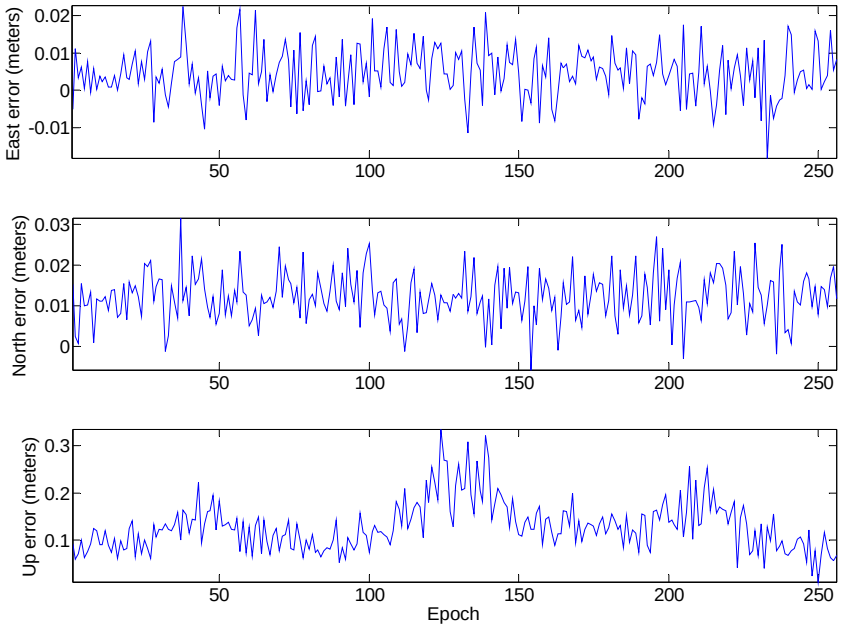

Figure 40: Example of Landing Aircraft ENU Position Error for h = 4000 meters and Altitude Varying in a Sinusoidal Fashion

As can be seen in Figure 37 and Figure 38 the GNAP and vertical position error for the orbiting aircraft do not change much with the addition of the sinusoidal pattern. The GNAP of the landing aircraft increases slightly, as seen in Figure 39, probably because the orbiting aircraft is, at times, dipping down lower which further reduces the slant angles between the landing aircraft and the orbiting aircraft. The bias in the vertical position error for the landing aircraft has been further reduced due to the greater geometric change between the orbiting aircraft and landing aircraft. Table 5 shows the reduction of the bias as the orbiting aircraft trajectory changes in this family of tests.

Table 5: Orbiting Aircraft Trajectory Change Compared to Average Vertical Positioning Error Bias

Orbiting Aircraft Trajectory	Average Vertical Positioning Error Bias for Landing Aircraft
Tight Orbit @ 15,000 meters	0.50 meters
Large Orbit @ 4,000 meters	0.15 meters
Large Orbit with Sinusoidal Altitude Change	0.10 meters

4.5.5 Orbiting Aircraft Results

By comparing the results of both the orbiting altitude, h, at 15,000 meters and 4,000 meters it appears to be that actions taken to better the geometry of the orbiting aircraft make the geometry for the landing aircraft worse and vice versa. Notice that when the orbiter was lowered to 4,000 meters and the circular orbit expanded, effectively decreasing the horrendous GNAP values from the 15,000-meter orbiter, the GNAP of the landing aircraft increased, even while the vertical position error bias decreased. The sinusoidal trajectory change did lower the bias further. However, when the orbiting

aircraft dipped lower towards the ground to create this trajectory it also lowered the slant angle between it and the landing aircraft, which increased the GNAP of the landing aircraft.

One possible solution to these problems would be to have the orbiting aircraft fly low and with a great deal of geometric variance before the test run so that the ambiguities can be solved for. Then, once the ambiguities are solved, have the orbiting aircraft fly to a very high altitude and hold a tight pattern over the runway to give the best geometry to the landing aircraft. This is of course assuming that all cycle slips can be detected and corrected between solving for the orbiters ambiguities and the test flight of the landing aircraft. If uncorrectable cycle slips do occur, then the orbiting aircraft would have descend and once again solve for its ambiguities.

4.6 Summary

This chapter described each of the simulations run during the course of this research, and their results. These simulations included the effects of elevation angle on geometry, the feasibility of deploying multiple Locatalites to aid in resolving the vertical positioning errors, and simulations involving a Locatalite onboard a mobile aircraft orbiting over the LocataNet to aid in reducing the vertical position errors. The next chapter will discuss the conclusions derived from these simulations.

V. Conclusion

5.1 Overview

The objective of this research was to develop methods for evaluating the geometry of a deployed pseudolite system with the goal of minimizing the position errors when tracking a landing aircraft. Of particular interest was the minimization of the vertical position error, which can be quite large due to poor slant angles between the local pseudolite transmitters and the receiver.

During the course of this research a new metric called GNAP has been developed to characterize the effects of geometry when the measurement error covariance matrix is not a pure diagonal, as is assumed when using DOP. This new value allows for a more accurate representation of the effects of geometry on position error because it takes the cross correlation terms, in the off diagonals of the measurement error covariance matrix, into account.

Several tests were run on a pseudolite simulator, based on the Locata reference system, which attempted to isolate the effect that different deployment geometries have on the position solution.

- The Elevation Angle Study: A single Locatalite was placed at a far distance, orthogonal to the runway. The height of this Locatalite above the ground was varied in order to yield slant angles ranging from 10^{o}-80^{o} from the middle of the runway. At each slant angle the VGNAP was taken to measure the relative vertical geometry quality that the lone elevated Locatalite gave to the system.

- Multiple Ground Level Locatalite Pairs Study: The number of Locatalite pairs was varied in this experiment. Each Locatalite in the pair was placed on opposite sides of the runway. In this case the Locatalites were not elevated above the ground.
- Multiple "Stepped" Locatalite Pairs Study: Similar to the "Multiple Ground Level Locatalite Pairs Study" except that every other Locatalite pair along the runway was elevated in a stair-step fashion from 0-100 meters.
- Centered Locatalites Study: Here the number of single Locatalites was varied as each Locatalite was placed along the centerline of the runway.
- Orbiting Aircraft Study: This test series involved placing a Locatalite and receiver in an aircraft that was to orbit above the runway as the test aircraft is on its landing approach.

5.2 Conclusions

The Elevation Angle study clearly shows that as the elevation angle increases between the receiver and the transmitter, the geometric errors decrease. There is a definite point of diminishing return after an elevation angle of 20^o. After this point the GNAP only improves by 0.75 over the course of 50^o of added elevation, corresponding to thousands of feet of added elevation. This means that raising the elevation angle to at least 20^o sees the most geometric improvement in the vertical range. It is also interesting to note that at an extremely high elevation angle of 80^o the GNAP drops to a value of 1, which shows that with a pseudolite almost directly overhead the vertical errors will be the same as the measurement errors.

In the multiple Locatalites study, multiple ground-based paired Locatalites yielded the poorest geometry of the three families of tests. It took over 500 Locatalite pairs to get the GNAP value down to a value of 4, which is still high and would yield high positioning errors in the vertical plane.

The single, centered Locatalites study did show some promise in that there was a significant reduction in GNAP, when compared to the multiple ground-based paired Locatalites study, with fewer Locatalites needed. In this case, the point of diminishing returns occured at about 100 Locatalites; however, the GNAP reduced to a value of just over 2 with only 50 Locatalites. Even though this geometry showed significant improvement in the GNAP for less cost, it is usually not very cost efficient to have 50 Locatalites in the LocataNet. Also with this geometry the transmitters would have to be practically embedded in the tarmac of the runway, which would pose a significant safety risk to the landing aircraft. Another concern with this geometry is that the aircraft could damage the transmitters once it touches down. These practical concerns limit the effectiveness of this deployment geometry.

Last among the multiple Locatalite deployment schemes was the multiple Locatalites arranged in a stair-step configuration. This study clearly provides the best geometry of all the multiple Locatalite studies, boasting a GNAP value of about 1 with only 10 Locatalite pairs. The point of diminishing returns occured with 20 Locatalite pairs and yields a GNAP value of less than 1. These results, while impressive, are unfortunately the result of a geometry that probably could not be utilized because of safety concerns with the tall towers that would need to be arranged right next to the runway.

The orbiting aircraft study shows some promising results that correlated well with the results of the elevation angle study. When the orbiting aircraft is high in the air, creating a high slant angle between the orbiter and the landing aircraft, the GNAP decreases down to a level less than 1 which would indicate that sub-centimeter level accuracy could be achieved with this geometry. However at high altitudes the geometry change of the orbiting aircraft in relation to the ground based LocataNet is not sufficient to solve for the carrier-phase ambiguities. Lowering the altitude, expanding the radius of the orbit, and varying the geometry of the trajectory can solve for the system ambiguities, yielding a lower GNAP for the orbiter. When the altitude of the orbiter decreases, to solve for the ambiguities, so do the slant angle seen between the orbiter and the landing aircraft, thus increasing the GNAP value for the landing aircraft.

It is interesting to notice that when the altitude decreases down to 4,000 meters the elevation angle between the landing aircraft and the orbiter is between about 45^{o} and the VGNAP values lay between 1 and 1.4. This data corresponds to what would has already been shown in the elevation angle study, where a slant angle between 40^{o} and 50^{o} yields GNAP values between 1 and 1.5.

In order to increase the efficiency of this geometry, which seems to yield promising results, it is recommended that the orbiting aircraft fly a low altitude flight pattern with a high degree of geometric change in trajectory in order to solve for the system ambiguities. Assuming that the cycle slips can be detected and corrected for, the orbiter could then fly to a high altitude and orbit there while the landing aircraft makes its descent. With the ambiguities solved for, the orbiting aircraft's GNAP should be low

enough to ensure that the position data the landing aircraft receives from the orbiter has the precision to yield low positioning errors in the landing aircrafts track.

5.3 Contributions

The following contributions have been made during the course of this research:

- The greatest contribution from this research stems from the development of a systematic method to test the effects that geometry has on a pseudolite based system.
- Results from the elevation studies and the multiple Locatalite studies clearly show the effects that those geometric deployments have on positioning error.
- The development of a feasible geometry, involving an orbiting aircraft, which could possibly be incorporated into an actual flight test of the Locata system and produce precision tracks of a landing aircraft.
- Development of the GNAP as a viable alternative to DOP when certain assumptions, common in GPS applications, cannot be made on a pseudolite based system.

5.4 Recommendations

While this research focused primarily on the geometry of pseudolite-based reference systems there is still much work to be done before these results can be applied to a real world deployment of a pseudolite network for the purpose of testing GPS. Listed below are recommendations for further research related to this topic.

- Many assumptions are made in the research, which limit the real world use of its results. Therefore, it is necessary to conduct a similar study of system geometry

that accounts for these assumptions (i.e. adding tropospheric errors, multipath errors, ambiguities, etc)

- This research conducted only limited tests into a large number of possible geometries, further research into other possible geometric deployments of the LocataNet should be investigated as well as combinations of the various geometries used in this study.
- Flight-testing of the Locata, Inc technology is required to verify that the system to validate the results which were simulated in this research.

Appendix A

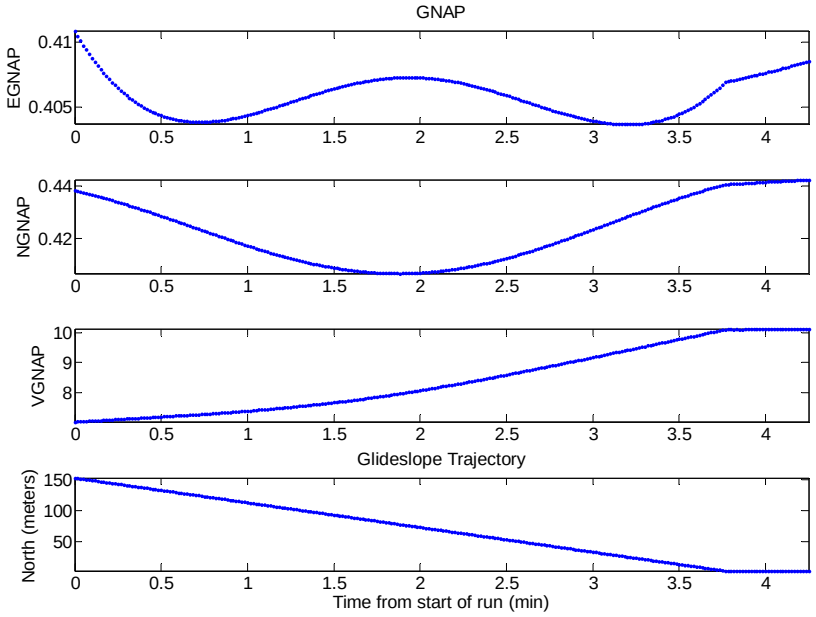

Figure 41: GNAP Plots of the 5^{o} Elevation Angle Test

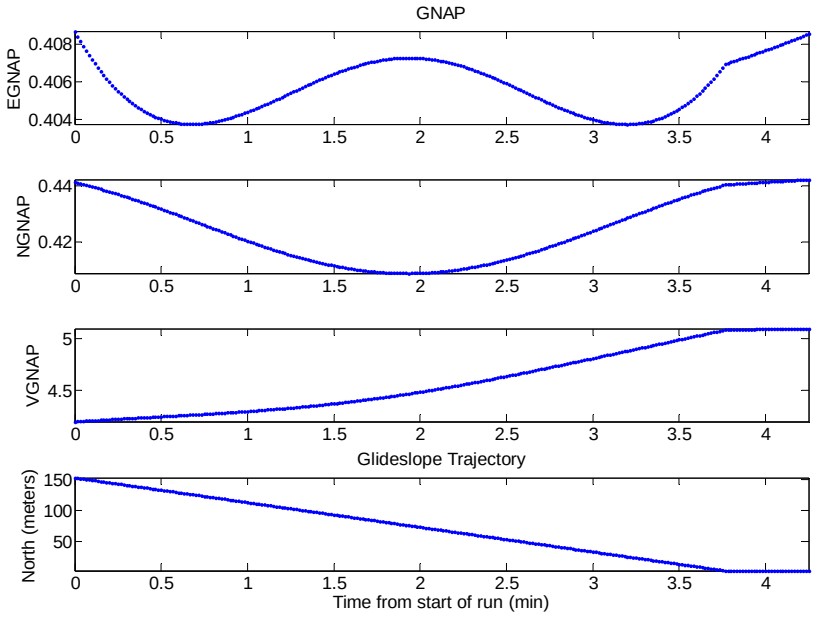

Figure 42: GNAP Plots of the 10^{o} Elevation Angle Test

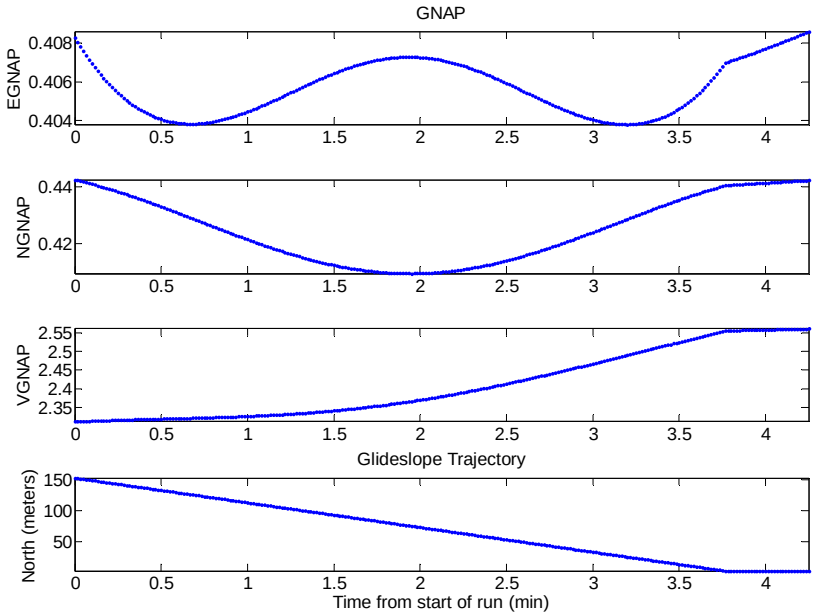

Figure 43: GNAP Plots of the 20^{o} Elevation Angle Test

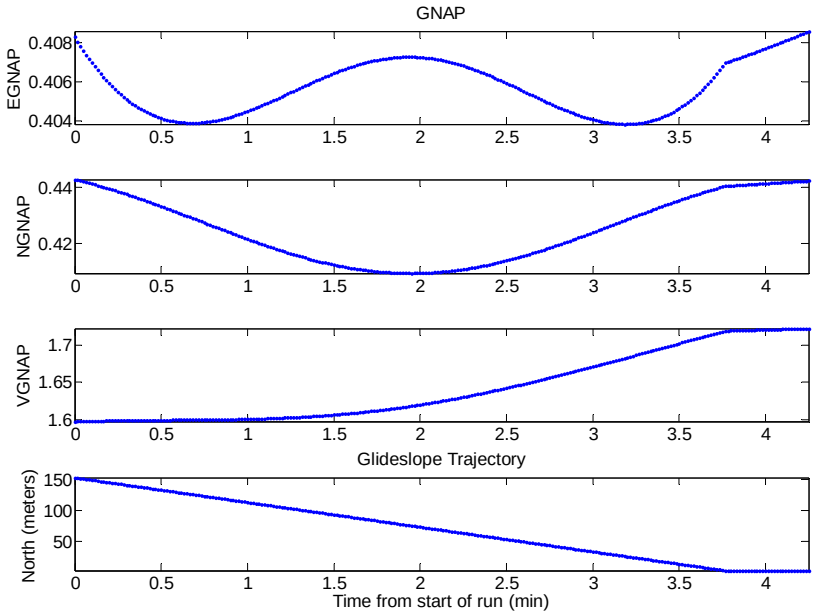

Figure 44: GNAP Plots of the 30^{o} Elevation Angle Test

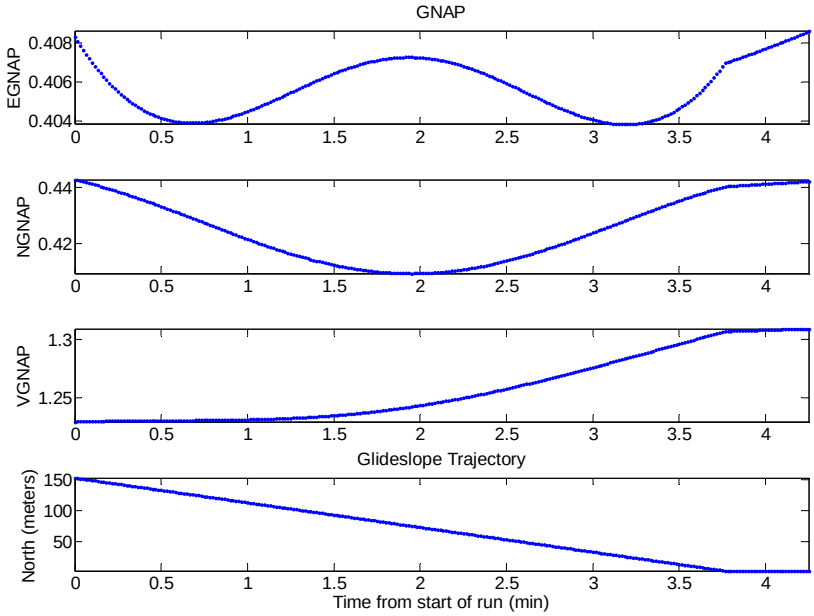

Figure 45: GNAP Plots of the 40^{o} Elevation Angle Test

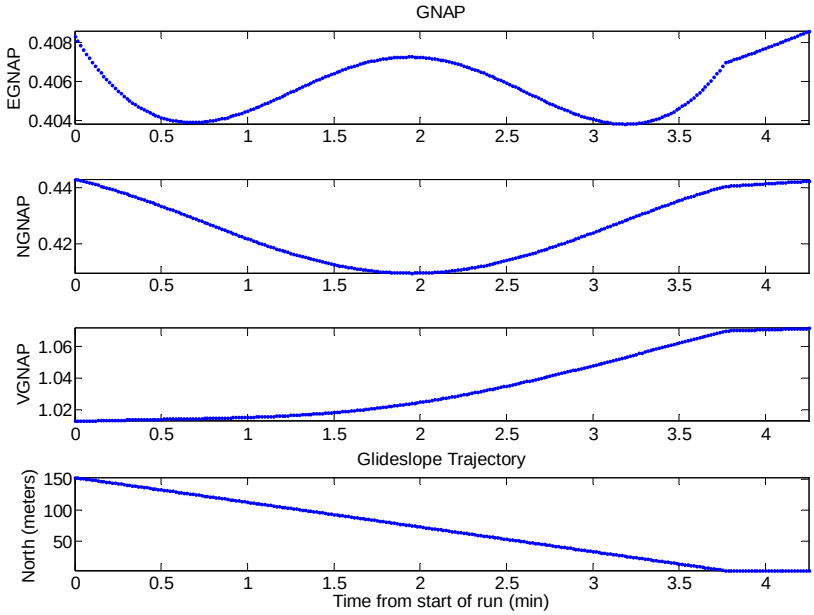

Figure 46: GNAP Plots of the 50^{o} Elevation Angle Test

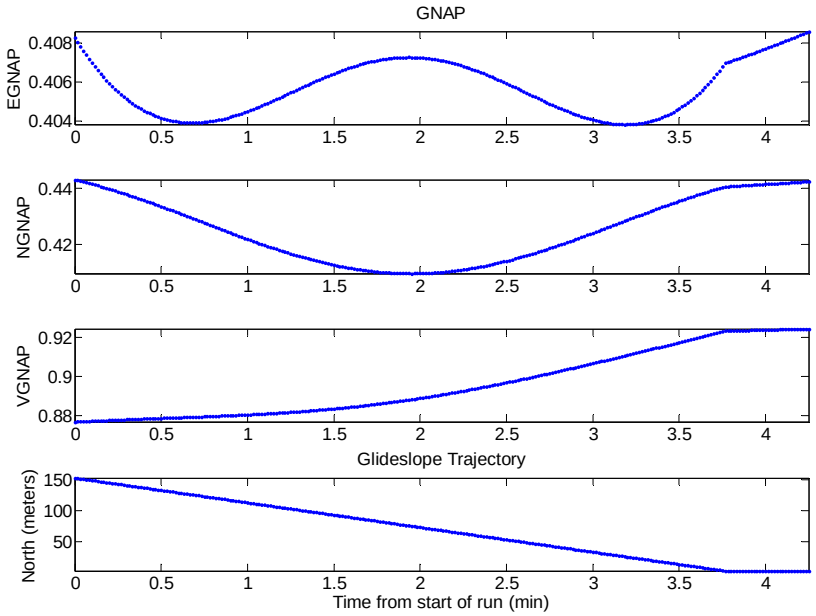

Figure 47: GNAP Plots of the 60^{o} Elevation Angle Test

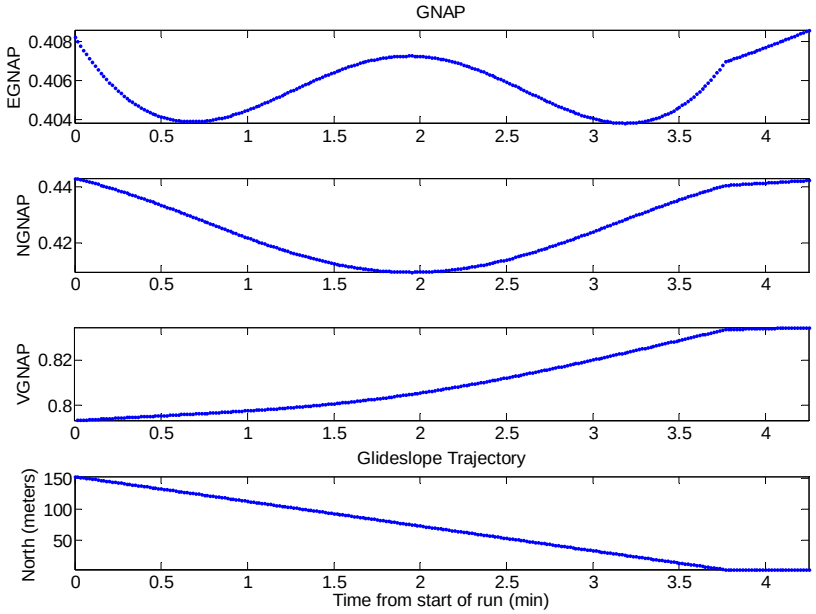

Figure 48: GNAP Plots of the 70^{o} Elevation Angle Test

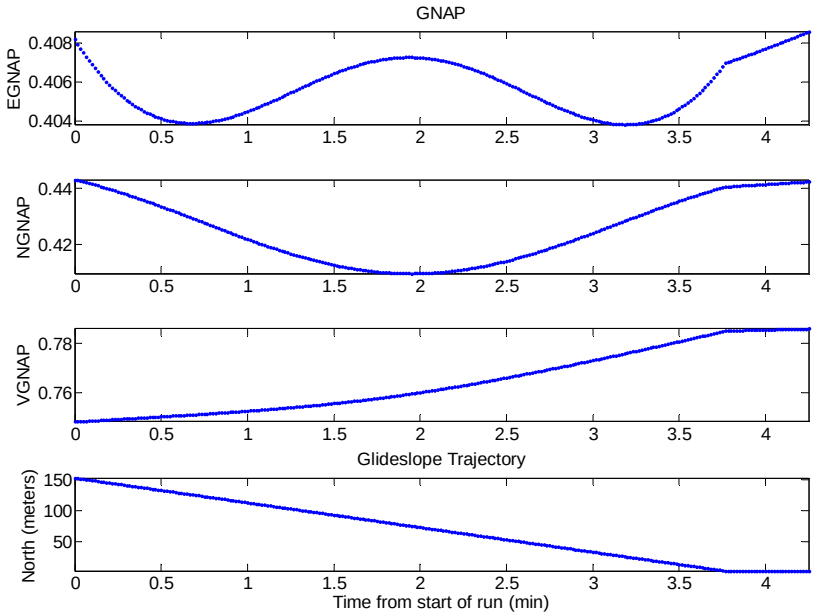

Figure 49: GNAP Plots of the 80^{o} Elevation Angle Test

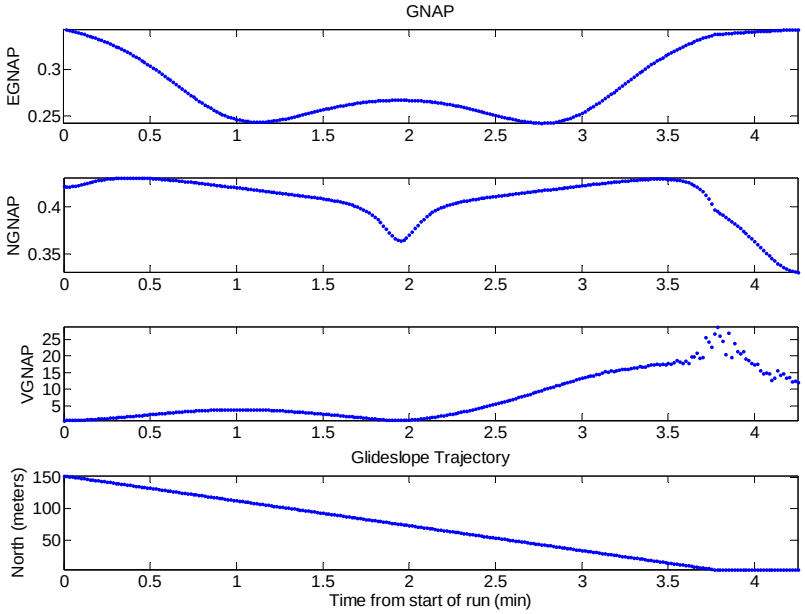

Figure 50: GNAP Plots of the Lots Case Study with 3 Pairs of Locatalites

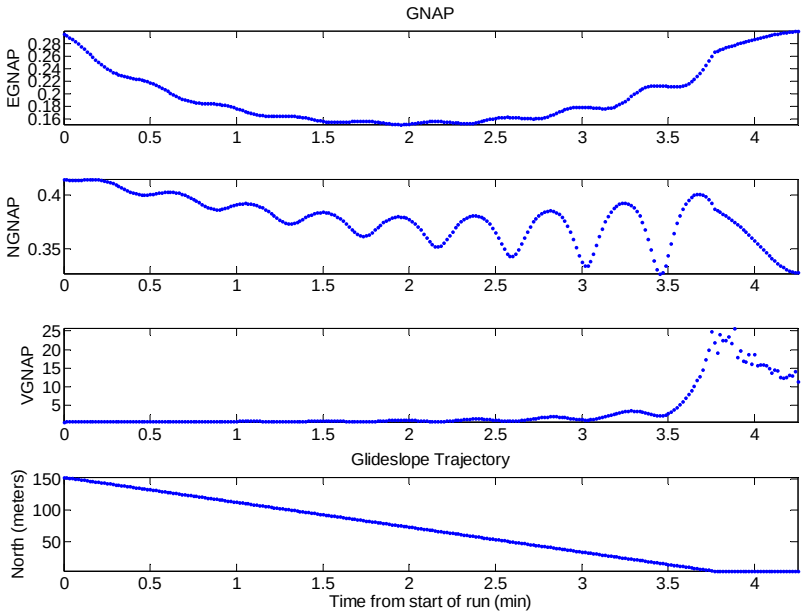

Figure 51: GNAP Plots of the Lots Case Study with 10 Pairs of Locatalites

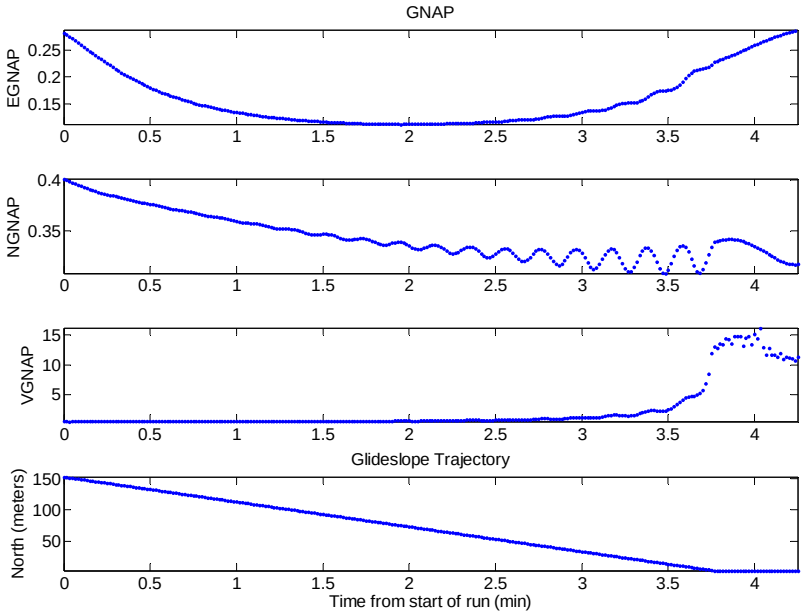

Figure 52: GNAP Plots of the Lots Case Study with 20 Pairs of Locatalites

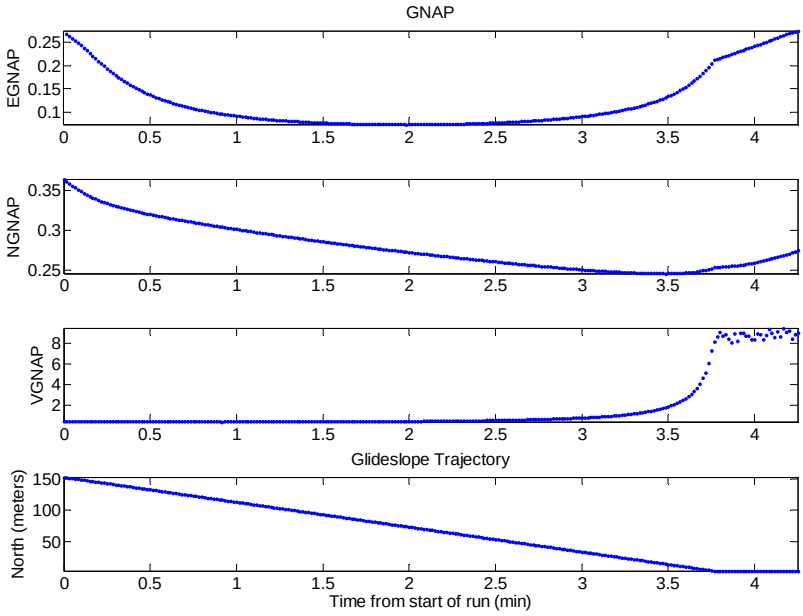

Figure 53: GNAP Plots of the Lots Case Study with 50 Pairs of Locatalites

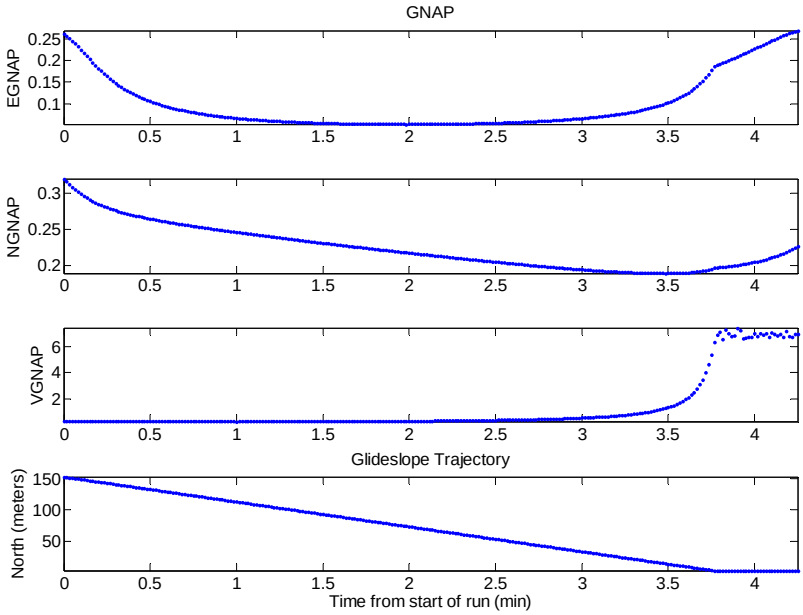

Figure 54: GNAP Plots of the Lots Case Study with 100 Pairs of Locatalites

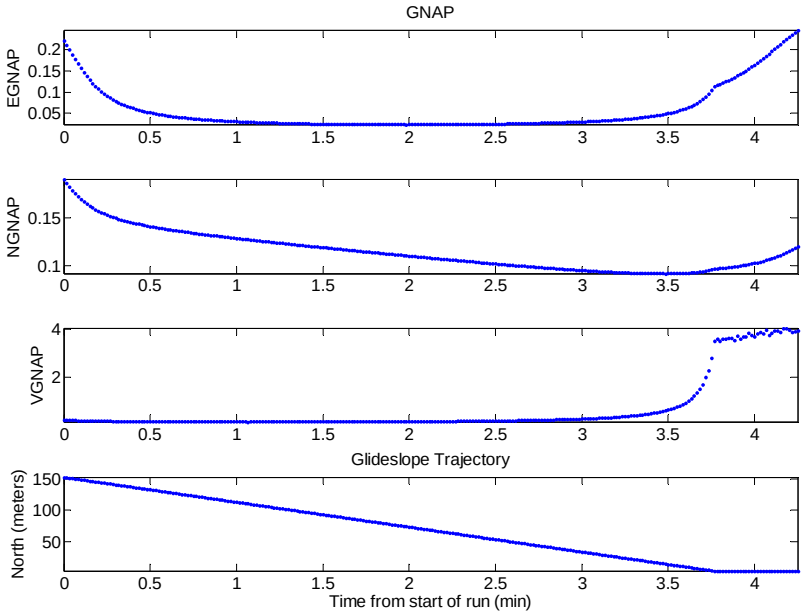

Figure 55: GNAP Plots of the Lots Case Study with 500 Pairs of Locatalites

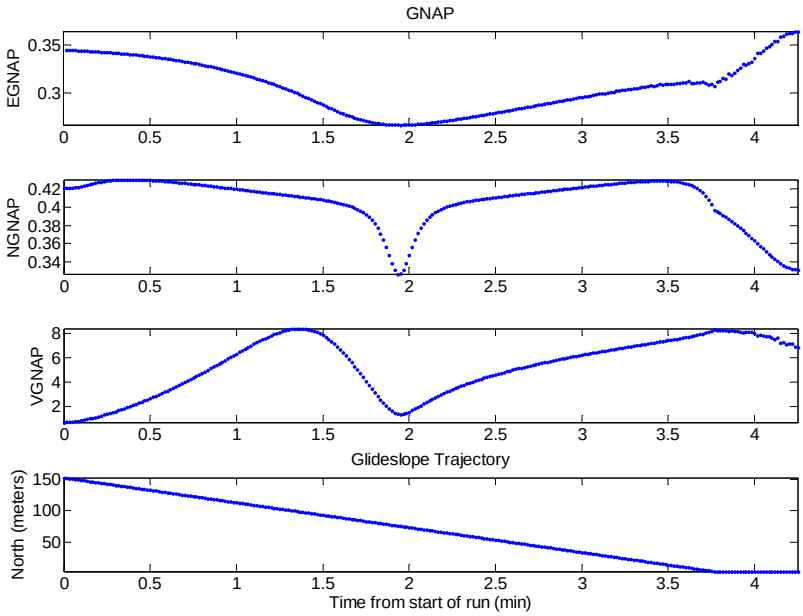

Figure 56: GNAP Plots of the Stair Stepped Case Study with 3 Pairs of Locatalites

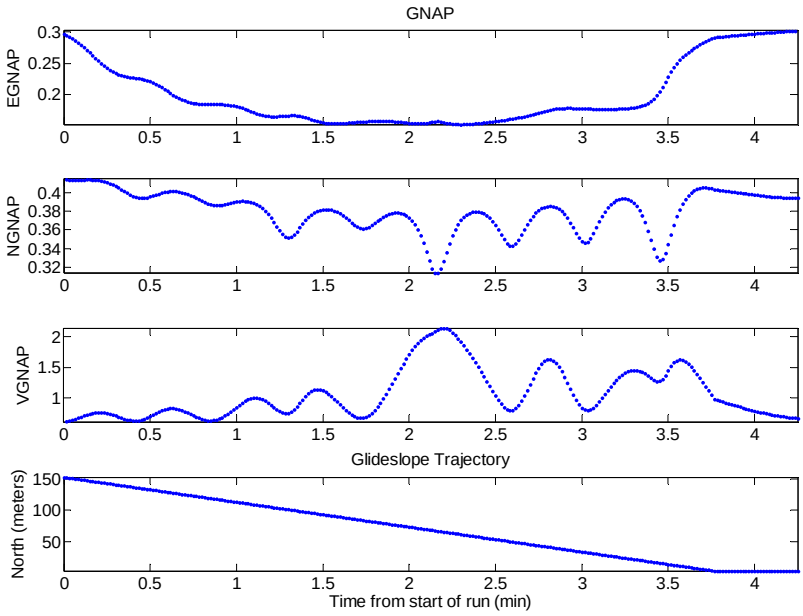

Figure 57: GNAP Plots of the Stair Stepped Case Study with 10 Pairs of Locatalites

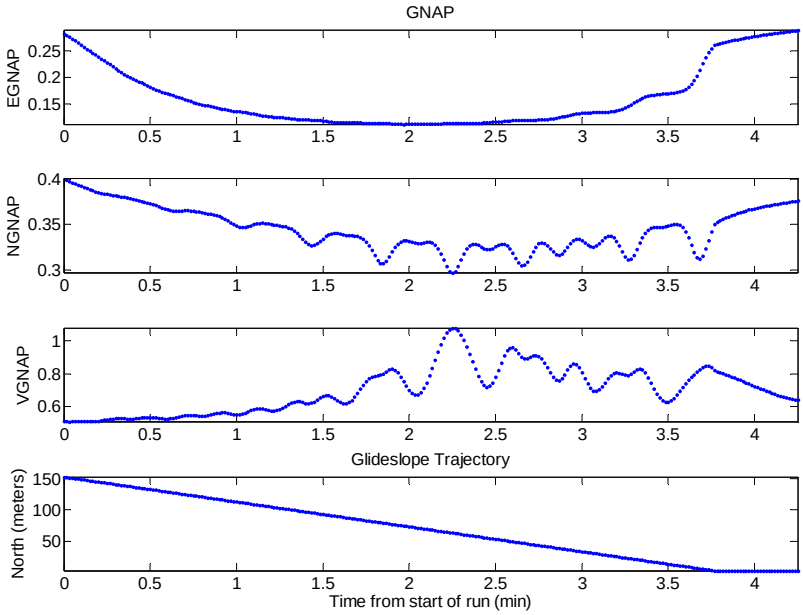

Figure 58: GNAP Plots of the Stair Stepped Case Study with 20 Pairs of Locatalites

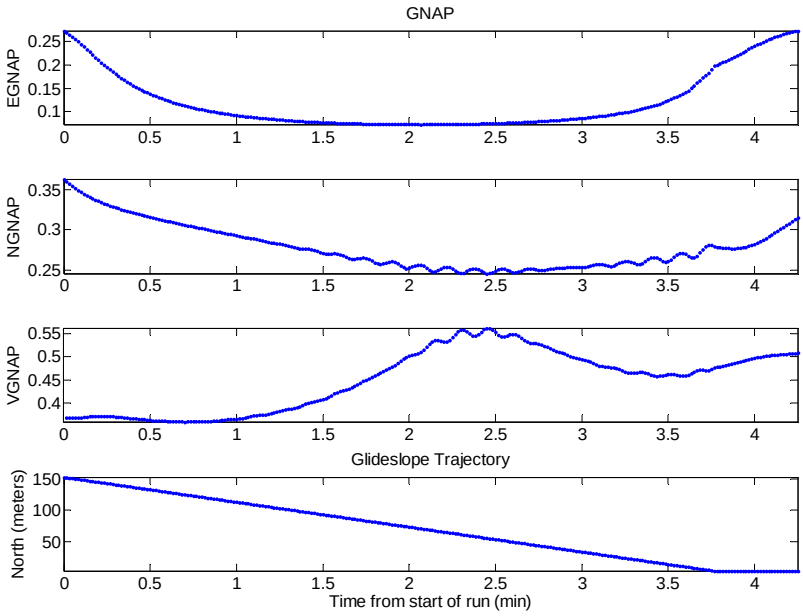

Figure 59: GNAP Plots of the Stair Stepped Case Study with 50 Pairs of Locatalites

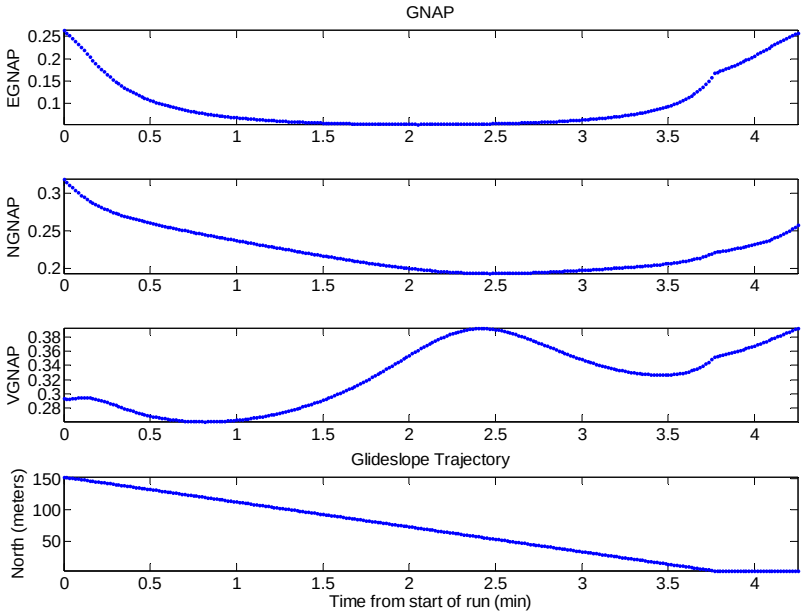

Figure 60: GNAP Plots of the Stair Stepped Case Study with 100 Pairs of Locatalites

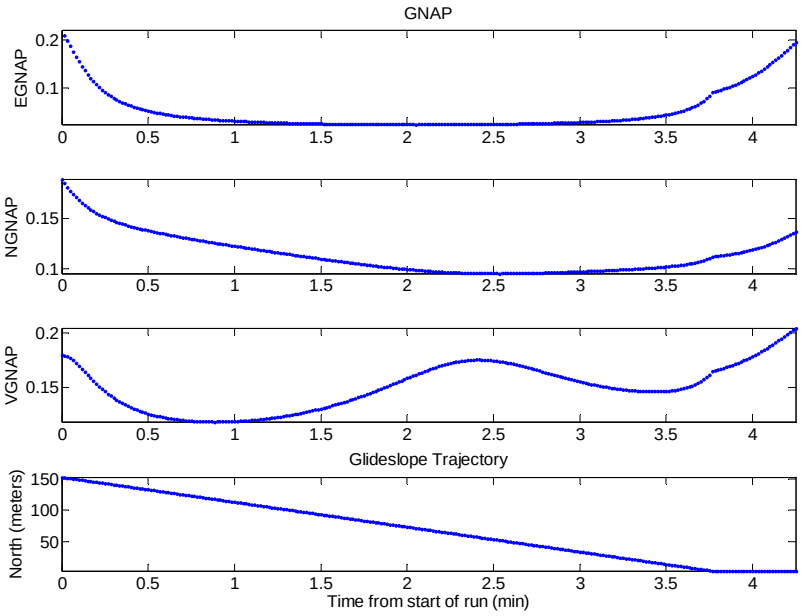

Figure 61: GNAP Plots of the Stair Stepped Case Study with 500 Pairs of Locatalites

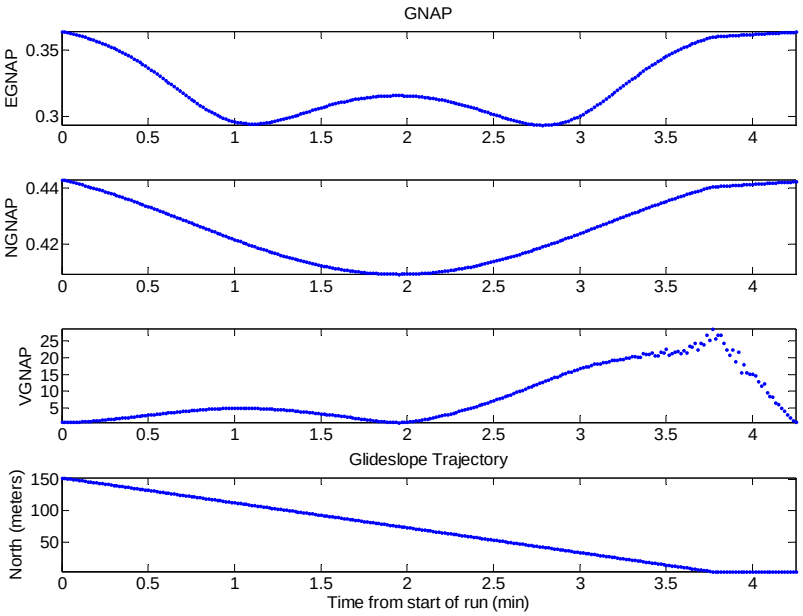

Figure 62: GNAP Plots of the Centered Case Study with 3 Locatalites

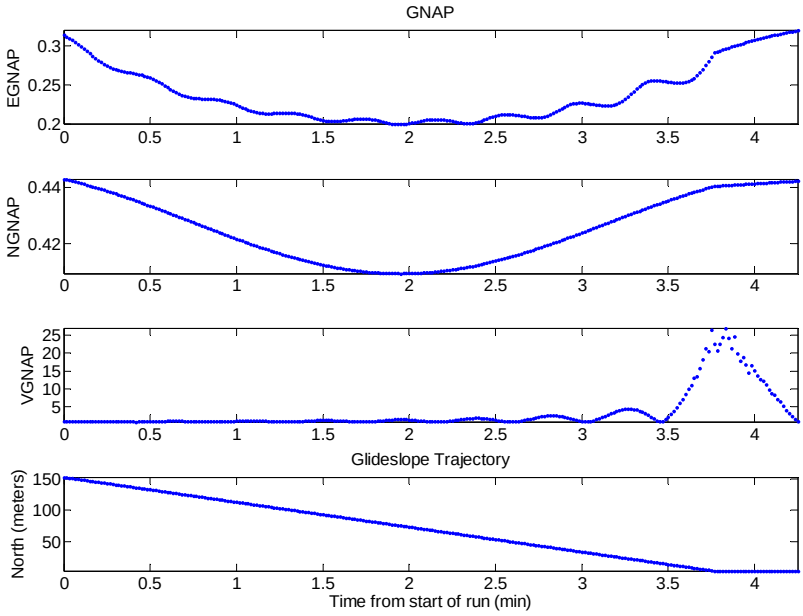

Figure 63: GNAP Plots of the Centered Case Study with 10 Locatalites

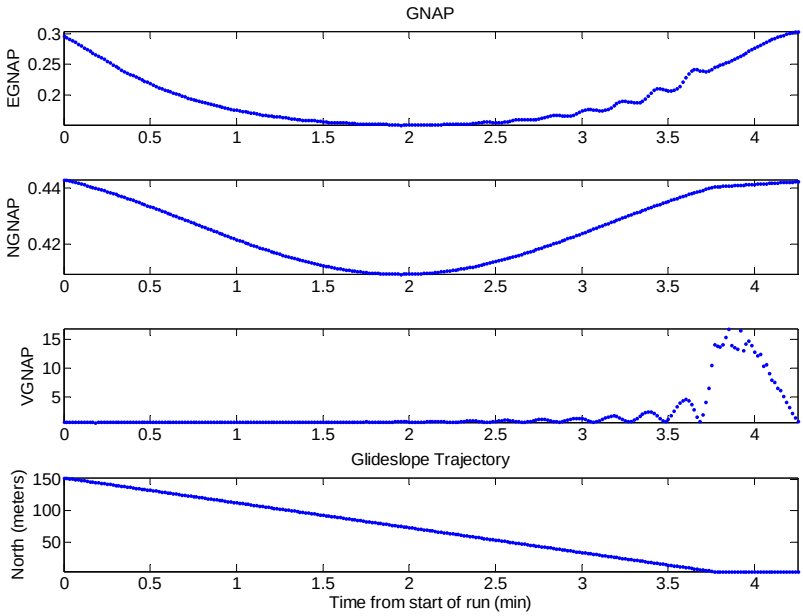

Figure 64: GNAP Plots of the Centered Case Study with 20 Locatalites

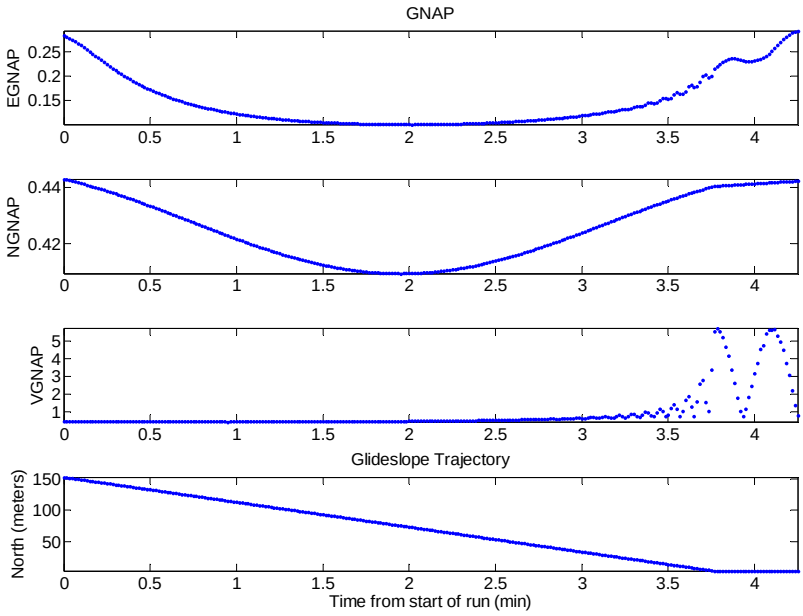

Figure 65: GNAP Plots of the Centered Case Study with 50 Locatalites

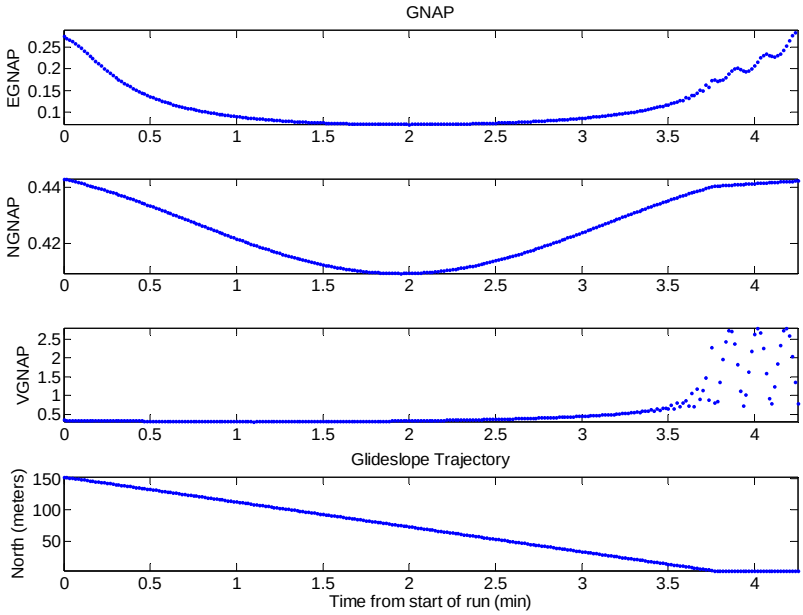

Figure 66: GNAP Plots of the Centered Case Study with 100 Locatalites

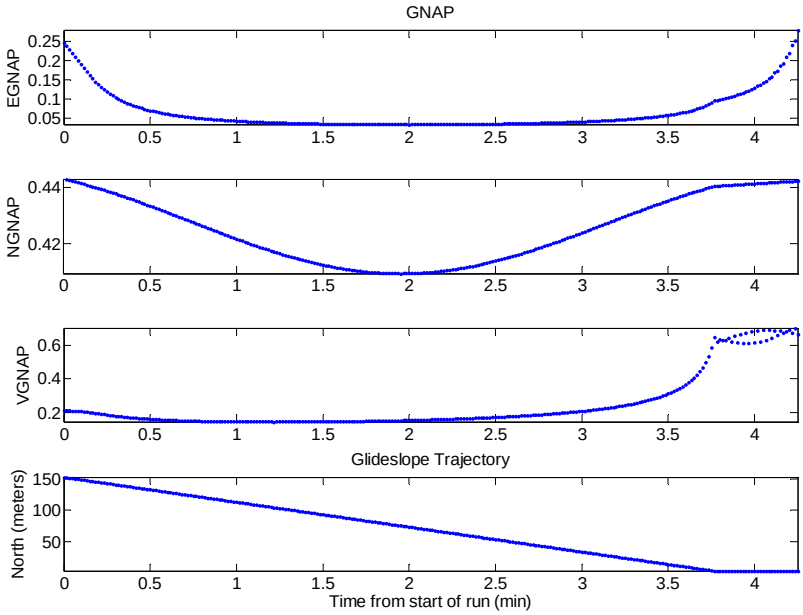

Figure 67: GNAP Plots of the Centered Case Study with 500 Locatalites

Bibliography

1. Amt, John R.H. *Methods For Aiding Height Determination in Pseudolite-Based Reference Systems Using Batch Least-Squares Estimation.* Master's Thesis, Air Force Institute of Technology, March 2006.

2. Barnes, J., C. Rizos, M. Kanli, A. Pahwa, D. Small, G. Voigt, N. Gambale, and J. Lamance. "High Accuracy Positioning Using Locata's Next Generation Technology".

3. Barnes, Joel, Chris Rizos, Mustafa Kanli, David Small, Gavin Voigt, Nunzio Gambale, Jimmy Lamance, Terry Nunan, and Chris Reid. "Indoor Industrial Manchine Guidance using Locata: A Pilot Study at BlueScope Steel". *Proceedings of the 2004 Annual Meeting of the Institute of Navigation*. Dayton, OH, June 2004.

4. Barnes, Joel, Chris Rizos, Mustafa Kanli, David Small, Gavin Voigt, Nunzio Gambale, and Jimmy Lamance. "Structural Deformation Monitoring Using Locata". *Proceedings of the 2004 International Symposium on Engineering Surveys for Construction Works and Structural Engineering.* Nottingham, UK, June 2003.

5. Barnes, Joel, Chris Rizos, Jinling Wang, David Small, Gavin Voigt, and Nunzio Gambale. "High Precision Indoor and Outdoor Positioning Using LocataNet". *Proceedings of the 2003 International Symposium on GPS/GNSS*. Tokyo, Japan, November 2003.

6. Barnes, Joel, Chris Rizos, Jinling Wang, David Small, Gavin Voigt, and Nunzio Gambale. "LocataNet: A New Positioning Technology for High Precision Indoor and Outdoor Positioning". *Proceedings of the 2003 International Technical Meeting of the Satellite Division of the US Institute of Navigation.* Portland, OR, September 2003.

7. Barnes, Joel, Chris Rizos, Jinling Wang, David Small, Gavin Voigt, and Nunzio Gambale. "Locata: The Positioning Technology of the Future?". *Proceedings of the 2003 International Symposium on Satellite Navigaion Technology Including Mobile Positioning and Location Services.* Melbourne, Austrialia, July 2003.

8. Bouska, Terry J. *Development and Simulation of a Pseudolite-based flight Reference System.* Master's Thesis, Air Force Institute of Technology, March 2003.

9. Brown, Alison, Frank Van Diggele, Thomas Kelecy, Peter Brown. "Flight Test Results Using Carrier Phase Kinematic Solutions for Aircraft precision Approach and Landing". *SPN*. Janurary 1995

10. Chao, C.C. "The Tropospheric Calibration Model for Mariner Mars." JPL Technical Report, 1971

11. Emporis Buildings. "KLIA Air Traffic Control Tower." *Excerpt from Technical Specifications*. http://www.emporis.com/en/wm/bu/?id=106042. 17 May 2006.

12. Federal Aviation Administration. "*Objects Affecting Navigable Airspace*." CFR Title 14 Part 77. Washington: GPO, 17 December 2004.

13. Lee, Hung Kyu, Jinling Wang, Chris Rizos, Joel Barnes, Toshiaki Tsujii, and Ben K.H. Soon. "Analysis of Pseudolite Augmentation for GPS Airborne Applications". *Proceedings of ION GPS 2002.* Portland, OR, September 2002.

14. Monda, Eric W., E. Lightsey, Kevin Key. "An Investigation of GPS Pseudolite Based Relative Navigation". *American Astronautical Society 03-529.* 2003

15. Paielli, R., R. Bach, B. McNally, R. Simmons, D. Warner, T. Forsyth, G. Kanning, C. Ahtye, D. Kaufmann, and J. Walton. "Carrier Phase Differential GPS Integrated with an Inertial Navigation system : Flight Test Evaluation with Auto-Coupled Precision Landing Guidance". *Proceedings of the 1995 National Technical Meeting of the Institute of Navigation.* Anaheim, CA, Janurary 1995.

16. Raquet, John, G. Lachapelle, W. Qiu, C. Pelletier, T. Nash, F.B. Snodgrass, P. Fenton, and T. Holden. "Development and Testing of a Mobile Pseudolite concept for Precise Positioning". *Navigation: Journal of the Institute of Navigation*. 43(2), 1996.

17. Raquet, John. "Class Notes to EENG 533". Air Force Institute of Technology, 2006.

18. Stone, Jonathan M., Edward LeMaster, J. Powell, Stephen Rock. "GPS Pseudolite Transceivers and their Applications". *Proceedings of the 1999 ION National Technical Meeting*. January 1999.

19. Wang, J. "Pseudolite Applications in Positioning and Navigation: Progress and Problems". *Journal of Global Positioning Systems: Vol. 1, No. 1*. 43-56. 2002.

Vita

Ensign Matthew Perri Crawford was born on 8 November, 1982 in London, England. He graduated, with honors, from West Springfield High School in 2000. After attending The Ohio State University for 5 years he graduated with a bachelor's degree in Aeronautical/Aerospace Engineering, and was commissioned a Naval Officer on 12 June 2005. His first assignment as a Naval Officer was to the Air Force Institute of Technology (AFIT) to attain his Master's degree in Aerospace Engineering. Upon graduation from AFIT he will report to NAS Pensacola to commence in flight training to become a Naval Aviator.

REPORT DOCUMENTATION PAGE

Form Approved
OMB No. 074-0188

1. REPORT DATE *(DD-MM-YYYY)*	**2. REPORT TYPE**	**3. DATES COVERED** *(From – To)*
13-06-2006	**Master's Thesis**	Jun 2005 – Jun 2006

4. TITLE AND SUBTITLE

Optimal Geometric Deployment of a Ground Based Pseudolite Navigation System to Track a Landing Aircraft

5a. CONTRACT NUMBER

5b. GRANT NUMBER

5c. PROGRAM ELEMENT NUMBER

6. AUTHOR(S)

Crawford, Matthew P., Ensign, USN

5d. PROJECT NUMBER

5e. TASK NUMBER

5f. WORK UNIT NUMBER

7. PERFORMING ORGANIZATION NAMES(S) AND ADDRESS(S)
Air Force Institute of Technology
Graduate School of Engineering and Management (AFIT/EN)
2950 Hobson Way
WPAFB OH 45433-7765

8. PERFORMING ORGANIZATION REPORT NUMBER

AFIT/GAE/ENG/06-02

9. SPONSORING/MONITORING AGENCY NAME(S) AND ADDRESS(ES)
AFRL/AFOSR
Attn: Dr. Arje Nachman
875 North Randolph Street
Suite 325, Room 3112
Arlington, Virginia 22203 Phone: (703) 696-8427 Email: arje.nachman@afosr.af.mil

10. SPONSOR/MONITOR'S ACRONYM(S)

11. SPONSOR/MONITOR'S REPORT NUMBER(S)

12. DISTRIBUTION/AVAILABILITY STATEMENT

APPROVED FOR PUBLIC RELEASE; DISTRIBUTION UNLIMITED.

13. SUPPLEMENTARY NOTES

14. ABSTRACT

With much of the military and civilian communities becoming dependent on GPS technology to navigate it has become imperative that the navigation systems be tested in situations in which GPS does not work. This testing is especially necessary for precise tasks such as landing an aircraft. Currently, research is being conducted into using a pseudolite-based reference system to use as a truth model for the GPS jamming test. Pseudolite systems have been proven to provide sub-centimeter level accuracy in the horizontal plane; however in the vertical plane the position error is still in the decimeter to meter level range. This is largely due to the fact that the geometry of a ground based pseudolite system provides poor slant angles in the vertical plane, which contributes to large positioning errors. The goal of this research is to study the effects of system geometry on the vertical plane solution.

The results of this effort show that elevation angles of greater than 20^{o}-30^{o} are necessary to attain resonably good positioning solutions. Multiple pseudolite deployments, while effective at reducing the geometry errors, are very cost ineffective and the geometries pose significant risks to a landing aircraft. The best geometry involved using an orbiting aircraft, with a pseudolite transmitter and receiver attached, as an elevated pseudolite to create better slant angles and thus better positioning solutions.

15. SUBJECT TERMS

Pseudolite, Global Positioning System, GPS; Precision Approach, Precision Landing, Locata, Network Geometry, DOP, GNAP, Batch Least Squares Estimation.

16. SECURITY CLASSIFICATION OF:			**17. LIMITATION OF ABSTRACT**	**18. NUMBER OF PAGES**	**19a. NAME OF RESPONSIBLE PERSON**
REPORT	**ABSTRACT**	**c. THIS PAGE**			Raquet, John F., Ph.D., (ENG)
U	**U**	**U**	**UU**	127	**19b. TELEPHONE NUMBER** *(Include area code)* (937) 255-3636, ext 4580 email: john.raquet@afit.edu